Ecological Cycle Optimizer: A novel nature-inspired metaheuristic algorithm for global optimization

Boyu Ma*,†, Jiaxiao Shi†, Yiming Ji and Zhengpu Wang

State Key Laboratory of Robotics and Systems, Harbin Institute of Technology, Harbin, 150001, China

ARTICLE INFO

Keywords:
Ecological Cycle Optimizer (ECO)
Metaheuristic algorithms
Nature-inspired
Global optimization
Engineering problems

ABSTRACT

This article proposes the Ecological Cycle Optimizer (ECO), a novel metaheuristic algorithm inspired by energy flow and material cycling in ecosystems. ECO draws an analogy between the dynamic process of solving optimization problems and ecological cycling. Unique update strategies are designed for the producer, consumer and decomposer, aiming to enhance the balance between exploration and exploitation processes. Through these strategies, ECO is able to achieve the global optimum, simulating the evolution of an ecological system toward its optimal state of stability and balance. Moreover, the performance of ECO is evaluated against five highly cited algorithms—CS, HS, PSO, GWO, and WOA—on 23 classical unconstrained optimization problems and 24 constrained optimization problems from IEEE CEC-2006 test suite, verifying its effectiveness in addressing various global optimization tasks. Furthermore, 50 recently developed metaheuristic algorithms are selected to form the algorithm pool, and comprehensive experiments are conducted on IEEE CEC-2014 and CEC-2017 test suites. Among these, five top-performing algorithms, namely ARO, CFOA, CSA, WSO, and INFO, are chosen for an in-depth comparison with the ECO on the IEEE CEC-2020 test suite, verifying the ECO's exceptional optimization performance. Finally, in order to validate the practical applicability of ECO in complex real-world problems, five state-ofthe-art algorithms, including NSM-SFS, FDB-SFS, FDB-AGDE, L-SHADE, and LRFDB-COA, along with four best-performing algorithms from the "CEC2020 competition on real-world single objective constrained optimization", namely SASS, ϵ sCMAgES, EnMODE, and COLSHADE, are selected for comparative experiments on five engineering problems from CEC-2020-RW test suite (real-world engineering problems), demonstrating that ECO achieves performance comparable to those of advanced algorithms. The source code of ECO is available at https://www.mathworks.com/ $\verb|matlabcentral/fileexchange/180852-ecological-cycle-optimizer-eco.| For detailed instructions and |$ presentation of ECO, please refer to https://github.com/jiaxiao-shi/ECO-Optimizer.

1. Introduction

Complex constrained optimization problems in the real world are often characterized by high dimensionality, nonlinearity, and non-convexity. Optimization, as a mathematical tool, plays a crucial role across various disciplines, aiming to identify global optima within constrained spaces. Traditional gradient-based methods, however, frequently encounter local optima when addressing such problems, limiting their global optimization capabilities (Nocedal and Wright, 1999; Boyd and Vandenberghe, 2004). In contrast, metaheuristic search (MHS) algorithms offer advantages such as simplicity in mathematical modeling, ease of implementation, black-box adaptability, and a high degree of randomness, making them effective at escaping local optima to find global solutions. As a result, MHS algorithms have been widely applied to large-scale complex constrained optimization problems in diverse fields.

In the past two decades, MHS algorithms have attracted significant attention within the academic community, driven by rapid advancements in the field. The inspiration for MHS algorithms often derives from natural phenomena,

Shi); 0009-0009-5694-7766 (Y. Ji); 0000-0002-0566-3087 (Z. Wang)

animal behaviors, physical laws, and human activities. Researchers model these patterns mathematically to develop intelligent optimizers for solving complex problems. Previous MHS algorithms are primarily inspired by *evolution*, *nature*, *physics*, *human behavior*, and *mathematics*, along with their related improved algorithms.

The implementation process of MHS algorithms includes population initialization and the iterative search process, the latter of which consists of three steps: guide selection, convergence search, and population update. The convergence search step of numerous MHS algorithms employ different strategies, resulting in diverse performance outcomes. Fundamentally, these convergence search models decompose the optimization process into two key phases: exploration and exploitation, which are essential components of the search-based problem-solving paradigm (Eiben and Schippers, 1998). Exploration allows the algorithm to broadly investigate the search space, identifying regions where a global optimum may exist, whereas exploitation focuses on intensively refining the search within those promising regions to locate the global optimum.

Although the expected performance of MHS algorithms may be comparable across constrained optimization problems, the balance between *exploration* and *exploitation* varies among different algorithms. Excessive *exploration* can result in a slower convergence rate, while overemphasis on *exploitation* risks the algorithm becoming trapped in

[†] These authors contributed equally to this work.

^{*} Corresponding author: mby9702@163.com (B. Ma)
ORCID(s): 0000-0002-9628-9886 (B. Ma); 0009-0003-7822-3087 (J.

local optima. These differences in balancing the two phases contribute to the varying performance of algorithms across different problems, which aligns with the No Free Lunch (NFL) theorem (Wolpert and Macready, 1997). This theorem asserts that no single algorithm is universally optimal for all constrained optimization problems. Consequently, researchers have proposed numerous MHS algorithms inspired by diverse concepts, making this an active area of research. In this article, we propose a novel nature-inspired metaheuristic optimizer, aimed at demonstrating superior performance compared to previous state-of-the-art (SOTA) MHS algorithms across a broader range of complex constrained optimization problems.

Drawing inspiration from energy flow and material cycling within ecosystems, we propose Ecological Cycle Optimizer (ECO). The dynamic optimization process of ECO is analogous to an ecological cycle, where the search for the global optimum resembles an ecosystem achieving balance and stability. We design specific iterative update strategies for different ecosystem roles, namely producers, consumers, and decomposers. For consumers, distinct predation strategies are developed for herbivores, carnivores, and omnivores, while decomposer strategies incorporate optimal, local random, and global random decomposition approaches. By enhancing the balance between exploration and exploitation, ECO addresses the limitations of previous MHS algorithms, such as slow convergence, low precision, and susceptibility to local optima, thereby achieving superior performance across a broader range of complex constrained optimization problems. Furthermore, the 23 classic optimization functions, IEEE CEC-2014, CEC-2017, CEC-2020 test suites, along with five classic real-world mechanical design engineering problems from CEC-2020 (real-world engineering problems, CEC-2020-RW), are used to validate the superior performance of ECO compared to various SOTA MHS algorithms.

The remainder of this article is organized as follows. The literature review is outlined in Section 2. Section 3 provides a detailed description of the inspiration and mathematical model underlying the proposed ECO. Section 4 introduces the experimental design and parameter settings of this paper, as well as the related evaluation criteria. In Section 5, the performance of ECO in solving unconstrained and constrained optimization functions has been verified. Section 6 focused on exploring the performance of ECO in solving single-objective optimization functions, and established an algorithm pool containing 50 comparative MHS algorithms to highlight the solving advantages of ECO. In Section 7, the application prospects and potential of ECO in solving real-world engineering problems have been verified. Finally, Section 8 concludes the article with some final remarks.

2. Literature review

To understand the latest research progress of MHS algorithms, this section reviews the literature on optimizers inspired by *evolution*, *nature*, *physics*, *human behavior*, and

mathematics, as well as their related improved algorithms, as shown in Table 1.

Evolution-inspired MHS algorithms draw inspiration from the process of biological evolution observed in nature, with algorithms in this category simulating key mechanisms of Darwinian evolution, such as selection, crossover, and mutation. One of the most representative algorithms is the Genetic Algorithm (GA) (Holland, 1992), which has significantly influenced the development of evolutionary optimization techniques. Genetic Programming (GP) (Koza, 1994) extended evolutionary principles to program evolution, while Differential Evolution (DE) (Storn and Price, 1997) introduced differential mutation strategies to handle continuous optimization problems. Evolutionary Programming (EP) (Yao et al., 1999) expanded evolutionary algorithms by focusing on optimization in stochastic environments, primarily using mutation-based operations without relying on crossover. Evolution Strategy (ES) (Beyer and Schwefel, 2002) optimized continuous problems through specialized mutation strategies and adaptive step-size adjustments. As evolutionary computation progressed, more specialized algorithms emerged. For instance, Queen-bee Evolution (QE) (Jung, 2003) incorporated roles inspired by bee colonies, while Biogeography-Based Optimizer (BBO) (Simon, 2008) drew on concepts from biogeography to enhance population diversity. Quantum-inspired Evolutionary Algorithm (QEA) (Talbi and Draa, 2017) leveraged principles from quantum computing to introduce probabilistic and superposition states into the evolutionary framework, enhancing its capability in exploring global optima. Recently, Liver Cancer Algorithm (LCA) (Houssein et al., 2023) introduced domain-specific adaptations, applying evolutionary concepts specifically tailored to complex medical data structures, reflecting the ongoing diversification of evolutionbased MHS algorithms across various domains and applications. Nature-inspired MHS algorithms, are metaheuristic approaches that emulate the social behaviors of biological populations, or the laws of nature. Foundational algorithms include Particle Swarm Optimization (PSO) (Kennedy and Eberhart, 1995), modeling bird flock predation strategies, and Ant Colony Optimization (ACO) (Dorigo et al., 1996), replicating ant foraging via pheromone trails. Artificial Bee Colony (ABC) algorithm (Karaboga, 2010) extended this paradigm by mimicking the foraging dynamics of honeybees, while Pigeon-Inspired Optimization (PIO) (Duan and Qiao, 2014) drew inspiration from the homing navigation behavior of pigeons. Grey Wolf Optimizer (GWO) (Mirjalili et al., 2014) simulated the leadership hierarchy and hunting tactics of wolf packs. Moth-Flame Optimization (MFO) (Mirjalili, 2015) was inspired by the spiral path of moths as they converge toward light sources. Whale Optimization Algorithm (WOA) (Mirjalili and Lewis, 2016) was based on the social dynamics and hunting methods of humpback whales. Beetle Antennae Search (BAS) (Jiang and Li, 2017) was modeled on the sensory and search behaviors of beetles. Moth Search Algorithm (MSA) (Wang, 2018) incorporated both the phototactic and Lévy flight patterns observed in

Table 1
Overview of MHS algorithms.

lassification	Algorithm	Abbrev.	Inspiration	Ref.
volution-	Genetic Algorithm	GA	Darwinian evolution theory	(Holland, 1992)
spired	Genetic Programming Differential Evolution	GP DE	Evolutionary processes for optimizing computer programs Biological evolutionary mechanisms	(Koza, 1994) (Storn and Price, 1997)
	Evolutionary Programming	EP	Evolutionary simulation of finite automata behavior	(?)
	Evolution Strategy	ES	Adaptive strategies for continuous optimization problems	(Beyer and Schwefel, 2002)
	Queen-bee Evolution	QE	Reproductive behavior of queen bees	(Jung, 2003)
	Biogeography-Based Optimization	BBO	Mathematics of biogeography	(Simon, 2008)
	Quantum-inspired Evolutionary Algorithm Liver Cancer Algorithm	QEA LCA	Quantum physics Behavior of liver tumors	(Talbi and Draa, 2017) (Houssein et al., 2023)
	-			
ture- pired	Particle Swarm Optimization Ant Colony Optimization	PSO ACO	Predation strategies of birds Foraging behavior of ants	(Kennedy and Eberhart, 1995) (Dorigo et al., 1996)
pireu	Artificial Bee Colony	ABC	Foraging strategies of bees	(Karaboga, 2010)
	Pigeon-Inspired Optimization	PIO	Homing behavior of pigeons	(Duan and Qiao, 2014)
	Grey Wolf Optimizer	GWO	Leadership hierarchy and foraging strategy	(Mirjalili et al., 2014)
	Moth-Flame Optimization	MFO	Spiral convergence of moths toward artificial lights	(Mirjalili, 2015)
	Whale Optimization Algorithm	WOA	Social behavior of humpback whales	(Mirjalili and Lewis, 2016)
	Beetle Antennae Search Moth Search Algorithm	BAS MSA	Detecting and searching behaviors of beetles Phototaxis and Lévy flights of moths	(Jiang and Li, 2017) (Wang, 2018)
	Butterfly Optimization Algorithm	BOA	Food search and mating behaviors of butterflies	(Arora and Singh, 2019)
	Harris Hawks Optimization	HHO	Harris' hawks collaborative attack behavior	(Heidari et al., 2019)
	Slime Mould Algorithm	SMA	Oscillation mode of slime mould	(Li et al., 2020)
	Sparrow Search Algorithm	SSA	Anti-predation and foraging behaviors of sparrows	(Xue and Shen, 2020)
	Chimp Optimization Algorithm	ChOA MRFO	Social hierarchy and hunting behavior of chimps	(Khishe and Mosavi, 2020) (Zhao et al., 2020)
	Manta Ray Foraging Optimization Aquila Optimizer	AO	Foraging behaviors of manta rays Hunting behavior of Aquila	(Abualigah et al., 2021c)
	African Vultures Optimization Algorithm	AVOA	Foraging and navigation behaviors of African vultures	(Abdollahzadeh et al., 2021)
	Red Fox Optimization	RFO	Hunting and social cooperation of red foxes	(Połap and Woźniak, 2021)
	Colony Predation Algorithm	CPA	Group hunting strategy	(Tu et al., 2021)
	Chameleon Swarm Algorithm	CSA	Hunting behavior and survival strategies of chameleons	(Braik, 2021)
	Remora Optimization Algorithm	ROA	Symbiotic relationship of remora with host species	(Jia et al., 2021)
	Hunger Games Search Golden Jackal Optimization	HGS GJO	Hunger-driven activities and behavioral choice of animals Collaborative hunting behavior of golden jackals	(Yang et al., 2021) (Chopra and Ansari, 2022)
	Snake Optimizer	SO	Mating mechanism of snakes	(Hashim and Hussien, 2022)
	Bottlenose Dolphin Optimizer	BDO	Echolocation and cooperative hunting of dolphins	(Srivastava and Das, 2022)
	Honey Badger Algorithm	HBA	Foraging behavior of honey badger	(Hashim et al., 2022)
	Artificial Rabbits Optimization	ARO	Survival behavior of rabbits	(Wang et al., 2022)
	Reptile Search Algorithm	RSA	Adaptive hunting and temperature regulation of reptiles	(Abualigah et al., 2022)
	Dandelion Optimizer	DO AHA	Long-distance flight of dandelion Energy-efficient hovering and searching behaviors	(Zhao et al., 2022a) (Zhao et al., 2022b)
	Artificial Hummingbird Algorithm Egret Swarm Optimization Algorithm	ESOA	Hunting behavior of egrets	(Zhao et al., 2022b) (Chen et al., 2022)
	Beluga Whale Optimization	BWO	Swimming, preying, and whale fall behaviors of beluga whales	(Zhong et al., 2022)
	White Shark Optimizer	WSO	Foraging and hunting behaviors of white sharks	(Braik et al., 2022)
	Dwarf Mongoose Optimization	DMO	Foraging behavior of dwarf mongooses	(Agushaka et al., 2022)
	Prairie Dog Optimization	PDO	Prairie dog behavior in natural habitat	(Ezugwu et al., 2022)
	Philippine Eagle Optimization Algorithm	PEOA FOX	Territorial hunting behavior of Philippine eagles	(Enriquez et al., 2022)
	FOX optimizer Crayfish Optimization Algorithm	CfOA	Foraging and hunting behaviors of foxes Summering, competition and foraging behaviors of crayfish	(Mohammed and Rashid, 2023) (Jia et al., 2023)
	Dung Beetle Optimizer	DBO	Food-search and orientation mechanisms of dung beetles	(Xue and Shen, 2023)
	Coati Optimization Algorithm	COA	Hunting and escape behaviors of coatis	(Dehghani et al., 2023)
	Gazalle Optimization Algorithm	GOA	Evasion behavior from predators	(Agushaka et al., 2023)
	Sea-Horse Optimizer	SHO	Courtship and foraging behavior of sea horses	(Zhao et al., 2023a)
	Nutcracker Optimization Algorithm	NOA	Food caching and seed dispersal behavior of nutcrackers	(Abdel-Basset et al., 2023d)
	Fire Hawk Optimizer Sand Cat Swarm Optimization	FHO SCSO	Foraging behavior of whistling kites, black kites and brown falcons Foraging and attacking behaviors of sand cats	(Azizi et al., 2023b) (Seyyedabbasi and Kiani, 2023)
	Electric Eel Foraging Optimization	EEFO	Electric sensing and foraging behavior of electric eels	(Zhao et al., 2024)
	Greylag Goose Optimization	GGO	Social behavior and dynamic activity of Greylag geese	(El-Kenawy et al., 2024)
	Pied Kingfisher Optimizer	PKO	Hunting behavior and symbiotic relationships of pied kingfishers	(Bouaouda et al., 2024)
	Puma Optimizer	PO	Intelligence and life of Pumas	(Abdollahzadeh et al., 2024)
	GOOSE algorithm	GOOSE	Swarming and foraging behaviors of geese	(Hamad and Rashid, 2024)
	Bitterling Fish Optimization	BFO BKA	Mating behavior of Bitterling Fish Hunting skills and migration habits of black-winged kites	(Zarcian et al., 2024)
	Black-winged Kite Algorithm FLood Algorithm	FLA	Intricate flow patterns in river flooding	(Wang et al., 2024) (Ghasemi et al., 2024)
	Hippopotamus Optimization	НО	Behavioral patterns of hippopotamuses	(Amiri et al., 2024)
	Multi-stategy Snow Ablation Optimizer	MSAO	Multi-phase snow ablation processes	(Xiao et al., 2024)
ysics-	Simulated Annealing	SA	Principle of solid annealing	(Kirkpatrick et al., 1983)
pired	Integrated Radiation Optimizer	IRO	Radiation distribution and optimization processes	(Chuang and Jiang, 2007)
•	Gravitational Search Algorithm	GSA	Law of gravity	(Rashedi et al., 2009)
	Charged System Search	CCS	Interaction of charged particles in an electric field	(Kaveh and Talatahari, 2010)
	Galaxy-Based Search Algorithm	GBSA	Gravitational interaction between galaxies	(Shah-Hosseini, 2011)
	Black Hole Optimization	BHO CBO	Gravitational pull and event horizon of black holes Collision dynamics of rigid bodies	(Hatamlou, 2013)
	Colliding Roding Ontimization		Comsion dynamics of rigid bodies	(Kaveh and Mahdavi, 2014)
	Colliding Bodies Optimization Kinetic Gas Molecules Optimization			(Moein and Logeswaran 2014)
	Colliding Bodies Optimization Kinetic Gas Molecules Optimization Ions Motion Optimization	KGMO IMO	Kinetic theory of gas molecules	(Moein and Logeswaran, 2014) (Javidy et al., 2015)
	Kinetic Gas Molecules Optimization Ions Motion Optimization Multi-Verse Optimizer	KGMO IMO MVO	Kinetic theory of gas molecules Motion of charged ions in a magnetic field Theory of multi-verse in physics	(Javidy et al., 2015) (Mirjalili et al., 2016)
	Kinetic Gas Molecules Optimization Ions Motion Optimization Multi-Verse Optimizer Thermal Exchange Optimization	KGMO IMO MVO TEO	Kinetic theory of gas molecules Motion of charged ions in a magnetic field Theory of multi-verse in physics Newton's law of cooling	(Javidy et al., 2015) (Mirjalili et al., 2016) (Kaveh and Dadras, 2017)
	Kinetic Gas Molecules Optimization lons Motion Optimization Multi-Verse Optimizer Thermal Exchange Optimization Henry Gas Solubility Optimization	KGMO IMO MVO TEO HGSO	Kinetic theory of gas molecules Motion of charged ions in a magnetic field Theory of multi-verse in physics Newton's law of cooling Henry's law of gas solubility	(Javidy et al., 2015) (Mirjailli et al., 2016) (Kaveh and Dadras, 2017) (Hashim et al., 2019)
	Kinetic Gas Molecules Optimization Ions Motion Optimization Multi-Verse Optimizer Thermal Exchange Optimization Henry Gas Solubility Optimization Nuclear Reaction Optimization	KGMO IMO MVO TEO HGSO NRO	Kinetic theory of gas molecules Motion of charged ions in a magnetic field Theory of multi-verse in physics Newton's law of cooling Henry's law of gas solubility Chain reactions in nuclear fission	(Javidy et al., 2015) (Mirjalili et al., 2016) (Kaveh and Dadras, 2017) (Hashim et al., 2019) (Wei et al., 2019)
	Kinetic Gas Molecules Optimization lons Motion Optimization Multi-Verse Optimizer Thermal Exchange Optimization Henry Gas Solubility Optimization Nuclear Reaction Optimization Atom Search Optimization	KGMO IMO MVO TEO HGSO NRO ASO	Kinetic theory of gas molecules Motion of charged ions in a magnetic field Theory of multi-verse in physics Newton's law of cooling Henry's law of gas solubility Chain reactions in nuclear fission Basic molecular dynamics	(Javidy et al., 2015) (Mirjalili et al., 2016) (Kaveh and Dadras, 2017) (Hashim et al., 2019) (Wei et al., 2019) (Zhao et al., 2019)
	Kinetic Gas Molecules Optimization Ions Motion Optimization Multi-Verse Optimizer Thermal Exchange Optimization Henry Gas Solubility Optimization Nuclear Reaction Optimization Atom Search Optimization Archimedes Optimization Algorithm	KGMO IMO MVO TEO HGSO NRO ASO AOA	Kinetic theory of gas molecules Motion of charged ions in a magnetic field Theory of multi-verse in physics Newton's law of cooling Henry's law of gas solubility Chain reactions in nuclear fission Basic molecular dynamics Buoyancy and principles of Archimedes	(Javidy et al., 2015) (Mirjalili et al., 2016) (Kaveh and Dadras, 2017) (Hashim et al., 2019) (Wei et al., 2019)
	Kinetic Gas Molecules Optimization lons Motion Optimization Multi-Verse Optimizer Thermal Exchange Optimization Henry Gas Solubility Optimization Nuclear Reaction Optimization Atom Search Optimization Archimedes Optimization Archimedes Optimization Algorithm Smell Agent Optimization Special Relativity Search	KGMO IMO MVO TEO HGSO NRO ASO AOA SAO SRS	Kinetic theory of gas molecules Motion of charged ions in a magnetic field Theory of multi-verse in physics Newton's law of cooling Henry's law of gas solubility Chain reactions in nuclear fission Basic molecular dynamics Buoyancy and principles of Archimedes Interaction between a smell agent, smell molecules, and a smell source Principles of Einstein's special relativity	(Javidy et al., 2015) (Mirjalili et al., 2016) (Kaveh and Dadras, 2017) (Hashim et al., 2019) (Wei et al., 2019) (Zhao et al., 2019) (Hashim et al., 2021) (Salawudeen et al., 2021) (Goodarzimehr et al., 2022)
	Kinetic Gas Molecules Optimization Ions Motion Optimization Multi-Verse Optimizer Thermal Exchange Optimization Henry Gas Solubility Optimization Nuclear Reaction Optimization Atom Search Optimization Archimedes Optimization Algorithm Smell Agent Optimization Algorithm Smell Agent Optimization Special Relativity Search RIME optimization algorithm	KGMO IMO MVO TEO HGSO NRO ASO AOA SAO SRS RIME	Kinetic theory of gas molecules Motion of charged ions in a magnetic field Theory of multi-verse in physics Newton's law of cooling Henry's law of gas solubility Chain reactions in nuclear fission Basic molecular dynamics Buoyaney and principles of Archimedes Interaction between a smell agent, smell molecules, and a smell source Principles of Einstein's special relativity Physical phenomenon of rime-ice	(Javidy et al., 2015) (Mirjalili et al., 2016) (Kaveh and Dadras, 2017) (Hashim et al., 2019) (Wei et al., 2019) (Zhao et al., 2019) (Hashim et al., 2021) (Salawudeen et al., 2021) (Goodarzimehr et al., 2022) (Su et al., 2023)
	Kinetic Gas Molecules Optimization lons Motion Optimization Multi-Verse Optimizer Thermal Exchange Optimization Henry Gas Solubility Optimization Nuclear Reaction Optimization Atom Search Optimization Ardom Search Optimization Archimedes Optimization Algorithm Smell Agent Optimization Special Relativity Search RIME optimization algorithm Energy Valley Optimizer	KGMO IMO MVO TEO HGSO NRO ASO AOA SAO SRS RIME EVO	Kinetic theory of gas molecules Motion of charged ions in a magnetic field Theory of multi-verse in physics Newton's law of cooling Henry's law of gas solubility Chain reactions in nuclear fission Basic molecular dynamics Buoyancy and principles of Archimedes Interaction between a smell agent, smell molecules, and a smell source Principles of Einstein's special relativity Physical phenomenon of rime-ice Energy potential valleys in physical systems	(Javidy et al., 2015) (Mirjalili et al., 2016) (Kaveh and Dadras, 2017) (Hashim et al., 2019) (Wei et al., 2019) (Zhao et al., 2019) (Hashim et al., 2021) (Salawudeen et al., 2021) (Goodarzimehr et al., 2022) (Su et al., 2023) (Azizi et al., 2023a)
	Kinetic Gas Molecules Optimization lons Motion Optimization Multi-Verse Optimizer Thermal Exchange Optimization Henry Gas Solubility Optimization Nuclear Reaction Optimization Atom Search Optimization Atom Search Optimization Archimedes Optimization Algorithm Smell Agent Optimization Special Relativity Search RIME optimization algorithm Energy Valley Optimizer Kepler Optimization Algorithm	KGMO IMO MVO TEO HGSO NRO ASO AOA SAO SRS RIME EVO KOA	Kinetic theory of gas molecules Motion of charged ions in a magnetic field Theory of multi-verse in physics Newton's law of cooling Henry's law of gas solubility Chain reactions in nuclear fission Basic molecular dynamics Buoyaney and principles of Archimedes Interaction between a smell agent, smell molecules, and a smell source Principles of Einstein's special relativity Physical phenomenon of rime-ice Energy potential valleys in physical systems Kepler's laws of planetary motion	(Javidy et al., 2015) (Mirjallii et al., 2016) (Kavch and Dadras, 2017) (Hashim et al., 2019) (Wei et al., 2019) (Zhao et al., 2019) (Hashim et al., 2021) (Salawudeen et al., 2021) (Goodarzimehr et al., 2022) (Su et al., 2023) (Azizi et al., 2023) (Abdel-Basset et al., 2023c)
	Kinetic Gas Molecules Optimization lons Motion Optimization Multi-Verse Optimizer Thermal Exchange Optimization Henry Gas Solubility Optimization Nuclear Reaction Optimization Atom Search Optimization Atom Search Optimization Archimedes Optimization Algorithm Smell Agent Optimization Special Relativity Search RIME optimization algorithm Energy Valley Optimizer Kepler Optimization Algorithm Young Double-Slit Experiment optimizer	KGMO IMO MVO TEO HGSO NRO ASO AOA SAO SRS RIME EVO	Kinetic theory of gas molecules Motion of charged ions in a magnetic field Theory of multi-verse in physics Newton's law of cooling Henry's law of gas solubility Chain reactions in nuclear fission Basic molecular dynamics Buoyancy and principles of Archimedes Interaction between a smell agent, smell molecules, and a smell source Principles of Einstein's special relativity Physical phenomenon of rime-ice Energy potential valleys in physical systems	(Javidy et al., 2015) (Mirjalili et al., 2016) (Kaveh and Dadras, 2017) (Hashim et al., 2019) (Wei et al., 2019) (Zhao et al., 2019) (Hashim et al., 2021) (Salawudeen et al., 2021) (Goodarzimehr et al., 2022) (Su et al., 2023) (Azizi et al., 2023a) (Abdel-Basset et al., 2023c) (Abdel-Basset et al., 2023b)
	Kinetic Gas Molecules Optimization lons Motion Optimization Multi-Verse Optimizer Thermal Exchange Optimization Henry Gas Solubility Optimization Nuclear Reaction Optimization Nuclear Reaction Optimization Ardom Search Optimization Ardom Search Optimization Ardom Search Optimization Ardom Search Optimization Special Relativity Search RIME optimization algorithm Energy Valley Optimizer Kepler Optimization Algorithm Young Double-Slit Experiment optimizer FATA morgana algorithm	KGMO IMO MVO TEO HGSO NRO ASO AOA SAO SRS RIME EVO KOA YDSE FATA	Kinetic theory of gas molecules Motion of charged ions in a magnetic field Theory of multi-verse in physics Newton's law of cooling Henry's law of gas solubility Chain reactions in nuclear fission Basic molecular dynamics Buoyaney and principles of Archimedes Interaction between a smell agent, smell molecules, and a smell source Principles of Einstein's special relativity Physical phenomenon of rime-ice Energy potential valleys in physical systems Kepler's laws of planetary motion Wave-particle duality and interference in quantum physics Mirage light filtering and refraction-reflection balance	(Javidy et al., 2015) (Mirjalili et al., 2016) (Kaveh and Dadras, 2017) (Hashim et al., 2019) (Wei et al., 2019) (Zhao et al., 2019) (Hashim et al., 2021) (Salawudeen et al., 2021) (Goodarzimehr et al., 2022) (Su et al., 2023) (Azizi et al., 2023) (Azizi et al., 2023) (Abdel-Basset et al., 2023b) (Qi et al., 2024)
	Kinetic Gas Molecules Optimization lons Motion Optimization Multi-Verse Optimizer Thermal Exchange Optimization Henry Gas Solubility Optimization Nuclear Reaction Optimization Atom Search Optimization Archimedes Optimization Archimedes Optimization Algorithm Smell Agent Optimization Algorithm Special Relativity Search RIME optimization algorithm Energy Valley Optimizer Kepler Optimization Algorithm Young Double-Slit Experiment optimizer FATA morgana algorithm Harmony Search	KGMO IMO MVO TEO HGSO NRO ASO AOA SAO SRS RIME EVO KOA YDSE FATA	Kinetic theory of gas molecules Motion of charged ions in a magnetic field Theory of multi-verse in physics Newton's law of cooling Henry's law of gas solubility Chain reactions in nuclear fission Basic molecular dynamics Buoyancy and principles of Archimedes Interaction between a smell agent, smell molecules, and a smell source Principles of Einstein's special relativity Physical phenomenon of rime-ice Energy potential valleys in physical systems Kepler's laws of planetary motion Wave-particle duality and interference in quantum physics Mirage light filtering and refraction-reflection balance Improvisation of musicians	(Javidy et al., 2015) (Mirjalili et al., 2016) (Kaveh and Dadras, 2017) (Hashim et al., 2019) (Wei et al., 2019) (Zhao et al., 2019) (Hashim et al., 2021) (Salawudeen et al., 2021) (Goodarzimehr et al., 2022) (Su et al., 2023) (Azizi et al., 2023a) (Abdel-Basset et al., 2023c) (Abdel-Basset et al., 2023b) (Qi et al., 2024) (Geem et al., 2024)
	Kinetic Gas Molecules Optimization lons Motion Optimization Multi-Verse Optimizer Thermal Exchange Optimization Henry Gas Solubility Optimization Nuclear Reaction Optimization Nuclear Reaction Optimization Atom Search Optimization Arbimedes Optimization Algorithm Smell Agent Optimization Special Relativity Search RIME optimization algorithm Energy Valley Optimizer Kepler Optimization Algorithm Young Double-Slit Experiment optimizer FATA morgana algorithm Harmony Search Imperialist Competitive Algorithm	KGMO IMO MVO TEO HGSO NRO ASO AOA SAO SRS RIME EVO KOA YDSE FATA	Kinetic theory of gas molecules Motion of charged ions in a magnetic field Theory of multi-verse in physics Newton's law of cooling Henry's law of gas solubility Chain reactions in nuclear fission Basic molecular dynamics Buoyaney and principles of Archimedes Interaction between a smell agent, smell molecules, and a smell source Principles of Einstein's special relativity Physical phenomenon of rime-ice Energy potential valleys in physical systems Kepler's laws of planetary motion Wave-particle duality and interference in quantum physics Mirage light filtering and refraction-reflection balance Improvisation of musicians Competition between empires for dominance	(Javidy et al., 2015) (Mirjalili et al., 2016) (Kaveh and Dadras, 2017) (Hashim et al., 2019) (Wei et al., 2019) (Zhao et al., 2019) (Hashim et al., 2021) (Salawudeen et al., 2021) (Goodarzimehr et al., 2022) (Su et al., 2023) (Azizi et al., 2023) (Azizi et al., 2023) (Abdel-Basset et al., 2023c) (Abdel-Basset et al., 2023b) (Qi et al., 2024) (Geem et al., 2001)
	Kinetic Gas Molecules Optimization lons Motion Optimization Multi-Verse Optimizer Thermal Exchange Optimization Henry Gas Solubility Optimization Nuclear Reaction Optimization Nuclear Reaction Optimization Atom Search Optimization Archimedes Optimization Algorithm Smell Agent Optimization Algorithm Special Relativity Search RIME optimization algorithm Energy Valley Optimizer Kepler Optimization Algorithm Young Double-Slit Experiment optimizer FATA morgana algorithm Harmony Search Imperialist Competitive Algorithm League Championship Algorithm League Championship Algorithm	KGMO IMO MVO TEO HGSO NRO ASO AOA SAO SRS RIME EVO KOA YDSE FATA HS	Kinetic theory of gas molecules Motion of charged ions in a magnetic field Theory of multi-verse in physics Newton's law of cooling Henry's law of gas solubility Chain reactions in nuclear fission Basic molecular dynamics Buoyancy and principles of Archimedes Interaction between a smell agent, smell molecules, and a smell source Principles of Einstein's special relativity Physical phenomenon of rime-ice Energy potential valleys in physical systems Kepler's laws of planetary motion Wave-particle duality and interference in quantum physics Mirage light filtering and refraction-reflection balance Improvisation of musicians	(Javidy et al., 2015) (Mirjalili et al., 2016) (Kaveh and Dadras, 2017) (Hashim et al., 2019) (Wei et al., 2019) (Zhao et al., 2019) (Hashim et al., 2021) (Salawudeen et al., 2021) (Goodarzimehr et al., 2022) (Su et al., 2023) (Azizi et al., 2023a) (Abdel-Basset et al., 2023c) (Abdel-Basset et al., 2023b) (Qi et al., 2024) (Geem et al., 2024)
	Kinetic Gas Molecules Optimization lons Motion Optimization Multi-Verse Optimizer Thermal Exchange Optimization Henry Gas Solubility Optimization Nuclear Reaction Optimization Nuclear Reaction Optimization Ardon Search Optimization Ardon Search Optimization Ardon Search Optimization Special Relativity Search RIME optimization algorithm Energy Valley Optimizer Kepler Optimization algorithm Young Double-Slit Experiment optimizer FATA morgana algorithm Harmony Search Imperials Competitive Algorithm League Championship Algorithm Teaching Learning-Based Optimization Soccer League Competition Algorithm	KGMO IMO MVO TEO HGSO NRO ASO AOA SAO SRS RIME EVO KOA YDSE FATA HS ICA LCA TLBO	Kinetic theory of gas molecules Motion of charged ions in a magnetic field Theory of multi-verse in physics Newton's law of cooling Henry's law of gas solubility Chain reactions in nuclear fission Basic molecular dynamics Buoyancy and principles of Archimedes Interaction between a smell agent, smell molecules, and a smell source Principles of Einstein's special relativity Physical phenomenon of rime-ice Energy potential valleys in physical systems Kepler's laws of planetary motion Wave-particle duality and interference in quantum physics Mirage light filtering and refraction-reflection balance Improvisation of musicians Competition between empires for dominance Competition among teams in a league Teachers' influence on learners Competition in soccer leagues	(Javidy et al., 2015) (Mirjalili et al., 2016) (Kaveh and Dadras, 2017) (Hashim et al., 2019) (Wei et al., 2019) (Zhao et al., 2019) (Hashim et al., 2019) (Hashim et al., 2021) (Gaodarzimehr et al., 2021) (Goodarzimehr et al., 2022) (Su et al., 2023) (Azizi et al., 2023) (Azizi et al., 2023) (Abdel-Basset et al., 2023b) (Qi et al., 2024) (Geem et al., 2001) (Atashpaz-Gargari and Lucas, 2007) (Kashan, 2009) (Rao et al., 2011) (Moosavian and Roodsari, 2014)
	Kinetic Gas Molecules Optimization lons Motion Optimization Multi-Verse Optimizer Thermal Exchange Optimization Henry Gas Solubility Optimization Nuclear Reaction Optimization Atom Search Optimization Archimedes Optimization Algorithm Smell Agent Optimization Algorithm Special Relativity Search RIME optimization algorithm Energy Valley Optimizer Kepler Optimization Algorithm Young Double-Slit Experiment optimizer FATA morgana algorithm Harmony Search Imperialist Competitive Algorithm League Championship Algorithm Teaching Learning-Based Optimization Soccer League Competition Algorithm Tug of War Optimization Tug of War Optimization	KGMO IMO TEO HGSO NRO ASO AOA SAO SRS RIME EVO KOA YDSE FATA HS ICA TLBO SLCA TWO	Kinetic theory of gas molecules Motion of charged ions in a magnetic field Theory of multi-verse in physics Newton's law of cooling Henry's law of gas solubility Chain reactions in nuclear fission Basic molecular dynamics Buoyancy and principles of Archimedes Interaction between a smell agent, smell molecules, and a smell source Principles of Einstein's special relativity Physical phenomenon of rime-ice Energy potential valleys in physical systems Kepler's laws of planetary motion Wave-particle duality and interference in quantum physics Mirage light filtering and refraction-reflection balance Improvisation of musicians Competition among teams in a league Teachers' influence on learners Competition in soccer leagues Tug-of-war contest between opposing forces	(Javidy et al., 2015) (Mirjallii et al., 2016) (Kaveh and Dadras, 2017) (Hashim et al., 2019) (Wei et al., 2019) (Zhao et al., 2019) (Hashim et al., 2021) (Salawudeen et al., 2021) (Salawudeen et al., 2021) (Su et al., 2023) (Azizi et al., 2023a) (Azizi et al., 2023a) (Abdel-Basset et al., 2023b) (Gi et al., 2024) (Geem et al., 2024) (Geem et al., 2021) (Kashan, 2009) (Rao et al., 2011) (Moosavian and Roodsari, 2014) (Kaveh and Zolghadr, 2016)
	Kinetic Gas Molecules Optimization lons Motion Optimization Multi-Verse Optimizer Thermal Exchange Optimization Henry Gas Solubility Optimization Nuclear Reaction Optimization Nuclear Reaction Optimization Ardom Search Optimization Ardom Search Optimization Ardom Search Optimization Special Relativity Search RIME optimization algorithm Search Relativity Search RIME optimization algorithm Energy Valley Optimizer Kepler Optimization Algorithm Young Double-Slit Experiment optimizer FATA morgana algorithm Harmony Search Imperialist Competitive Algorithm League Championship Algorithm Teaching Learning-Based Optimization Soccer League Competition Algorithm Tug of War Optimization Collective Decision Optimization Algorithm	KGMO IMO MVO TEO HGSO NRO ASO ASO SAO SRS RIME EVO KOA YDSE FATA HS ICA LCA TUBO SLCA TWO CDDOA	Kinetic theory of gas molecules Motion of charged ions in a magnetic field Theory of multi-verse in physics Newton's law of cooling Henry's law of gas solubility Chain reactions in nuclear fission Basic molecular dynamics Buoyancy and principles of Archimedes Interaction between a smell agent, smell molecules, and a smell source Principles of Einstein's special relativity Physical phenomenon of rime-ice Energy potential valleys in physical systems Kepler's laws of planetary motion Wave-particle duality and interference in quantum physics Mirage light filtering and refraction-reflection balance Improvisation of musicians Competition between empires for dominance Competition among teams in a league Teacher's influence on learners Competition in soccer leagues Tug-of-war contest between opposing forces Consensus of human decision-making	(Javidy et al., 2015) (Mirjalili et al., 2016) (Kaveh and Dadras, 2017) (Hashim et al., 2019) (Wei et al., 2019) (Zhao et al., 2019) (Hashim et al., 2021) (Salawudeen et al., 2021) (Goodarzimehr et al., 2022) (Su et al., 2023) (Azizi et al., 2023) (Azizi et al., 2023) (Abdiel-Basset et al., 2023b) (Qi et al., 2024) (Geem et al., 2024) (Geem et al., 2001) (Kashan, 2009) (Kashan, 2009) (Rao et al., 2011) (Moosavian and Roodsari, 2014) (Kaveh and Zolghadr, 2016) (Zhang et al., 2017)
	Kinetic Gas Molecules Optimization lons Motion Optimization Multi-Verse Optimizer Thermal Exchange Optimization Henry Gas Solubility Optimization Nuclear Reaction Optimization Nuclear Reaction Optimization Ardom Search Optimization Ardom Search Optimization Archimedes Optimization Algorithm Smell Agent Optimization Algorithm Special Relativity Search RIME optimization algorithm Energy Valley Optimizer Kepler Optimization Algorithm Young Double-Slit Experiment optimizer FATA morgana algorithm Harmony Search Imperialist Competitive Algorithm League Championship Algorithm Teaching Learning-Based Optimization Soccer League Competition Algorithm Tug of War Optimization Collective Decision Optimization Algorithm Human Mental Search	KGMO IMO MVO TEO HGSO NRO ASO ASO ASO SAO SRS RIME EVO KOA YDSE ICA TLBO SLCA TUBO SLCA TWO CDOA	Kinetic theory of gas molecules Motion of charged ions in a magnetic field Theory of multi-verse in physics Newton's law of cooling Henry's law of gas solubility Chain reactions in nuclear fission Basic molecular dynamics Buoyancy and principles of Archimedes Interaction between a smell agent, smell molecules, and a smell source Principles of Einstein's special relativity Physical phenomenon of rime-ice Energy potential valleys in physical systems Kepler's laws of planetary motion Wave-particle duality and interference in quantum physics Mirage light filtering and refraction-reflection balance Improvisation of musicians Competition among teams in a league Teachers' influence on learners Competition in soccer leagues Tug-of-war contest between opposing forces Consensus of human decision-making Cognitive strategies for mental searching	(Javidy et al., 2015) (Mirjalli et al., 2016) (Kaveh and Dadras, 2017) (Hashim et al., 2019) (Wei et al., 2019) (Zhao et al., 2019) (Zhao et al., 2019) (Hashim et al., 2021) (Salawudeen et al., 2021) (Goodarzimehr et al., 2022) (Su et al., 2023) (Azizi et al., 2023a) (Azizi et al., 2023a) (Abdel-Basset et al., 2023b) (Qi et al., 2024) (Geem et al., 2011) (Atashpaz-Gargari and Lucas, 2007) (Kashan, 2009) (Rao et al., 2011) (Moosavian and Roodsari, 2014) (Kaveh and Zolghadr, 2016) (Zhang et al., 2017) (Mousavirad and Ebrahimpour-Komleh, 2017)
	Kinetic Gas Molecules Optimization lons Motion Optimization Multi-Verse Optimizer Thermal Exchange Optimization Henry Gas Solubility Optimization Nuclear Reaction Optimization Nuclear Reaction Optimization Ardom Search Optimization Ardom Search Optimization Archimedes Optimization Algorithm Smell Agent Optimization Special Relativity Search RIME optimization algorithm Energy Valley Optimizer Kepler Optimization Algorithm Young Double-Slit Experiment optimizer FATA morgana algorithm Harmony Search Imperialist Competitive Algorithm League Championship Algorithm League Championship Algorithm Taching Learning-Based Optimization Soccer League Competition Algorithm Tug of War Optimization Collective Decision Optimization Algorithm Human Mental Search Poor and Rich Optimization Algorithm	KGMO IMO MVO TEO HGSO NRO ASO ASO ASO SAO SRS RIME EVO KOA YDSE FATA HS ICA LCA TUBO SLCA TWO CDOA HMS	Kinetic theory of gas molecules Motion of charged ions in a magnetic field Theory of multi-verse in physics Newton's law of cooling Henry's law of gas solubility Chain reactions in nuclear fission Basic molecular dynamics Buoyancy and principles of Archimedes Interaction between a smell agent, smell molecules, and a smell source Principles of Einstein's special relativity Physical phenomenon of rime-ice Energy potential valleys in physical systems Kepler's laws of planetary motion Wave-particle duality and interference in quantum physics Mirage light filtering and refraction-reflection balance Improvisation of musicians Competition among teams in a league Teachers' influence on learners Competition in soccer leagues Tug-of-war contest between opposing forces Consensus of human decision-making Cognitive strategies for mental searching Weath disparity and economic dynamics	(Javidy et al., 2015) (Mirjalili et al., 2016) (Kaveh and Dadras, 2017) (Hashim et al., 2019) (Wei et al., 2019) (Zhao et al., 2019) (Hashim et al., 2021) (Salawudeen et al., 2021) (Goodarzimehr et al., 2022) (Sue et al., 2023) (Azizi et al., 2023) (Azizi et al., 2023a) (Abdel-Basset et al., 2023c) (Abdel-Basset et al., 2023b) (Qi et al., 2024) (Geem et al., 2024) (Geem et al., 2001) (Atashpaz-Gargari and Lucas, 2007) (Kashan, 2009) (Rao et al., 2011) (Moosavian and Roodsari, 2014) (Kaveh and Zolghadr, 2016) (Zhang et al., 2017) (Mousavirad and Ebrahimpour-Komleh, 2017) (Moosavian da Bardsiri, 2019)
	Kinetic Gas Molecules Optimization lons Motion Optimization Multi-Verse Optimizer Thermal Exchange Optimization Henry Gas Solubility Optimization Nuclear Reaction Optimization Nuclear Reaction Optimization Ardon Search Optimization Ardon Search Optimization Archimedes Optimization Algorithm Special Relativity Search RIME optimization algorithm Energy Valley Optimizer Kepler Optimization algorithm Young Double-Slit Experiment optimizer FATA morgana algorithm Harmony Search Imperialist Competitive Algorithm League Championship Algorithm Teaching Learning-Based Optimization Soccer League Competition Algorithm Tug of War Optimization Collective Decision Optimization Algorithm Human Whental Search Poor and Rich Optimization Algorithm Human Human Urbanization Algorithm	KGMO IMO MVO TEO HGSO NRO ASO ASO ASO SAO SRS RIME EVO KOA YDSE FATA HS ICA TUBO SLCA TUBO SLCA TWO CDOA HMS PROA HUA	Kinetic theory of gas molecules Motion of charged ions in a magnetic field Theory of multi-verse in physics Newton's law of cooling Henry's law of gas solubility Chain reactions in nuclear fission Basic molecular dynamics Buoyancy and principles of Archimedes Interaction between a smell agent, smell molecules, and a smell source Principles of Einstein's special relativity Physical phenomenon of rime-ice Energy potential valleys in physical systems Kepler's laws of planetary motion Wave-particle duality and interference in quantum physics Mirage light filtering and refraction-reflection balance Improvisation of musicians Competition between empires for dominance Competition among teams in a league Teachers' influence on learners Competition in soccer leagues Tug-of-war contest between opposing forces Consensus of human decision-making Cognitive strategies for mental searching Wealth disparity and economic dynamics Urban development and human settlement behaviors	(Javidy et al., 2015) (Mirjalili et al., 2016) (Kaveh and Dadras, 2017) (Hashim et al., 2019) (Wei et al., 2019) (Zhao et al., 2019) (Hashim et al., 2019) (Hashim et al., 2021) (Goodarzimehr et al., 2021) (Goodarzimehr et al., 2022) (Su et al., 2023) (Azizi et al., 2023) (Azizi et al., 2023) (Abdel-Basset et al., 2023b) (Qi et al., 2024) (Geem et al., 2011) (Gasabara, 2024) (Geem et al., 2011) (Mossavian and Roodsari, 2014) (Kaveh and Zolghadr, 2016) (Zhang et al., 2017) (Moosavian da Bardsiri, 2019) (Moosavian da Bardsiri, 2019) (Gosavenian et al., 2020)
	Kinetic Gas Molecules Optimization lons Motion Optimization Multi-Verse Optimizer Thermal Exchange Optimization Henry Gas Solubility Optimization Nuclear Reaction Optimization Archimedes Optimization Archimedes Optimization Archimedes Optimization Algorithm Smell Agent Optimization Special Relativity Search RIME optimization algorithm Energy Valley Optimizer Kepler Optimization Algorithm Young Double-Slit Experiment optimizer FATA morgana algorithm Harmony Search Imperialist Competitive Algorithm Teaching Learning-Based Optimization Soccer League Competition Algorithm Tug of War Optimization Collective Decision Optimization Algorithm Human Mental Search Poor and Rich Optimization Algorithm Human Wental Search Poor and Rich Optimization Algorithm Human Urbanization Algorithm Human Urbanization Algorithm	KGMO IMO MVO TEO HGSO NRO ASO AOA SAO SRS RIME EVO KOA YDSE FATA HS ICA TLBO SLCA TWO CDOA HMS PROA HUA SPBO	Kinetic theory of gas molecules Motion of charged ions in a magnetic field Theory of multi-verse in physics Newton's law of cooling Henry's law of gas solubility Chain reactions in nuclear fission Basic molecular dynamics Buoyancy and principles of Archimedes Interaction between a smell agent, smell molecules, and a smell source Principles of Einstein's special relativity Physical phenomenon of rime-ice Energy potential valleys in physical systems Kepler's laws of planetary motion Wave-particle duality and interference in quantum physics Mirage light filtering and refraction-reflection balance Improvisation of musicians Competition among teams in a league Teachers' influence on learners Competition in soccer leagues Tug-of-war contest between opposing forces Consensus of human decision-making Cognitive strategies for mental searching Wealth disparity and economic dynamics Urban development and human settlement behaviors Learning and psychological adaptation strategies	(Javidy et al., 2015) (Mirjalili et al., 2016) (Kavch and Dadras, 2017) (Hashim et al., 2019) (Wei et al., 2019) (Zhao et al., 2019) (Zhao et al., 2019) (Hashim et al., 2021) (Salawudeen et al., 2021) (Salawudeen et al., 2021) (Goodarzimehr et al., 2022) (Su et al., 2023) (Azizi et al., 2023a) (Abdel-Basset et al., 2023b) (Qi et al., 2024) (Geem et al., 2001) (Atashpaz-Gargari and Lucas, 2007) (Kashan, 2009) (Rao et al., 2011) (Moosavian and Roodsari, 2014) (Kavch and Zolghadr, 2016) (Zhang et al., 2017) (Mousavirad and Ebrahimpour-Komleh, 2017) (Moosavi and Bardsiri, 2019) (Ghasemian et al., 2020) (Das et al., 2000)
	Kinetic Gas Molecules Optimization lons Motion Optimization Multi-Verse Optimizer Thermal Exchange Optimization Henry Gas Solubility Optimization Nuclear Reaction Optimization Nuclear Reaction Optimization Ardon Search Optimization Ardon Search Optimization Archimedes Optimization Algorithm Special Relativity Search RIME optimization algorithm Energy Valley Optimizer Kepler Optimization algorithm Young Double-Slit Experiment optimizer FATA morgana algorithm Harmony Search Imperialist Competitive Algorithm League Championship Algorithm Teaching Learning-Based Optimization Soccer League Competition Algorithm Tug of War Optimization Collective Decision Optimization Algorithm Human Whental Search Poor and Rich Optimization Algorithm Human Human Urbanization Algorithm	KGMO IMO MVO TEO HGSO NRO ASO ASO ASO SAO SRS RIME EVO KOA YDSE FATA HS ICA TUBO SLCA TUBO SLCA TWO CDOA HMS PROA HUA	Kinetic theory of gas molecules Motion of charged ions in a magnetic field Theory of multi-verse in physics Newton's law of cooling Henry's law of gas solubility Chain reactions in nuclear fission Basic molecular dynamics Buoyancy and principles of Archimedes Interaction between a smell agent, smell molecules, and a smell source Principles of Einstein's special relativity Physical phenomenon of rime-ice Energy potential valleys in physical systems Kepler's laws of planetary motion Wave-particle duality and interference in quantum physics Mirage light filtering and refraction-reflection balance Improvisation of musicians Competition between empires for dominance Competition among teams in a league Teachers' influence on learners Competition in soccer leagues Tug-of-war contest between opposing forces Consensus of human decision-making Cognitive strategies for mental searching Wealth disparity and economic dynamics Urban development and human settlement behaviors	(Javidy et al., 2015) (Mirjalili et al., 2016) (Kaveh and Dadras, 2017) (Hashim et al., 2019) (Wei et al., 2019) (Zhao et al., 2019) (Hashim et al., 2019) (Hashim et al., 2021) (Goodarzimehr et al., 2021) (Goodarzimehr et al., 2022) (Su et al., 2023) (Azizi et al., 2023) (Azizi et al., 2023) (Abdel-Basset et al., 2023b) (Qi et al., 2024) (Geem et al., 2011) (Gasabara, 2024) (Geem et al., 2011) (Mossavian and Roodsari, 2014) (Kaveh and Zolghadr, 2016) (Zhang et al., 2017) (Moosavian da Bardsiri, 2019) (Moosavian da Bardsiri, 2019) (Gosavenian et al., 2020)
	Kinetic Gas Molecules Optimization lons Motion Optimization Multi-Verse Optimizer Thermal Exchange Optimization Henry Gas Solubility Optimization Nuclear Reaction Optimization Nuclear Reaction Optimization Ardon Search Optimization Ardon Search Optimization Archimedes Optimization Algorithm Smell Agent Optimization Special Relativity Search RIME optimization algorithm Energy Valley Optimizer Kepler Optimization algorithm Young Double-Slit Experiment optimizer FATA morgana algorithm Harmony Search Imperialist Competitive Algorithm League Championship Algorithm Teaching Learning-Based Optimization Soccer League Competition Algorithm Tug of War Optimization Collective Decision Optimization Algorithm Human Mental Search Poor and Rich Optimization Algorithm Human Urbanization Algorithm Human Urbanization Algorithm Human Urbanization Algorithm Student Psychology Based Optimization Giza Pyramids Construction algorithm	KGMO IMO MYO TEO MYO TEO NRO ASO ASO ASO SAO SAO SAO KOA YDSE FATA HS ICA TLBO SLCA TWO CDOA HMS PROA HUA SPBO GPC	Kinetic theory of gas molecules Motion of charged ions in a magnetic field Theory of multi-verse in physics Newton's law of cooling Henry's law of gas solubility Chain reactions in nuclear fission Basic molecular dynamics Buoyancy and principles of Archimedes Interaction between a smell agent, smell molecules, and a smell source Principles of Einstein's special relativity Physical phenomenon of rime-ice Energy potential valleys in physical systems Kepler's laws of planetary motion Wave-particle duality and interference in quantum physics Mirage light filtering and refraction-reflection balance Improvisation of musicians Competition between empires for dominance Competition among teams in a league Teachers' influence on learners Competition in soccer leagues Tug-of-war contest between opposing forces Consensus of human decision-making Cognitive strategies for mental searching Wealth disparity and economic dynamics Urban development and human settlement behaviors Learning and psychological adaptation strategies Construction of the Giza Pyramids by ancient workers	(Javidy et al., 2015) (Mirjalili et al., 2016) (Kaveh and Dadras, 2017) (Hashim et al., 2019) (Wei et al., 2019) (Zhao et al., 2019) (Hashim et al., 2021) (Salawudeen et al., 2021) (Goodarzimehr et al., 2022) (Su et al., 2023) (Azizi et al., 2023) (Azizi et al., 2023) (Abdel-Basset et al., 2023c) (Abdel-Basset et al., 2023b) (Qi et al., 2024) (Geem et al., 2011) (Kashapa-Cargari and Lucas, 2007) (Kashan, 2009) (Rao et al., 2011) (Moosavian and Roodsari, 2014) (Kaveh and Zolghadr, 2016) (Zhang et al., 2017) (Mousavirad and Ebrahimpour-Komleh, 2017) (Moosavi and Bardsiri, 2019) (Ghasemian et al., 2020) (Das et al., 2020)
	Kinetic Gas Molecules Optimization lons Motion Optimization Multi-Verse Optimizer Thermal Exchange Optimization Henry Gas Solubility Optimization Nuclear Reaction Optimization Nuclear Reaction Optimization Ardom Search Optimization Ardom Search Optimization Archimedes Optimization Algorithm Smell Agent Optimization Algorithm Special Relativity Search RIME optimization algorithm Energy Valley Optimizer Kepler Optimization Algorithm Young Double-Slit Experiment optimizer FATA morgana algorithm Harmony Search Imperialist Competitive Algorithm League Championship Algorithm Teaching Learning-Based Optimization Soccer League Competition Algorithm Tug of War Optimization Collective Decision Optimization Algorithm Human Urbanization Algorithm Student Psychology Based Optimization Giza Pyramids Construction algorithm Sudent Psychology Based Optimization Giza Pyramids Construction algorithm Swing Training-Based Optimization Skill Optimization Algorithm Skill Optimization Algorithm	KGMO IMO MYO TEO HGSO NRO ASO ASO ASO SAS RIME EVO KOA YDSE FATA HS ICA TLBO SLCA TWO CDOA HMS PROA HUA SPBO GGPC STBO SOA	Kinetic theory of gas molecules Motion of charged ions in a magnetic field Theory of multi-verse in physics Newton's law of cooling Henry's law of gas solubility Chain reactions in nuclear fission Basic molecular dynamics Buoyancy and principles of Archimedes Interaction between a smell agent, smell molecules, and a smell source Principles of Einstein's special relativity Physical phenomenon of rime-ice Energy potential valleys in physical systems Kepler's laws of planetary motion Wave-particle duality and interference in quantum physics Mirage light filtering and refraction-reflection balance Improvisation of musicians Competition among teams in a league Teachers' influence on learners Competition in soccer leagues Tug-of-war contest between opposing forces Consensus of human decision-making Cognitive strategies for mental searching Wealth disparity and economic dynamics Urban development and human settlement behaviors Learning and psychological adaptation strategies Construction of the Giza Pyramids by ancient workers Skill learning through repeated practice Acquisition and enhancement of skills Rural fishermen fishing in ponds	(Javidy et al., 2015) (Mayidh et al., 2016) (Kaveh and Dadras, 2017) (Hashim et al., 2019) (Wei et al., 2019) (Zhao et al., 2019) (Hashim et al., 2019) (Hashim et al., 2021) (Salawudeen et al., 2021) (Gaodarzimehr et al., 2021) (Abdel-Basset et al., 2023a) (Azizi et al., 2023a) (Abdel-Basset et al., 2023b) (Gj et al., 2024) (Geem et al., 2011) (Atashpaz-Gargari and Lucas, 2007) (Kashan, 2009) (Rao et al., 2011) (Moosavian and Roodsari, 2014) (Kaveh and Zoighadr, 2016) (Zhang et al., 2017) (Moosavi and Bardsiri, 2019) (Ghasemian et al., 2020) (Das et al., 2020) (Das et al., 2021) (Dehghani et al., 2022) (Givi and Hubalovska, 2023) (Jia et al., 2024)
	Kinetic Gas Molecules Optimization lons Motion Optimization Multi-Verse Optimizer Thermal Exchange Optimization Henry Gas Solubility Optimization Nuclear Reaction Optimization Nuclear Reaction Optimization Atom Search Optimization Archimedes Optimization Algorithm Smell Agent Optimization Special Relativity Search RIME optimization algorithm Energy Valley Optimizer Kepler Optimization Algorithm Young Double-Slit Experiment optimizer FATA morgana algorithm Harmony Search Imperialist Competitive Algorithm League Championship Algorithm League Championship Algorithm Tug of War Optimization Soccer League Competition Algorithm Tug of War Optimization Collective Decision Optimization Algorithm Human Mental Search Poor and Rich Optimization Algorithm Human Urbanization Algorithm Human Urbanization Algorithm Student Psychology Based Optimization Giza Pyramids Construction algorithm Sewing Training-Based Optimization Skill Optimization Algorithm Catch Fish Optimization Algorithm Catch Fish Optimization Algorithm Catch Fish Optimization Algorithm Catch Fish Optimization Algorithm	KGMO IMO MVO TEO HGSO NRO ASO ASO SAO SRS RIME EVO KOA YDSE FATA HS ICA LCA TLBO SLCA TWO CDOA HMS PROA HUA SPBO GPC STBO SOA CFOA	Kinetic theory of gas molecules Motion of charged ions in a magnetic field Theory of multi-verse in physics Newton's law of cooling Henry's law of gas solubility Chain reactions in nuclear fission Basic molecular dynamics Buoyancy and principles of Archimedes Interaction between a smell agent, smell molecules, and a smell source Principles of Einstein's special relativity Physical phenomenon of rime-ice Energy potential valleys in physical systems Kepler's laws of planetary motion Wave-particle duality and interference in quantum physics Mirage light filtering and refraction-reflection balance Improvisation of musicians Competition between empires for dominance Competition among teams in a league Teachers' influence on learners Competition in soccer leagues Tug-of-war contest between opposing forces Consensus of human decision-making Cognitive strategies for mental searching Wealth disparity and economic dynamics Urban development and human settlement behaviors Learning and psychological adaptation strategies Construction of the Giza Pyramids by ancient workers Skill learning through repeated practice Acquisition and enhancement of skills Rural fishermen fishing in ponds Experiences of hikers summitting mountains, hills, or rocks	(Javidy et al., 2015) (Mirjalili et al., 2016) (Kavch and Dadras, 2017) (Hashim et al., 2019) (Wei et al., 2019) (Zhao et al., 2019) (Zhao et al., 2019) (Hashim et al., 2021) (Salawudeen et al., 2021) (Goodarzimehr et al., 2022) (Azizi et al., 2023) (Azizi et al., 2023) (Azizi et al., 2023a) (Abdel-Basset et al., 2023c) (Abdel-Basset et al., 2023b) (Qi et al., 2024) (Geem et al., 2001) (Atashpaz-Gargari and Lucas, 2007) (Kashan, 2009) (Rao et al., 2011) (Moosavian and Roodsari, 2014) (Kavch and Zolghadr, 2016) (Zhang et al., 2017) (Mousavirad and Ebrahimpour-Komleh, 2017) (Moosavian da Bardsiri, 2019) (Ghasemian et al., 2020) (Harifi et al., 2021) (Dehghani et al., 2022) (Givi and Hubalovska, 2023) (Jia et al., 2024)
uman- pired	Kinetic Gas Molecules Optimization lons Motion Optimization Multi-Verse Optimizer Thermal Exchange Optimization Henry Gas Solubility Optimization Nuclear Reaction Optimization Nuclear Reaction Optimization Ardom Search Optimization Ardom Search Optimization Archimedes Optimization Algorithm Smell Agent Optimization Algorithm Special Relativity Search RIME optimization algorithm Energy Valley Optimizer Kepler Optimization Algorithm Young Double-Slit Experiment optimizer FATA morgana algorithm Harmony Search Imperialist Competitive Algorithm League Championship Algorithm Teaching Learning-Based Optimization Soccer League Competition Algorithm Tug of War Optimization Collective Decision Optimization Algorithm Human Urbanization Algorithm Student Psychology Based Optimization Giza Pyramids Construction algorithm Sudent Psychology Based Optimization Giza Pyramids Construction algorithm Swing Training-Based Optimization Skill Optimization Algorithm Skill Optimization Algorithm	KGMO IMO MYO TEO HGSO NRO ASO ASO ASO SAS RIME EVO KOA YDSE FATA HS ICA TLBO SLCA TWO CDOA HMS PROA HUA SPBO GGPC STBO SOA	Kinetic theory of gas molecules Motion of charged ions in a magnetic field Theory of multi-verse in physics Newton's law of cooling Henry's law of gas solubility Chain reactions in nuclear fission Basic molecular dynamics Buoyancy and principles of Archimedes Interaction between a smell agent, smell molecules, and a smell source Principles of Einstein's special relativity Physical phenomenon of rime-ice Energy potential valleys in physical systems Kepler's laws of planetary motion Wave-particle duality and interference in quantum physics Mirage light filtering and refraction-reflection balance Improvisation of musicians Competition among teams in a league Teachers' influence on learners Competition in soccer leagues Tug-of-war contest between opposing forces Consensus of human decision-making Cognitive strategies for mental searching Wealth disparity and economic dynamics Urban development and human settlement behaviors Learning and psychological adaptation strategies Construction of the Giza Pyramids by ancient workers Skill learning through repeated practice Acquisition and enhancement of skills Rural fishermen fishing in ponds	(Javidy et al., 2015) (Mayidh et al., 2016) (Kaveh and Dadras, 2017) (Hashim et al., 2019) (Wei et al., 2019) (Zhao et al., 2019) (Hashim et al., 2019) (Hashim et al., 2021) (Salawudeen et al., 2021) (Gaodarzimehr et al., 2021) (Abdel-Basset et al., 2023a) (Azizi et al., 2023a) (Abdel-Basset et al., 2023b) (Gj et al., 2024) (Geem et al., 2011) (Atashpaz-Gargari and Lucas, 2007) (Kashan, 2009) (Rao et al., 2011) (Moosavian and Roodsari, 2014) (Kaveh and Zoighadr, 2016) (Zhang et al., 2017) (Moosavi and Bardsiri, 2019) (Ghasemian et al., 2020) (Das et al., 2020) (Das et al., 2021) (Dehghani et al., 2022) (Givi and Hubalovska, 2023) (Jia et al., 2024)

Table 1Overview of MHS algorithms (continued).

Classification	Algorithm	Abbrev.	Inspiration	Ref.	Year
Mathematics-	Stochastic Fractal Search	SFS	Fractal concept and its diffusion property	(Salimi, 2015)	2015
inspired	Sine Cosine Algorithm	SCA	Sine and Cosine functions	(Mirjalili, 2016)	2016
	Golden Sine Algorithm	GSA	Golden ratio applied to sinusoidal functions	(Tanyildizi and Demir, 2017)	2017
	RUNge kutta optimizer	RUN	Foundations of the Runge Kutta method	(Ahmadianfar et al., 2021)	2021
	Arithmetic Optimization Algorithm	AOA	Distribution behavior of arithmetic operators	(Abualigah et al., 2021a)	2021
	Circle Search Algorithm	CSA	Geometric properties of circles	(Qais et al., 2022)	2022
	weIghted meaN oF vectOrs	INFO	Concept of the weighted mean of vectors	(Ahmadianfar et al., 2022)	2022
	Tangent Search Algorithm	TSA	Tangent function	(Layeb, 2022)	2022
	Exponential Distribution Optimizer	EDO	Exponential probability distribution model	(Abdel-Basset et al., 2023a)	2023
	Quadratic Interpolation Optimization	QIO	Generalized quadratic interpolation method	(Zhao et al., 2023b)	2023
	Newton-Raphson-Based Optimizer	NRBO	Newton-Raphson method for root-finding	(Sowmya et al., 2024)	2024
	Exponential-Trigonometric Optimization	ETO	Sophisticated combination of exponential and trigonometric functions	(Luan et al., 2024)	2024
Improved	ES with Covariance Matrix Adaptation	CMA-ES	Introduction of covariance matrix adaptation in ES	(Hansen and Ostermeier, 2001)	2001
	Success-History based Adaptive DE	SHADE	Introduction of success-history-based parameter adaptation in DE	(Tanabe and Fukunaga, 2013)	2013
	Improved constrained DE	rank-iMDDE	Introduction of ranking-based mutation operator and improved dynamic diversity mechanism in DE	(Gong et al., 2014)	2014
	SHADE using Linear population size reduction	L-SHADE	Introduction of linear population size reduction in SHADE	(Tanabe and Fukunaga, 2014)	2014
	L-SHADE with Ensemble pool of Sinusoidal parameter adaptation	LSHADE-EpSin	Introduction of ensemble sinusoidal approach in L-SHADE	(Awad et al., 2016)	2016
	LSHADE-EpSin with covariance matrix adaptation and Euclidean neighborhood	LSHADE-cnEpSin	Introduction of covariance matrix learning for crossover operator in LSHADE-EpSin	(Awad et al., 2017)	2017
	LSHADE with Semi-Parameter Adaptation hybrid with CMA-ES	LSHADE-SPACMA	Introduction of semi-parameter adaptation and CMA-ES in LSHADE	(Mohamed et al., 2017)	2017
	Teaching-Learning-based ABC	TLABC	Combination of TLBO and ABC	(Chen et al., 2018)	2018
	Adaptive SCA integrated with PSO	ASCA-PSO	Combination of SCA and PSO	(Issa et al., 2018)	2018
	Adaptive Guided DE	AGDE	Introduction of novel mutation and parameter adaptation schemes in DE	(Mohamed and Mohamed, 2019)	2019
	Chaotic SSA	CSSA	Introduction of chaotic logistic mapping in SSA	(Zhang and Ding, 2021)	2021
	BAS based GWO	BGWO	Combination of BAS and GWO	(Fan et al., 2021)	2021
	SFS with Fitness-Distance Balance	FDB-SFS	Introduction of Fitness-Distance Balance method in SFS	(Aras et al., 2021)	2021
	AGDE with Fitness-Distance Balance	FDB-AGDE	Introduction of Fitness-Distance Balance method in AGDE	(Guvenc et al., 2021)	2021
	Coyote Optimization Algorithm with Lévy Roulette and Fitness-Distance Balance	LRFDB-COA	Introduction of Lévy flight and Fitness-Distance Balance method in Coyote Optimization Algorithm	(Duman et al., 2021)	2021
	Adaptive L-SHADE	AL-SHADE	Introduction of adaptive selection strategy for mutation in L-SHADE	(Li et al., 2022)	2022
	MFRO with Dynamic Fitness-Distance Balance	DFDB-MRFO	Introduction of Dynamic Fitness-Distance Balance method in MFRO	(Kahraman et al., 2022)	2022
	AGDE with Fitness-Distance-Constraint	FDC-AGDE	Introduction of Fitness-Distance-Constraint method in AGDE	(Ozkaya et al., 2023)	2023
	SFS with Natural Survivor Method	NSM-SFS	Introduction of Natural Survivor Method method in SFS	(Kahraman et al., 2023)	2023
	TLABC with Natural Survivor Method	NSM-TLABC	Introduction of Natural Survivor Method method in TLABC	(Kahraman et al., 2023)	2023
	LSHADE-SPACMA with Natural Survivor Method	NSM-LSHADE-SPACMA	Introduction of Natural Survivor Method method in LSHADE-SPACMA	(Kahraman et al., 2023)	2023
	ARO with Adaptive Fitness-Distance Balance	AFDB-ARO	Introduction of Adaptive Fitness-Distance Balance method in ARO	(Ozkaya et al., 2024)	2024
	Adaptive Differential Learning TLBO	ADL-TLBO	Introduction of enhanced search and adaptive mechanisms in TLBO	(Tao et al., 2025)	2025

moths. Butterfly Optimization Algorithm (BOA) (Arora and Singh, 2019) was based on the food searching and mating behaviors of butterflies. Harris Hawks Optimization (HHO) (Heidari et al., 2019) imitated the coordinated hunting techniques of Harris' hawks. Slime Mould Algorithm (SMA) (Li et al., 2020) simulated the oscillation mode exhibited by slime moulds. Sparrow Search Algorithm (SSA) (Xue and Shen, 2020) modeled the foraging and anti-predation strategies of sparrows. Chimp Optimization Algorithm (ChOA) (Khishe and Mosavi, 2020) was inspired by the social structure and hunting strategies of chimpanzees. Manta Ray Foraging Optimization (MRFO) (Zhao et al., 2020) was based on the foraging behavior of manta rays. Aquila Optimizer (AO) (Abualigah et al., 2021c) simulated the hunting tactics of Aquila birds. African Vultures Optimization Algorithm (AVOA) (Abdollahzadeh et al., 2021) mirrored the foraging and navigation behaviors of African vultures. Red Fox Optimization (RFO) (Polap and Woźniak, 2021) was inspired by the hunting and cooperative behaviors of red foxes. Colony Predation Algorithm (CPA) (Tu et al., 2021) emulated the group hunting strategies of animals. Chameleon Swarm Algorithm (CSA) (Braik, 2021) was based on the hunting and survival techniques of chameleons. Remora Optimization Algorithm (ROA) (Jia et al., 2021) modeled the symbiotic relationship between remoras and their host species. Hunger Games Search (HGS) (Yang et al., 2021) was based on the hunger-driven activities and behavioral choices of animals. Golden Jackal Optimization (GJO) (Chopra and Ansari, 2022) simulated the collaborative hunting tactics of golden jackals. Snake Optimizer (SO) (Hashim and Hussien, 2022) was inspired by the mating mechanisms of snakes. Bottlenose Dolphin Optimizer (BDO) (Srivastava and Das, 2022) replicated the echolocation and cooperative hunting behaviors of dolphins. Honey Badger Algorithm (HBA) (Hashim et al., 2022) was based on the foraging behavior of honey badgers.

Artificial Rabbits Optimization (ARO) (Wang et al., 2022) was inspired by the survival strategies of rabbits. Reptile Search Algorithm (RSA) (Abualigah et al., 2022) mimicked the hunting and temperature regulation strategies of reptiles. Dandelion Optimizer (DO) (Zhao et al., 2022a) was based on the long-distance dispersal of dandelion seeds. Artificial Hummingbird Algorithm (AHA) (Zhao et al., 2022b) modeled the energy-efficient hovering and searching behaviors of hummingbirds. Egret Swarm Optimization Algorithm (ESOA) (Chen et al., 2022) was inspired by the hunting techniques of egrets. Beluga Whale Optimization (BWO) (Zhong et al., 2022) simulated the swimming, foraging, and whale fall behaviors of beluga whales. White Shark Optimizer (WSO) (Braik et al., 2022) was based on the foraging and hunting tactics of white sharks. Dwarf Mongoose Optimization (DMO) (Agushaka et al., 2022) modeled the foraging behavior of dwarf mongooses. Prairie Dog Optimization (PDO) (Ezugwu et al., 2022) was inspired by the social behaviors and communication of prairie dogs. Philippine Eagle Optimization Algorithm (PEOA) (Enriquez et al., 2022) replicated the territorial hunting strategies of Philippine eagles. Fox optimizer (FOX) (Mohammed and Rashid, 2023) was based on the foraging and hunting techniques of foxes. Crayfish Optimization Algorithm (CfOA) (Jia et al., 2023) simulated the foraging, competition, and summering behaviors of crayfish. Dung Beetle Optimizer (DBO) (Xue and Shen, 2023) mirrored the food-searching and orientation behaviors of dung beetles. Coati Optimization Algorithm (COA) (Dehghani et al., 2023) was inspired by the hunting and escape behaviors of coatis. Gazelle Optimization Algorithm (GOA) (Agushaka et al., 2023) mimicked the evasion strategies of gazelles. Sea-Horse Optimizer (SHO) (Zhao et al., 2023a) was based on the courtship and foraging behaviors of sea horses. Nutcracker Optimization Algorithm (NOA) (Abdel-Basset et al., 2023d) simulated the food caching and seed dispersal behaviors of nutcrackers. Fire Hawk Optimizer (FHO) (Azizi et al., 2023b) was inspired by the foraging behaviors of whistling kites, black kites, and brown falcons. Sand Cat Swarm Optimization (SCSO) (Seyvedabbasi and Kiani, 2023) mirrored the foraging and hunting tactics of sand cats. Electric Eel Foraging Optimization (EEFO) (Zhao et al., 2024) simulated the electric sensing and foraging techniques of electric eels. Greylag Goose Optimization (GGO) (El-Kenawy et al., 2024) was based on the social dynamics and migratory patterns of Greylag geese. Pied Kingfisher Optimizer (PKO) (Bouaouda et al., 2024) modeled the hunting behaviors and symbiotic relationships of pied kingfishers. Puma Optimizer (PO) (Abdollahzadeh et al., 2024) was inspired by the intelligence and survival techniques of pumas. Goose algorithm (GOOSE) (Hamad and Rashid, 2024) mimicked the swarming and foraging behaviors of geese. Bitterling Fish Optimization (BFO) (Zareian et al., 2024) was based on the mating behavior of bitterling fish. Black-winged Kite Algorithm (BKA) (Wang et al., 2024) was inspired by the hunting skills and migratory behaviors of black-winged kites. Flood Algorithm (FLA) (Ghasemi et al., 2024) modeled the flow patterns during river flooding. Hippopotamus Optimization (HO) (Amiri et al., 2024) was based on the behavioral patterns of hippopotamuses. Multi-strategy Snow Ablation Optimizer (MSAO) (Xiao et al., 2024) simulated the processes of multiphase snow ablation.

Physics-inspired MHS algorithms are inspired by fundamental physical laws and phenomena. One of the first algorithms in this category is Simulated Annealing (SA) (Kirkpatrick et al., 1983), which mimicked the metal annealing process to find optimal solutions. Integrated Radiation Optimizer (IRO) (Chuang and Jiang, 2007) followed radiation distribution and optimization processes, while Gravitational Search Algorithm (GSA) (Rashedi et al., 2009) modeled the law of gravity for solving optimization tasks. Charged System Search (CSS) (Kaveh and Talatahari, 2010) algorithm was inspired by the interaction of charged particles in an electric field. Galaxy-Based Search Algorithm (GBSA) (Shah-Hosseini, 2011) expanded the inspiration to gravitational interactions between galaxies, and Black Hole Optimization (BHO) (Hatamlou, 2013) drew from the gravitational pull and event horizon dynamics of black holes. Colliding Bodies Optimization (CBO) (Kaveh and Mahdavi, 2014) simulated collision dynamics of rigid bodies, while Kinetic Gas Molecules Optimization (KGMO) (Moein and Logeswaran, 2014) was based on the kinetic theory of gas molecules. Ions Motion Optimization (IMO) (Javidy et al., 2015) modeled the motion of charged ions in a magnetic field. Multi-Verse Optimizer (MVO) (Mirjalili et al., 2016) was inspired by the theory of the multi-verse in physics. Thermal Exchange Optimization (TEO) (Kaveh and Dadras, 2017) drew from Newton's law of cooling to simulate thermal energy transfer, and Henry Gas Solubility Optimization (HGSO) (Hashim et al., 2019) followed Henry's law of gas solubility. Nuclear Reaction Optimization (NRO) (Wei et al., 2019) was inspired by chain reactions in nuclear fission, while Atom Search Optimization

(ASO) (Zhao et al., 2019) used basic molecular dynamics to model atomic-level interactions. Archimedes Optimization Algorithm (AOA) (Hashim et al., 2021) simulated buoyancy, based on Archimedes' principle, while Smell Agent Optimization (SAO) (Salawudeen et al., 2021) modeled the interaction between a smell agent, smell molecules, and a smell source. Special Relativity Search (SRS) (Goodarzimehr et al., 2022) algorithm drew from the principles of Einstein's special relativity to guide optimization processes. Rime optimization algorithm (RIME) (Su et al., 2023) was inspired by the physical phenomenon of rime-ice, and Energy Valley Optimizer (EVO) (Azizi et al., 2023a) modeled energy potential valleys in physical systems. Kepler Optimization Algorithm (KOA) (Abdel-Basset et al., 2023c) was based on Kepler's laws of planetary motion, and Young Double-Slit Experiment optimizer (YDSE) (Abdel-Basset et al., 2023b) was inspired by wave-particle duality and interference patterns in quantum physics. Fata morgana algorithm (FATA) (Oi et al., 2024) was inspired by the mirage light filtering and refraction-reflection balance.

Human-inspired MHS algorithms simulate human characteristics such as cooperation, learning, and behaviors within communities. One of the earliest algorithms in this category is Harmony Search (HS) (Geem et al., 2001), inspired by the improvisation process of musicians seeking a perfect harmony. Imperialist Competitive Algorithm (ICA) (Atashpaz-Gargari and Lucas, 2007) followed, modeling the competition between empires for dominance, and League Championship Algorithm (LCA) (Kashan, 2009) was introduced to simulate league-based competition among teams. Teaching-Learning-Based Optimization (TLBO) (Rao et al., 2011) built upon these concepts by simulating the teacherstudent interaction in a classroom setting. Soccer League Competition Algorithm (SLCA) (Moosavian and Roodsari, 2014) simulated the dynamics of soccer leagues to optimize search strategies. Tug of War Optimization (TWO) (Kaveh and Zolghadr, 2016) and Collective Decision Optimization Algorithm (CDOA) (Zhang et al., 2017) introduced competitive and decision-making behaviors observed in human activities. Subsequent developments included Human Mental Search (HMS) (Mousavirad and Ebrahimpour-Komleh, 2017), which emulated human cognitive processes in problem-solving, and Poor and Rich Optimization Algorithm (PROA) (Moosavi and Bardsiri, 2019), inspired by the socio-economic dynamics between rich and poor individuals. Human Urbanization Algorithm (HUA) (Ghasemian et al., 2020) drew on the urbanization process to model optimization, while Student Psychology Based Optimization (SPBO) (Das et al., 2020) used psychological factors influencing student behavior as a basis for optimization. Additionally, Giza Pyramids Construction Algorithm (GPC) (Harifi et al., 2021) was inspired by the construction of the Giza Pyramids by ancient workers, emphasizing human collaboration and skill enhancement in large-scale projects. Sewing Training-Based Optimization (STBO) (Dehghani et al., 2022) and Skill Optimization Algorithm (SOA) (Givi

and Hubalovska, 2023), expanded the scope by incorporating training and skill development processes observed in human societies. Skill Optimization Algorithm (SOA) (Givi and Hubalovska, 2023) focused on skill acquisition and improvement. Catch Fish Optimization Algorithm (CFOA) (Jia et al., 2024) simulated rural fishermen fishing in ponds, reflecting patience and precision. Hiking Optimization Algorithm (HOA) (Oladejo et al., 2024) mirrored the experiences of hikers summiting mountains, hills, or rocks, focusing on perseverance and decision-making. Information Acquisition Optimizer (IAO) (Wu et al., 2024) modeled human behaviors related to information gathering and processing for optimal decision-making. Competition of Tribes and Cooperation of Members algorithm (CTCM) (Chen et al., 2025) reflected the competition and cooperation among ancient tribes, showcasing the balance between conflict and collaboration. Dream Optimization Algorithm (DOA) (Lang and Gao, 2025) was inspired by human consciousness and traits in dreams, simulating unconscious thought processes and their potential role in optimization.

Mathematics-inspired MHS algorithms are inspired by mathematical functions, formulas, and theories, capturing their inherent properties to guide the optimization process. Early contributions include Stochastic Fractal Search (SFS) (Salimi, 2015) algorithm, utilized the fractal concept in mathematics and its diffusion property for more efficient search space exploration. Next, Sine Cosine Algorithm (SCA) (Mirjalili, 2016) was designed, utilizing trigonometric functions to generate diverse solutions for exploration and exploitation. Golden Sine Algorithm (GSA) (Tanyildizi and Demir, 2017) employed the golden ratio properties combined with trigonometric functions for optimization, showcasing the effectiveness of mathematical constants in enhancing search strategies. Runge Kutta optimizer (RUN) (Ahmadianfar et al., 2021) applied numerical integration techniques inspired by the Runge-Kutta method to navigate the solution space. Arithmetic Optimization Algorithm (AOA) (Abualigah et al., 2021a) emerged by utilizing the distribution behavior of arithmetic operators, striking a balance between exploration and exploitation in optimization problems. Circle Search Algorithm (CSA) (Qais et al., 2022) modeled the geometric properties of circles to refine the search paths, while weighted mean of vectors algorithm (INFO) (Ahmadianfar et al., 2022) applied the concept of weighted means of vectors to guide the optimization process. More recently, Tangent Search Algorithm (TSA) (Layeb, 2022) took inspiration from the tangent function to efficiently explore and refine solutions, while Exponential Distribution Optimizer (EDO) (Abdel-Basset et al., 2023a) leveraged exponential distribution to enhance convergence rates. Quadratic Interpolation Optimization (QIO) (Zhao et al., 2023b) utilized quadratic interpolation methods to optimize the search direction further. Newton-Raphson-Based Optimizer (NRBO) (Sowmya et al., 2024) applied the Newton-Raphson method for refining solutions, while Exponential-Trigonometric Optimization (ETO) (Luan et al., 2024) combined exponential and trigonometric functions to create a sophisticated optimization technique.

The aforementioned MHS, inspired by various innovative origins, exhibit distinct optimization capabilities in terms of exploration and exploitation during the convergence search process. Additionally, several studies combined different MHS algorithms to develop novel algorithms that further enhance the performance of the original optimizers, including Teaching-Learning-based ABC (TLABC) (Chen et al., 2018), Adaptive SCA integrated with PSO (ASCA-PSO) (Issa et al., 2018), and BAS based GWO (BGWO) (Fan et al., 2021). Moreover, numerous studies have focused on improving the convergence search step of previous MHS, with new algorithms such as ES with Covariance Matrix Adaptation (CMA-ES) (Hansen and Ostermeier, 2001), rank-iMDDE (Gong et al., 2014), Adaptive Guided DE (AGDE) (Mohamed and Mohamed, 2019), Chaotic SSA (CSSA) (Zhang and Ding, 2021), and Adaptive Differential Learning TLBO (ADL-TLBO) (Tao et al., 2025). Some outstanding improvement algorithms include Success-History based Adaptive DE (SHADE) (Tanabe and Fukunaga, 2013), SHADE using Linear population size reduction (L-SHADE) (Tanabe and Fukunaga, 2014), L-SHADE with Ensemble pool of Sinusoidal parameter adaptation (LSHADE-EpSin) (Awad et al., 2016), LSHADE-EpSin with covariance matrix adaptation with Euclidean neighborhood (LSHADE-cnEpSin) (Awad et al., 2017), LSHADE with Semi-Parameter Adaptation hybrid with CMA-ES (LSHADE-SPACMA) (Mohamed et al., 2017), and Adaptive L-SHADE (AL-SHADE) (Li et al., 2022). In recent years, research on the guide selection and population update steps of MHS algorithms has made some progress. For the guide selection step, researchers have proposed several innovative methods, including Fitness-Distance Balance (FDB) (Kahraman et al., 2020), Dynamic FDB (DFDB) (Kahraman et al., 2022), Adaptive FDB (AFDB) (Duman et al., 2023), and Fitness-Distance-Constraint (FDC) (Ozkaya et al., 2023). These methods have been applied to develop corresponding novel algorithms, such as FDB-SFS (Aras et al., 2021), FDB-AGDE (Guvenc et al., 2021), Coyote Optimization Algorithm with Lévy Roulette and FDB (LRFDB-COA) (Duman et al., 2021), DFDB-MRFO (Kahraman et al., 2022), AFDB-ARO (Ozkaya et al., 2024), and FDC-AGDE (Ozkaya et al., 2023). Regarding the population update step, a promising Natural Survivor Method (NSM) has been proposed and applied in the design of the NSM-SFS, NSM-TLABC, and NSM-LSHADE-SPACMA algorithms (Kahraman et al., 2023).

3. Ecological Cycle Optimizer (ECO)

This section introduces a novel nature-inspired MHS algorithm, referred to as ECO. First, the inspiration for ECO is described, followed by a detailed description of its mathematical model and solution process.

3.1. Inspiration

An ecosystem is a unified whole formed by the interaction between biological communities (including plants, animals, microorganisms, etc.) and inorganic environment (including soil, water, climate, etc.), including producers, consumers, decomposers, and non-living matter and energy (Odum and Barrett, 1971). Producers, typically plants, are the cornerstone of the ecosystem. They convert carbon dioxide and water into organic matter through photosynthesis using solar energy, and provide food and oxygen for consumers, marking the beginning of energy flow within the ecosystem. Consumers, primarily including herbivores, carnivores, and omnivores, occupy different trophic levels of the food chain and facilitate energy flow and material cycling through predation within the ecosystem. Decomposers break down the remains of plants and animals into inorganic substances, which are reabsorbed by producers, thus contributing to the material cycle.

Energy flow and material cycling are the primary functions of an ecosystem. Matter serves as the carrier of energy, allowing energy to flow unidirectionally along the food chain, progressively decreasing across trophic levels. Energy, as the driving force, enables the continuous cycling of matter between biological communities and the inorganic environment. Through energy flow and material cycling, the various components of the ecosystem are closely interconnected, forming a relatively balanced ecological cycle that collectively maintains the balance and stability of the ecosystem.

The inspiration for the ECO comes from the aforementioned natural phenomena, drawing an analogy between dynamic optimization and ecological cycles. Mathematical models are established for the iterative update strategies of producers, consumers, and decomposers, thereby simulating energy flow and material cycling. As the number of iterations increases, the ECO progressively searches for the theoretical global optimal solution, simulating the ecosystem as it reaches an optimal state of balance and stability.

3.2. Mathematical model

This section establishes the ECO's mathematical model, simulating the iterative update strategies of producers, consumers, and decomposers.

First, the following five rules are formulated for the ECO algorithm:

- (1) The consumers in the population include only herbivores, carnivores, and omnivores, with trophic levels specified as: herbivore < carnivore < omnivore;
- (2) Herbivores feed on producers, carnivores feed on herbivores, and omnivores can prey on producers, herbivores, and carnivores. It is specified that all consumers cannot prey on organisms at the same trophic level;
- (3) The proportions of producers, herbivores, carnivores, and omnivores in the population are 20%, 30%, 30%, and 20%, respectively. After each iteration cycle, they are all decomposed by decomposers;

- (4) The fitness of individuals in the population is inversely proportional to their energy; higher energy indicates lower fitness;
- (5) After each individual in the population is updated iteratively, it is retained if its fitness improves, and eliminated if its fitness worsens, while the individual's historical best is still preserved, thereby simulating the survival of the fittest within the ecosystem.

Based on these rules, Fig. 1 visually presents a schematic of an ecosystem.

For the ECO algorithm, population initialization is performed by random sampling within the constrained space. During the iterative search phase, the roulette wheel selection-based multi-elite guiding strategy is used to guide selection, while the fitness value-based method is employed for population updates to simulate the survival of the fittest in nature. For the most critical convergence search operators that influence the ECO's *exploration* and *exploitation* phases, unique strategies for producers, consumers and decomposers are proposed and detailed in this section.

3.2.1. Population initialization

Before the algorithm begins, the population needs to be initialized. The population size is defined as $N_{\rm pop}$, with the number of producers being $N_{\rm Pro}$. Among consumers, the numbers of herbivores, carnivores, and omnivores are $N_{\rm Her}$, $N_{\rm Car}$, and $N_{\rm Omn}$, respectively. Therefore, $N_{\rm pop} = N_{\rm Pro} + N_{\rm Her} + N_{\rm Car} + N_{\rm Omn}$. The objective function of the optimization problem is $f(\cdot)$, with a dimension of D. The upper and lower bounds of the constrained space are $U_{\rm b} \in \mathbb{R}^D$ and $L_{\rm b} \in \mathbb{R}^D$, respectively. The current number of iterations is k, and the maximum number of iterations is $k_{\rm max}$, hence $1 \leq k \leq k_{\rm max}$.

Randomly initialize population individual $X_i \in \mathbb{R}^D$ within the constrained space:

$$X_i = L_b + rand(U_b - L_b), \quad i = 1, 2, ..., N_{pop},$$
 (1)

where $rand \in \mathbb{R}$ is a random number in the range [0, 1].

Therefore, producers $X_{\text{Pro}} \in \mathbb{R}^{N_{\text{Pro}} \times D}$, herbivores $X_{\text{Her}} \in \mathbb{R}^{N_{\text{Her}} \times D}$, carnivores $X_{\text{Car}} \in \mathbb{R}^{N_{\text{Car}} \times D}$, and omnivores $X_{\text{Omn}} \in \mathbb{R}^{N_{\text{Omn}} \times D}$ are initialized as follows:

$$X_{\text{Pro}} = \left[X_i\right]_{i=1}^{N_{\text{Pro}}},\tag{2}$$

$$X_{\text{Her}} = \left[X_i\right]_{i=N_{\text{Pro}}+1}^{N_{\text{Pro}}+N_{\text{Her}}},\tag{3}$$

$$X_{\text{Car}} = [X_i]_{i=N_{\text{Pro}}+N_{\text{Her}}+1}^{N_{\text{Pro}}+N_{\text{Her}}+N_{\text{Car}}},$$
 (4)

$$X_{\text{Omn}} = \left[X_i\right]_{i=N_{\text{Pro}}+N_{\text{Her}}+N_{\text{Car}}+1}^{N_{\text{pop}}},\tag{5}$$

where X_{Pro} , X_{Her} , X_{Car} , and X_{Omn} are formed by vertically stacking X_i over the indicated index ranges.

During each loop iteration, after the producer and consumer update according to their respective strategy, the individuals in the population are decomposed one by one based on the decomposition strategy to generate inorganic

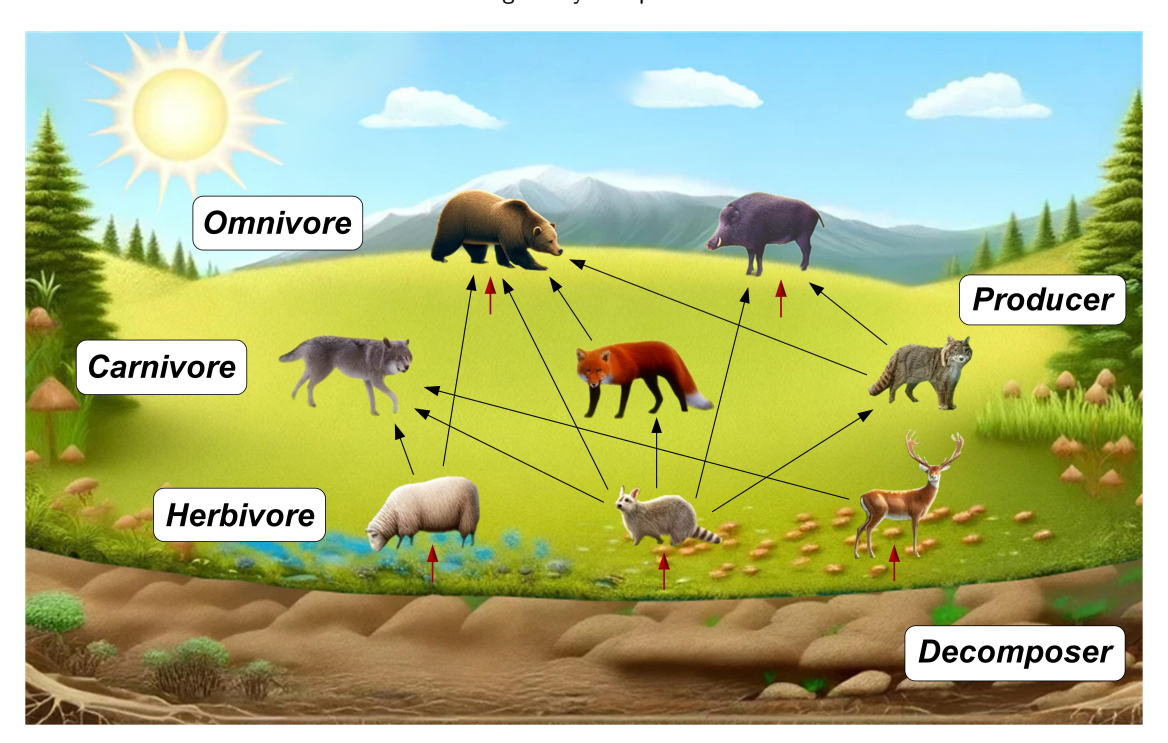


Figure 1: Schematic of an ecosystem.

substances. In ECO, these inorganic substances are regarded as decomposers $\boldsymbol{X}_{\mathrm{Dec}} \in \mathbb{R}^{N_{\mathrm{pop}} \times D}$, so there is no need to initialize the decomposers.

Additionally, when updating the population individuals, if their position exceeds the bounds of the constrained space, they are re-initialized according to (1).

3.2.2. Producer strategy

During material cycling within the ecosystem, producers can reabsorb the inorganic substances generated by decomposers from the decomposition of plant and animal remains to meet their nutritional needs.

In ECO, the individuals formed after the decomposition of producers and consumers simulate the inorganic substances produced by decomposers, while the current producer individuals are regarded as the existing nutrients. During each iteration, the producers select $N_{\rm Pro}$ units with the highest energy (i.e., lowest fitness) from the existing nutrients and inorganic substances to absorb nutrients, considering this process as the updating strategy for producers, expressed as follows:

$$X_{\text{nut}}(k+1) = Sort \begin{bmatrix} X_{\text{Pro}}(k) \\ X_{\text{Dec}}(k) \end{bmatrix},$$
 (6)

$$X_{\text{Pro}}(k+1) = [X_{\text{nut}}(k+1)]_{1:N_{\text{Pro}}},$$
 (7)

where $\boldsymbol{X}_{\text{nut}} \in \mathbb{R}^{\left(N_{\text{Pro}}+N_{\text{Dec}}\right) \times D}$ is the nutrients required by the producers, sorted by energy level, $Sort\left[\cdot\right]$ is the sorting function that reorders the elements according to certain rules, and $\left[\cdot\right]_{1:N_{\text{Pro}}}$ selects the elements from index 1 to N_{Pro} .

The sorting rule of the $Sort\left[\cdot\right]$ function is based on the fitness values $f\left[\boldsymbol{X}_{Pro}\left(k\right)\right]$ and $f\left[\boldsymbol{X}_{Dec}\left(k\right)\right]$ in ascending order, meaning that the elements of $\boldsymbol{X}_{Pro}\left(k\right)$ and $\boldsymbol{X}_{Dec}\left(k\right)$ are rearranged by fitness values from lowest to highest.

3.2.3. Consumer strategy

Consumers promote the energy flow and material cycling within the ecosystem by preying on organisms with lower trophic levels than themselves. During the predation process, consumers often lurk in the shadows, constantly monitoring the movements of their prey and waiting for the opportune moment to strike. Therefore, the mathematical model for the predation behavior of the consumers is designed as the following (8), where the operator \otimes denotes element-wise multiplication between two vectors. Here, $\boldsymbol{X}_{\text{Con}} \in \mathbb{R}^D$ represents the position of the consumer individual, $\boldsymbol{X}_{\text{prey}} \in \mathbb{R}^D$ denotes the predation factor vector corresponding to the consumer.

$$\boldsymbol{X}_{\text{Con}}(k+1) = \boldsymbol{X}_{\text{Con}}(k) + \boldsymbol{G}(k) \otimes \left\{ rand \left[\boldsymbol{X}_{\text{prey}}(k+1) - \boldsymbol{X}_{\text{Con}}(k) \right] \right\}, \tag{8}$$

Fig. 2 depicts the schematic of the consumer preying on the prey. There are multiple factors in nature that jointly constrain the predation behavior of consumers. For instance, obstacles present along the predation path may hinder the predator's movement and pursuit; additionally, the prey's camouflage, defense mechanisms, and ability to flee further reduce the success rate of predation. Therefore, for the predation model (8), random numbers within the interval [0, 1] are employed to simulate these complex stochastic factors, adding random weights to the predator's movement vector toward the prey. This enhances the randomness in the ECO's optimization process, thereby contributing to the prevention of the algorithm becoming trapped in local optima.

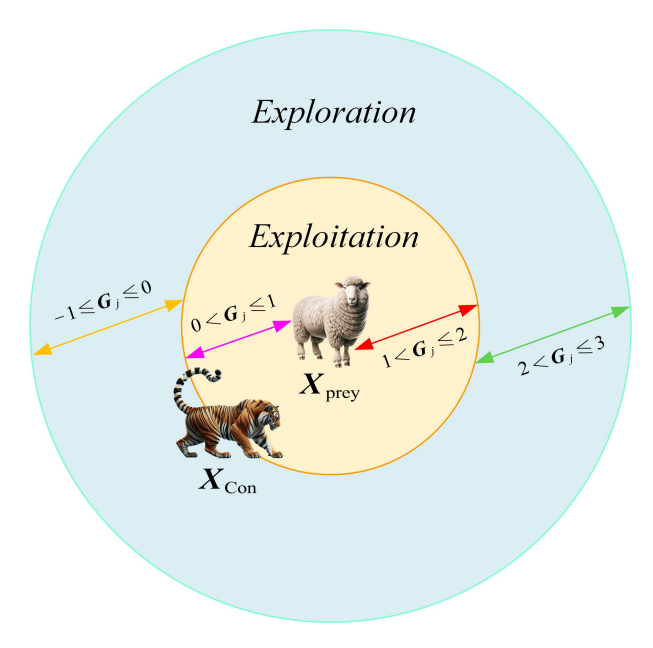


Figure 2: Consumer-prey predatory dynamics.

(1) Predation factor vector function G

Each dimension G_j of the consumer's predation factor vector function G is calculated according to the following formula:

$$G_j(k) = 1 + 2 \, rand \, e^{-9\left(\frac{k}{k_{\text{max}}}\right)^3} (-1)^{randi([1,2])},$$

 $j = 1, 2, ..., D,$
(9)

where randi([1,2]) randomly takes an integer value of 1 or 2.

The graph of $G_j(k)$ is shown in Fig. 3. The incorporation of the random numbers rand and randi([1,2]) in $G_j(k)$ allows it to take values within the interval [-1,3], enabling ECO to exhibit different behaviors at various phases of the iteration process. By combining Fig. 2 and Fig. 3, we further analyze the impact of the predation factor G on the performance of the ECO.

In the initial phase of the iteration, G_j can randomly take values within the interval $[-1,0] \cup (2,3]$, prompting ECO to exhibit a greater tendency toward *exploration*. The algorithm extensively searches the regions where the global

optimum may exist, reducing the risk of becoming trapped in local optima. Such behavior is akin to a situation in which the current prey fails to satisfy the consumer's energy needs, and the consumer has not yet found the prey that maximizes its energy intake (*i.e.*, the prey with the lowest fitness). To conserve energy, the consumer abandons the current target and searches a broader region for more energy-rich prey.

As the number of iterations k increases, G_j adaptively adjusts and gradually reduces its range of random values, allowing ECO to transition from *exploration* to *exploitation*. When $G_j \in (0,2]$, ECO enters the *exploitation* phase, intensively searching for the global optimum within a multidimensional hypersphere of random radius $\|X_{\text{prey}} - X_{\text{Con}}\|$. Such behavior is akin to a situation where the consumer launches an attack on the prey within a circular region centered on the prey, with a radius of $\|X_{\text{prey}} - X_{\text{Con}}\|$.

Due to $\lim_{k \to k_{\text{max}}} G_j = 1$, in the later phase of the iteration, ECO continuously performs *exploitation* within the neighborhood of the global optimum, while refining and uncovering the highly precise global optimum X_{best} .

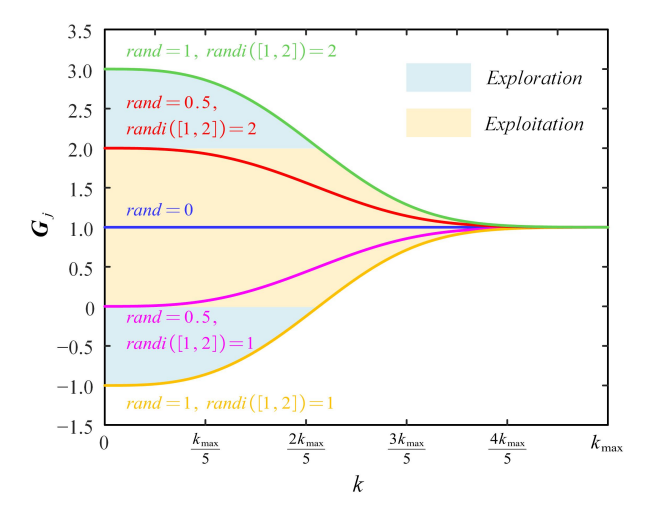


Figure 3: Variation of predation factor $G_i(k)$ over iterations.

(2) Herbivore predation strategy

In ECO, each herbivore is only allowed to prey on three producers, guided by the top three elite individuals. The predation principle applies the roulette wheel selection (Goldberg, 1989; Lipowski and Lipowska, 2012) to the producer population, with selection determined probabilistically based on their energy levels. The higher the energy of a producer (*i.e.*, the smaller the fitness), the greater the probability of being preyed upon. Define the *i*th herbivore as $\boldsymbol{X}_{\mathrm{Her}\,(i)} \in \mathbb{R}^D$ ($i=1,2,...,N_{\mathrm{Her}}$), and the three producers it preys on as $\boldsymbol{X}_{\mathrm{Pro}\,(A)} \in \mathbb{R}^D$, $\boldsymbol{X}_{\mathrm{Pro}\,(B)} \in \mathbb{R}^D$, and $\boldsymbol{X}_{\mathrm{Pro}\,(C)} \in \mathbb{R}^D$. Based on the consumer predation model (8), the herbivore's predation strategy is designed in (10).

(3) Carnivore predation strategy

ECO specifies that each carnivore preys on three herbivores using the roulette wheel selection rule. Define the

$$\begin{aligned} \boldsymbol{X}_{\mathsf{Her}(i)}(k+1) &= \boldsymbol{X}_{\mathsf{Her}(i)}(k) + \boldsymbol{G}(k) \otimes \left\{ rand \left[\boldsymbol{X}_{\mathsf{Pro}(A)}(k+1) - \boldsymbol{X}_{\mathsf{Her}(i)}(k) \right] \right. \\ &+ rand \left[\boldsymbol{X}_{\mathsf{Pro}(B)}(k+1) - \boldsymbol{X}_{\mathsf{Her}(i)}(k) \right] + rand \left[\boldsymbol{X}_{\mathsf{Pro}(C)}(k+1) - \boldsymbol{X}_{\mathsf{Her}(i)}(k) \right] \right\}, \quad i = 1, 2, ..., N_{\mathsf{Her}}, \end{aligned} \tag{10}$$

$$\begin{split} \boldsymbol{X}_{\mathsf{Car}(i)}(k+1) &= \boldsymbol{X}_{\mathsf{Car}(i)}(k) + \boldsymbol{G}(k) \otimes \left\{ rand \left[\boldsymbol{X}_{\mathsf{Her}(A)}(k+1) - \boldsymbol{X}_{\mathsf{Car}(i)}(k) \right] \right. \\ &+ rand \left[\boldsymbol{X}_{\mathsf{Her}(B)}(k+1) - \boldsymbol{X}_{\mathsf{Car}(i)}(k) \right] + rand \left[\boldsymbol{X}_{\mathsf{Her}(C)}(k+1) - \boldsymbol{X}_{\mathsf{Car}(i)}(k) \right] \right\}, \quad i = 1, \, 2, \dots, \, N_{\mathsf{Car}}, \end{split}$$

$$\begin{split} \boldsymbol{X}_{\mathsf{Omn}(i)}(k+1) &= \boldsymbol{X}_{\mathsf{Omn}(i)}(k) + \boldsymbol{G}(k) \otimes \left\{ rand \left[\boldsymbol{X}_{\mathsf{Pro}(D)}(k+1) - \boldsymbol{X}_{\mathsf{Omn}(i)}(k) \right] + rand \left[\boldsymbol{X}_{\mathsf{Her}(D)}(k+1) - \boldsymbol{X}_{\mathsf{Omn}(i)}(k) \right] \right. \\ &+ rand \left[\boldsymbol{X}_{\mathsf{Car}(A)}(k+1) - \boldsymbol{X}_{\mathsf{Omn}(i)}(k) \right] + rand \left[\boldsymbol{X}_{\mathsf{Car}(B)}(k+1) - \boldsymbol{X}_{\mathsf{Omn}(i)}(k) \right] \right\}, \qquad i = 1, 2, ..., N_{\mathsf{Omn}}. \end{split}$$

*i*th carnivore as $\boldsymbol{X}_{\operatorname{Car}(i)} \in \mathbb{R}^D$ ($i = 1, 2, ..., N_{\operatorname{Car}}$), with $\boldsymbol{X}_{\operatorname{Her}(A)} \in \mathbb{R}^D$, $\boldsymbol{X}_{\operatorname{Her}(B)} \in \mathbb{R}^D$, and $\boldsymbol{X}_{\operatorname{Her}(C)} \in \mathbb{R}^D$ representing the three preyed herbivores. According to (8), the predation strategy of the carnivore is expressed in (11).

(4) Omnivore predation strategy

The omnivore randomly preys on one producer, one herbivore, and two carnivores based on the roulette wheel selection, which constitutes a four-elite guiding approach. Define the ith omnivore as $\boldsymbol{X}_{\mathrm{Omn}\,(i)} \in \mathbb{R}^D$ ($i=1,2,...,N_{\mathrm{Omn}}$), with $\boldsymbol{X}_{\mathrm{Pro}\,(\mathrm{D})} \in \mathbb{R}^D$ and $\boldsymbol{X}_{\mathrm{Her}\,(\mathrm{D})} \in \mathbb{R}^D$ representing the preyed producer and herbivore, respectively, and $\boldsymbol{X}_{\mathrm{Car}\,(\mathrm{A})} \in \mathbb{R}^D$ and $\boldsymbol{X}_{\mathrm{Car}\,(\mathrm{B})} \in \mathbb{R}^D$ as the two preyed carnivores. In accordance with (8), the predation strategy of the omnivore is presented in (8).

(5) Roulette wheel selection for elite individuals

ECO adopts the roulette wheel selection-based multielite guiding strategy, which increases the probability of consumers preying on higher-energy (*i.e.*, lower-fitness) prey to meet their energy intake requirements. This behavior leads to local *exploitation* by the algorithm in the neighborhood of the optimal solution. Simultaneously, it avoids the drawback of prioritizing the selection of all elite individuals, which could lead the algorithm into local optima and premature convergence, thereby enhancing the global *exploration* capability of ECO.

In the candidate pool for the roulette wheel selection, individuals with lower fitness are considered superior and have a higher probability of being selected. Taking the producer population as an example, the number of individuals participating in the roulette wheel selection is N_{Pro} . Define the *i*th producer as $X_{\text{Pro}(i)} \in \mathbb{R}^D$ ($i = 1, 2, ..., N_{\text{Pro}}$), and its probability of being selected is given by:

$$P_{\text{ECO}}\left[\boldsymbol{X}_{\text{Pro}(i)}\right] = \frac{1/f\left[\boldsymbol{X}_{\text{Pro}(i)}\right]}{\sum_{j=1}^{N_{\text{Pro}}} 1/f\left[\boldsymbol{X}_{\text{Pro}(j)}\right]}.$$
 (13)

The sum of the probabilities of the first i individuals represents the cumulative probability corresponding to $X_{\text{Pro}(i)}$, expressed as follows:

$$q_{\text{ECO}}\left[\boldsymbol{X}_{\text{Pro}(i)}\right] = \sum_{i=1}^{i} P_{\text{ECO}}\left[\boldsymbol{X}_{\text{Pro}(j)}\right]. \tag{14}$$

A random number rand is generated within the interval [0,1]. If $rand \leqslant q_{\text{ECO}}\left[\boldsymbol{X}_{\text{Pro}(1)}\right]$, the first individual is selected. Otherwise, the process iterates until $q_{\text{ECO}}\left[\boldsymbol{X}_{\text{Pro}(i-1)}\right] < rand \leqslant q_{\text{ECO}}\left[\boldsymbol{X}_{\text{Pro}(i)}\right]$ ($i=2,3,...,N_{\text{Pro}}$), selecting the ith individual. To select multiple elite individuals, this process is repeated the corresponding number of times.

The pseudocode of the roulette wheel selection for elite individuals is shown in Algorithm 1.

3.2.4. Decomposer strategy

Decomposers constitute a critical part of the ecosystem, facilitating the breakdown of plant and animal remains, as well as excretions, into inorganic substances, thus promoting ecological cycling and ensuring the stability of the ecosystem. In each iteration of ECO, decomposers are required to decompose producers and consumers sequentially.

Accordingly, this section presents a mathematical model for the decomposition process and introduces three probability-based decomposition strategies to balance the process of *exploration* and *exploitation* in ECO.

For each individual in the population, there is an equal probability (50%) of undergoing either optimal decomposition or random decomposition. In the case of random decomposition, there is a 50% probability of performing either local or global random decomposition.

(1) Optimal decomposition

When any individual \boldsymbol{X}_i ($i \in [1, 2, ..., N_{pop}]$) in the population is selected with a 50% probability for optimal decomposition, the individual $\boldsymbol{X}_{bestk} \in \mathbb{R}^D$ with the highest energy (i.e., lowest fitness) in the current iteration is chosen. The selected individual is decomposed toward the neighborhood of \boldsymbol{X}_{bestk} , promoting the decomposer to provide the most nutrient-rich inorganic matter to the producers, thereby enhancing material cycling. This process will significantly enhance the *exploitation* capability of ECO, improving the algorithm's convergence speed and solution accuracy.

The multidimensional neighborhood $X_{\text{nei}} \in \mathbb{R}^D$ of X_{bestk} is defined as follows:

$$X_{\text{nei}, j}(k+1) = rand X_{\text{bestk}, j}(k+1),$$

 $j = 1, 2, ..., D,$ (15)

Algorithm 1: Pseudocode of the roulette wheel selection for elite individuals.

Input: Population individual fitness $f\left[X_{\text{Pro}(i)}\right]$ $(i = 1, 2, ..., N_{\text{Pro}})$ and the number of selected individuals (*i.e.*, the number of roulette wheel selections)

Output: All selected individuals

- 1 Probability $P_{\text{ECO}}\left[X_{\text{Pro}(i)}\right]$ of each individual being selected by the roulette wheel selection according to (13);
- 2 Cumulative probability $q_{\text{ECO}}\left[\boldsymbol{X}_{\text{Pro}(i)}\right]$ corresponding to each individual calculated according to (14);

```
3 for each roulette wheel selection do
         Generate a random number rand within [0, 1];
 4
         if rand \leq q_{ECO} \left[ X_{Pro(i)} \right] then
 5
             Select the first individual:
 6
 7
              while no individual selected do
 8
                   if q_{\text{ECO}}\left[X_{\text{Pro}(i-1)}\right] < rand \leqslant
                    q_{\text{ECO}}[X_{\text{Pro}(i)}] (i = 2, 3, ..., N_{\text{Pro}}) then
                       Select the ith individual;
10
                       break;
11
                  end
12
             end
13
14
         Record the selected individual;
15
16 end
```

where $X_{\text{nei},j} \in \mathbb{R}$ and $X_{\text{bestk},j} \in \mathbb{R}$ are *j*th dimensional elements of the neighborhood X_{nei} and the best individual X_{bestk} in the current iteration, respectively.

The population individual X_i is decomposed along the direction of $X_{\text{nei}} - X_i$ to a random position within a distance $\pm 0.2 \|X_{\text{nei}} - X_i\|$ from the center X_{nei} , and the inorganic matter generated at this point is regarded as the *i*th decomposer $X_{\text{Dec}(i)} \in \mathbb{R}^D$. The optimal decomposition strategy is designed as follows:

$$\begin{split} \boldsymbol{X}_{\mathrm{Dec}\,(i)}\,(k+1) &= \boldsymbol{X}_{\mathrm{nei}}\,(k+1) + (0.4\,rand - 0.2) \\ &\left[\boldsymbol{X}_{\mathrm{nei}}\,(k+1) - \boldsymbol{X}_{i}\,(k+1)\right], \quad i \in \left[1,\,2,\,...,\,N_{\mathrm{pop}}\right]. \end{split} \tag{16}$$

(2) Local random decomposition

17 **return** all selected individuals

The remaining population individuals undergo random decomposition, with a 50% probability of being further selected for local random decomposition. In this process, individual \boldsymbol{X}_i is radially decomposed to a random position within a multidimensional hypersphere centered at itself, with an *exploration* radius of $\|\boldsymbol{X}_{\text{bestk}} - \boldsymbol{X}_i\|$. The range of the radial distance is $[0, \|\boldsymbol{X}_{\text{bestk}} - \boldsymbol{X}_i\|]$.

Define a random vector $V_{rand} \in \mathbb{R}^D$, with each of its elements as:

$$V_{rand, j} = 2rand - 1, \quad j = 1, 2, ..., D.$$
 (17)

The local random decomposition strategy is designed as follows:

$$X_{\text{Dec}(i)}(k+1) = X_{i}(k+1) + rand \| X_{\text{bestk}}(k+1) - X_{i}(k+1) \| \frac{V_{rand}}{\| V_{rand} \|}, \quad i \in [1, 2, ..., N_{\text{pop}}].$$
(18)

In the initial phase of the iteration, local random decomposition enables population individuals to perform radial *exploration* within a larger hypersphere, facilitating the search for regions that may contain the global optimum. As iterations increase, most population individuals converge near $X_{\rm bestk}$ in the later phase of the algorithm, leading to a gradual decrease in the maximum *exploration* radius $\|X_{\rm bestk} - X_i\|$. Individuals continue to search for the optimal solution around $X_{\rm bestk}$ with a certain probability, further enhancing the algorithm's *exploitation* capability. Therefore, the local random decomposition strategy effectively balances the *exploration* and *exploitation* processes of the ECO.

(3) Global random decomposition

The rest of the population is selected for global random decomposition. In this process, individual X_i is decomposed to a random position through a random walk, enhancing the algorithm's global *exploration* capability. The maximum step size for the random walk is set to $2/3 \min \left(L_b - U_b \right)$ across all dimensions of the constrained space, in order to prevent the random walk from exceeding the boundaries of the constrained space. The step size of the random walk is denoted as $\boldsymbol{w}_{rand} \in \mathbb{R}^D$, with each dimension calculated as follows:

$$\boldsymbol{w}_{rand, j} = \frac{2}{3} rand H (k) \min \left(\boldsymbol{L}_{b} - \boldsymbol{U}_{b} \right),$$

$$j = 1, 2, ..., D,$$
(19)

where $H(\cdot)$ is a global random walk coefficient function, designed as follows:

$$H(k) = \cos(rand\pi) \left(1 - \frac{k}{1.5k_{\text{max}}}\right)^{\left(\frac{5k}{k_{\text{max}}}\right)}.$$
 (20)

Define a weight $rand_{wei} \in \mathbb{R}$ for the random walk as a random number within the interval [0,1], and apply a random weight to individual X_i and the step size w_{rand} of the random walk, thereby increasing the randomness of the *exploration*. Thus, the global random decomposition strategy is designed as follows:

$$\mathbf{X}_{\text{Dec}(i)}(k+1) = rand_{wei}\mathbf{X}_{i}(k+1) + (1 - rand_{wei})\mathbf{w}_{rand}, \quad i \in [1, 2, ..., N_{pop}].$$
(21)

Algorithm 2: Pseudocode of the Ecological Cycle Optimizer (ECO).

```
Input: Population size N_{\text{pop}}, the maximum number of iterations k_{\text{max}}, objective function f(\cdot), dimension D, and
            the upper bound \hat{U}_{\rm h} and lower bound L_{\rm h} of the constrained space
   Output: The optimal solution X_{\text{best}} and optimal fitness f(X_{\text{best}})
 1 Calculate the numbers of producers N_{\text{Pro}}, herbivores N_{\text{Her}}, carnivores N_{\text{Car}}, and omnivores N_{\text{Omn}} proportionally;
 2 Initialize X_{Pro}, X_{Her}, X_{Car}, and X_{Omn} sequentially according to (1)–(5);
 3 for each iteration k (k = 1, 2, ..., k_{max}) do
        if k \neq 1 then
            Producer update rule: apply production strategy (6) and (7) to update X_{Pro};
 5
        end
 6
        Calculate the predation factor vector \mathbf{G} of the consumer according to (9);
 7
        for each herbivore X_{\text{Her}(i)} (i = 1, 2, ..., N_{\text{Her}}) do
 8
            Select three producers X_{Pro(A)}, X_{Pro(B)}, and X_{Pro(C)} using roulette wheel selection Algorithm 1;
            Herbivore update rule: apply predation strategy (10) to update X_{\text{Her}(i)};
10
            Perform function evaluation of f(X_{\text{Her}(i)});
11
        end
12
        for each carnivore X_{\text{Car}(i)} (i = 1, 2, ..., N_{\text{Car}}) do
13
            Select three herbivores X_{\text{Her (A)}}, X_{\text{Her (B)}}, and X_{\text{Her (C)}} using roulette wheel selection Algorithm 1;
14
            Carnivore update rule: apply predation strategy (11) to update X_{Car(i)};
15
            Perform function evaluation of f(X_{Car(i)});
16
17
        for each omnivore X_{\text{Omn}(i)} (i = 1, 2, ..., N_{\text{Omn}}) do
18
            Select one producer X_{Pro(D)}, one herbivore X_{Her(D)}, and two carnivores X_{Car(A)} and X_{Car(B)} using roulette
19
              wheel selection Algorithm 1;
            Omnivore update rule: apply predation strategy (12) to update X_{Omn(i)};
20
            Perform function evaluation of f(X_{Omn(i)});
21
22
        for each decomposer X_{\text{Dec}(i)} (i = 1, 2, ..., N_{\text{pop}}) do
23
            if rand < 0.5 then
24
                Optimal decomposition rule: apply (16) to perform decomposition of X_i (i \in [1, 2, ..., N_{pop}]);
25
            else
26
                if rand < 0.5 then
27
                     Local random decomposition rule: apply (18) to perform decomposition of X_i
28
                       (i \in [1, 2, ..., N_{pop}]);
                 else
29
30
                     Global random decomposition rule: apply (21) to perform decomposition of X_i (i \in [1, 2, ..., N_{\text{pop}}]);
                end
31
            end
32
            Perform function evaluation of f(X_{Dec(i)});
33
34
        Update the historical optimal population individual X_{\text{best}} and the global optimum f(X_{\text{best}});
35
36 end
37 return X_{\text{best}} and f(X_{\text{best}})
```

With the introduction of rand in function H, it takes random values within the interval [-1,1], and $\lim_{k\to k_{\max}} H=0$. In the initial phase of the iteration, the value range of H is relatively large, leading to a larger random walk step size \boldsymbol{w}_{rand} , enabling population individuals to perform extensive exploration within the constrained space. With increasing iterations, the value range of H adaptively decreases, and the random walk step size decreases accordingly. In the later phase of the iteration, as convergence stabilizes, ECO

demonstrates a strong capability to escape local optima, particularly for objective functions where many local optima are densely distributed around the global optimum.

3.3. ECO workflow

The pseudocode and flowchart of the ECO are presented in Algorithm 2 and Fig. 4, respectively.

Many previous metaheuristic algorithms rely on multiple parameters that significantly influence their performance

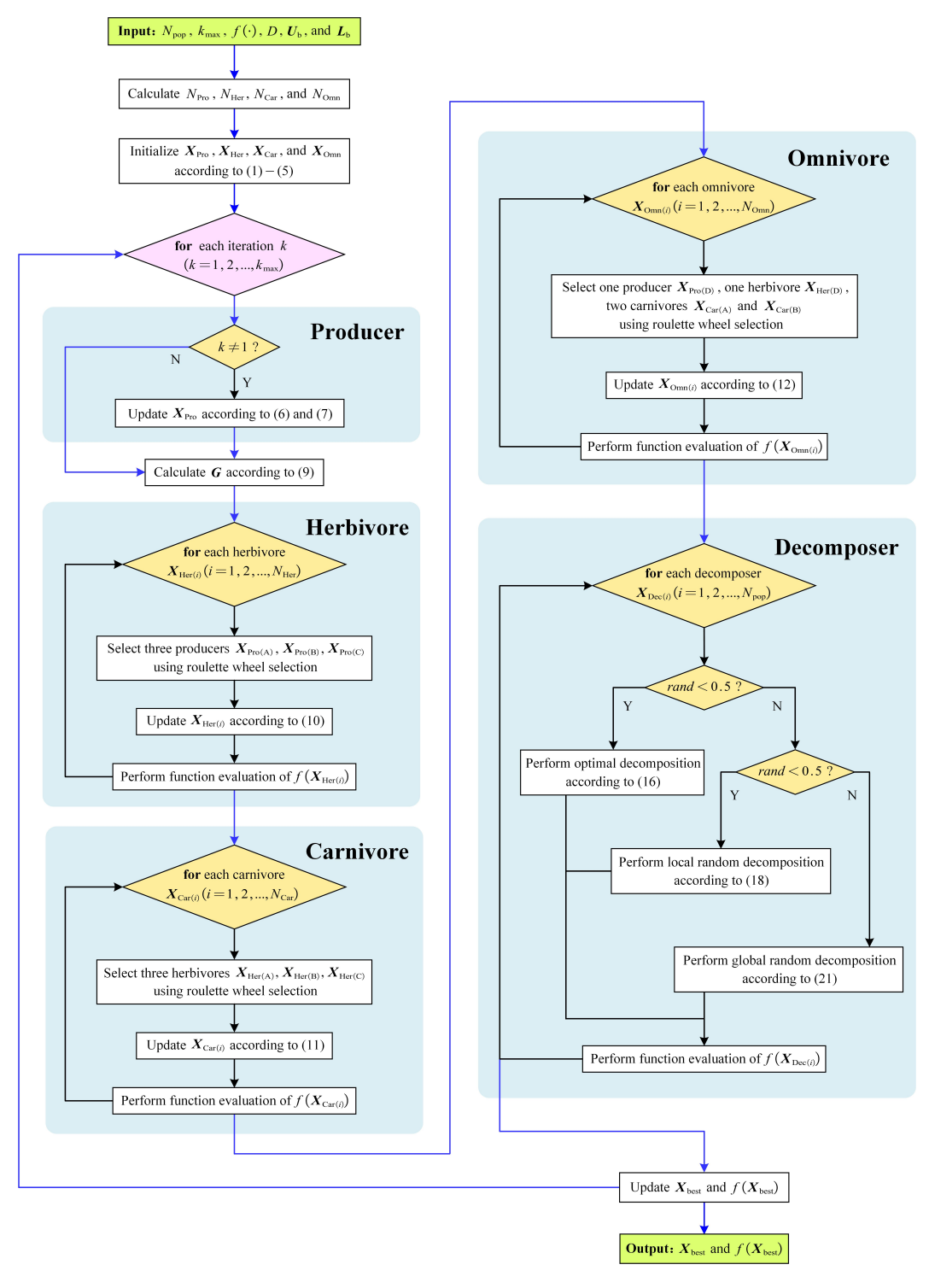


Figure 4: Flowchart of Ecological Cycle Optimizer (ECO).

and are highly sensitive to parameter settings. To achieve an optimal balance between *exploration* and *exploitation* for superior solution performance, these algorithms often require extensive parameter tuning.

In contrast, the mathematical model and solution process of the ECO indicate that its implementation is more convenient, requiring only the setting of two universally applicable parameters: the population size $N_{\rm pop}$ and the maximum

number of iterations $k_{\rm max}$, without the need for additional parameter settings. The unique strategies of production, consumption, and decomposition in ECO allow the algorithm to dynamically adjust the processes of *exploration* and *exploitation*, enhancing its stability and resulting in extremely fast convergence speed, high solution accuracy, and strong ability to escape local optima. Therefore, ECO demonstrates

outstanding solution performance when addressing more complex constrained optimization problems.

3.4. Computational complexity analysis

Computational complexity analysis is essential for evaluating the efficiency and scalability of optimization algorithms when solving problems of different scales and dimensions. It offers a theoretical perspective that reveals how the computational cost of an algorithm grows with the increase of algorithm parameters. For the ECO algorithm, the computational complexity is primarily related to the population size $N_{\rm pop}$, the problem dimension D, and the maximum number of iterations $k_{\rm max}$. This section analyzes the time and space complexity of the ECO algorithm.

3.4.1. Time complexity

Time complexity reflects the computational burden required to execute the algorithm. During the ECO process, the computational complexity of population initialization is $O\left(N_{\mathrm{pop}}D\right)$. In each iteration, the computational complexity of calculating the predation factor vector function G is $O\left(D\right)$, and that of the roulette wheel selection is $O\left(N_{\mathrm{pop}}\right)$. Updating the population individuals has a computational complexity of $O\left(N_{\mathrm{pop}}D\right)$, while the complexity of function evaluation is $O\left(N_{\mathrm{pop}}F\left(D\right)\right)$, where $F\left(D\right)$ denotes the time complexity of the objective function in the optimization problem. Therefore, the overall dominant time complexity of the ECO algorithm is given as follows:

$$\begin{split} O_{\text{time}}\left(\text{ECO}\right) &\approx O(N_{\text{pop}}D + k_{\text{max}}(D + N_{\text{pop}} + N_{\text{pop}}D \\ &+ N_{\text{pop}}F\left(D\right))) \\ &\approx O\left(k_{\text{max}}N_{\text{pop}}\left[D + F\left(D\right)\right]\right). \end{split} \tag{22}$$

If the objective function is computationally simple, the time complexity of the ECO algorithm reduces to $O\left(k_{\max}N_{\text{pop}}D\right)$.

3.4.2. Space complexity

Space complexity measures the memory resources needed to store data structures and intermediate results during computation. The ECO algorithm mainly requires storing several variables, including the predation factor vector function G, which has a space complexity of O(D); population individuals with space complexity $O\left(N_{\rm pop}D\right)$; personal best positions and fitness values requiring $O\left(N_{\rm pop}D\right)$ and $O\left(N_{\rm pop}\right)$; and the global optimal solution $X_{\rm best}$ and its optimal fitness $f\left(X_{\rm best}\right)$, requiring $O\left(D\right)$ and $O\left(1\right)$, respectively. Therefore, the overall space complexity of the ECO algorithm is:

$$\begin{split} O_{\rm space}\left(\text{ECO}\right) &\approx O(D + N_{\rm pop}D + N_{\rm pop}D + N_{\rm pop} + D + 1) \\ &\approx O\left(N_{\rm pop}D\right). \end{split}$$

Since the dominant term is $O(N_{pop}D)$, other terms can be neglected in asymptotic analysis.

4. Experimental overview

Similar to other MHS algorithms, ECO is originally designed to address complex optimization problems, which are frequently formulated as non-convex models. Such problems can be classified as either *unconstrained* or *constrained* optimization problems.

Starting from this chapter, experiments will be conducted to verify the performance of ECO in solving these optimization problems. The experimental procedure is presented systematically along with the evaluation criteria and methodologies employed to analyze the results. This approach enables a rigorous assessment of the algorithm's effectiveness across diverse problem configurations.

4.1. Experimental design

To conduct the experiment, standardized optimization functions must be selected as benchmarks. Numerous studies have adopted classic benchmarks and IEEE CEC test suites for this purpose. The CEC test suites encompass comprehensive optimization categories, covering all problem classifications mentioned above along with constrained optimization problems from the real-world, which integrates practical engineering scenarios. It should be noted that the optimization problems from the IEEE CEC test suites are all single-objective. Detailed information is specified in the official technical reports for each test suite.

The initial verification of MHS algorithms usually focuses on their performance in solving single-objective optimization problems. Additional classifications of optimization problems are also needed to comprehensively evaluate their problem solving capabilities. SOTA MHS algorithms are selected for comparative analysis in various optimization problems to thoroughly explore the performance potential of ECO.

Therefore, our experiments will be structured into three distinct components, each with explicitly defined objectives and methodological frameworks as outlined below:

(1) Overall verification

Firstly, the comprehensive performance of ECO will be verified. Specifically, we choose the 23 classic optimization functions to verify the performance of ECO in solving unconstrained optimization problems, and CEC-2006 to verify its performance in solving constrained optimization problems. Five famous highly cited MHS algorithms will be adopted along with ECO for comparative analysis.

(2) Single-objective potential

Secondly, the performance of ECO in solving single-objective optimization problems will be tested mainly. For this purpose, we select CEC-2014, CEC-2017, and CEC-2020 as benchmarks, covering various types of single-objective optimization problems ranging from simple to complex. To explore the potential performance of ECO, 50 SOTA MHS algorithms will be compared with ECO through experiments.

 Table 2

 Description of benchmarks used in the experiment.

Experimental goal	Benchmarks	Type of optimization problems	Ref. of technical report
Overall verification	23 classic optimization functions	Unconstrained	(Yao et al., 1999)
	CEC-2006	Constrained	(Liang et al., 2006)
Single-objective potential	CEC-2014	Single-objective	(Liang et al., 2013)
	CEC-2017	Single-objective	(Wu et al., 2017)
	CEC-2020	Single-objective	(Yue et al., 2019)
Engineering applications	CEC-2020-RW	Constrained from real-world	(Kumar et al., 2020c)

(3) Engineering applications

Finally, the performance of ECO in solving real-world engineering problems will be explored. In this part, the CEC-2020-RW test suite is adopted, which consists of constrained engineering problems derived from real-world scenarios. Five classic problems and five powerful MHS algorithms that are widely used are selected as benchmarks for comparison with ECO.

The information of these test suites used in the experiment is presented in Table 2.

4.2. Performance metrics

In this section, the evaluation criteria and methods adopted for analyzing numerical results are introduced. The analysis of MHS algorithms' numerical results usually includes comparing the performance superiority of different MHS algorithms and their distinct problem-solving characteristics.

Since experiments will be conducted independently and repeatedly, a set of data will be obtained from the solution result. Thus, it can be regarded as a statistical analysis (Carrasco et al., 2020). For MHS, statistical analysis must be performed with nonparametric testing methods to obtain rigor and accurate conclusions (Derrac et al., 2011; Eftimov et al., 2017).

In summary, statistical data results of the experiments must first be derived, followed by nonparametric testing methods to conclude. When analyzing algorithmic performance superiority, both a detailed comparison of ECO with each competing MHS algorithm on individual functions and a macro-level comprehensive performance ranking of all algorithms (including ECO) across the entire test suite are required to highlight their problem solving characteristics. Therefore, pairwise comparison and multiple comparison from nonparametric testing (Carrasco et al., 2020) will be employed.

4.2.1. Statistical data results

On each test suite, all MHS algorithms will search N times independently on each optimization function. The minimum (Min), average (Ave) and standard deviation (Std) values of these search results are recorded, and box plots are generated to visually illustrate the distribution of solution values.

Differences between MHS algorithms must be further compared and analyzed. It is important to clarify a premise regarding algorithmic performance evaluation: an MHS algorithm is considered superior if it achieves a smaller Ave value on a optimization function. However, this premise alone is insufficient and lacks rigor. The influence of algorithmic randomness on experimental outcomes must be excluded. A common practice involves determining whether there are significant differences between solutions obtained by different MHS: (1) if the differences between MHS algorithms are statistically significant, Ave values can be reliably used for comparison; and (2) if no significant differences are observed, a smaller Ave value may result from randomness and cannot serve as a criterion to evaluate algorithmic superiority. This constitutes the rationale for employing nonparametric methods (Derrac et al., 2011).

4.2.2. Pairwise comparisons

To compare the differences between ECO and other competing MHS algorithms on each optimization function, a widely adopted method is the **Wilcoxon test**. Noted that the Wilcoxon test comprises two distinct tests:

• Wilcoxon signed-rank test

Requires paired samples, where the data of two groups are correspondence to each other (Wilcoxon, 1945b).

• Wilcoxon rank-sum test (Mann-Whitney *U* test) Makes no such assumption about pairwise correspondence, which indicates that the length of two data groups can be different (Wilcoxon, 1945a).

Both tests share the same null hypothesis H_0 : "there is no significant difference between the two groups of data", or equivalently "both groups originate from populations with identical distributions". The result of these tests is the statistical significance p-value. The similarities and difference are listed in Table 3.

In this experiment, although the numerical results of each MHS algorithm on any optimization function contain N elements, these results are not inherently pairwise matched. Therefore, the more rigorous approach is to perform the Wilcoxon rank-sum test on the two groups of data.

After obtained the *p*-value, it is compared to a predefined significance level α . Together with the Ave (\overline{X}) values, the superiority of MHS algorithms can be concluded: if *p*-value $< \alpha$, H_0 is rejected, indicating statistically significant

Table 3
Similarities and difference between the two Wilcoxon tests.

Content	Similarities
H_0	There is no significant difference between the two groups of data Both groups originate from populations with identical distributions
Output	p-value
Content	Difference
Input	Wilcoxon signed-rank test: paired samples from 2 groups Wilcoxon rank-sum test: 2 groups of data

differences between the groups. This enables conclusions based on the Ave (\overline{X}) values:

- p-value $< \alpha$, H_0 is rejected, indicating statistically significant differences between the groups. If $\overline{X_A} < \overline{X_B}$, then MHS algorithm A is recognized better than MHS algorithm B, where A will be denoted as "+" and B as "-"
- p-value $\geq \alpha$, H_0 cannot be rejected. Thus, conservatively conclude that the performance of the two MHS algorithms is statistically equivalent to ensure experimental rigor, marked as "=", as the influence of stochastic factors cannot be excluded.

4.2.3. Multiple comparisons

To comprehensively compare the overall performance of ECO and all competing MHS, a global ranking across the entire test suite must be given. This approach requires aggregating all numerical results rather than focusing on pairwise algorithm comparisons or individual functions, which falls under the category of multiple comparisons.

A widely adopted and intuitive method involves: (1) rank all algorithms on each function, where the smaller \overline{X} indicates a higher rank; (2) calculate the average rank for each algorithm on all optimization functions; and (3) generate a global ranking based on these average ranks. This procedure constitutes the core principle of the **Friedman mean rank** method.

Using Wilcoxon rank-sum tests for global ranking introduces three critical issues. Firstly, for m MHS algorithms and n optimization functions, $C_n^m = nm(m-1)/2$ tests are required, which will intensify computational cost. Secondly, the "=" equivalence classification will create ranking indeterminacy. Last but not least, from a statistical perspective, the loss of control over the Family-Wise Error Rate (FWER) implies that the probability of committing one or more Type I errors (false discoveries) across all hypotheses increases substantially when performing multiple pairwise comparisons (Derrac et al., 2011).

As a result, the **Friedman test** is adopted to resolve these limitations. The Null hypothesis H_0 of the Friedman test is: "no significant difference exist among m groups of data", in this circumstance means that no significant differences exist among the m MHS algorithm performances (Friedman, 1940). Similarly to the Wilcoxon test, the output of the

Friedman test is the statistical significance p-value. If p-value < α , the H_0 is rejected. In this case, an overall ranking can be given by ascending the Friedman mean rank.

5. ECO performance verification

In this chapter, the performance of ECO will be evaluated in solving both unconstrained and constrained optimization problems. The 23 classic optimization functions are utilized for unconstrained optimization problems, while the CEC-2006 test suite is utilized for constrained optimization problems. Detailed experimental configurations are described in the following sections.

5.1. Competing algorithms and parameter settings

Five highly cited and well-performed MHS algorithms CS (Yang and Deb, 2009), HS (Geem et al., 2001), PSO (Kennedy and Eberhart, 1995), GWO (Mirjalili et al., 2014), and WOA (Mirjalili and Lewis, 2016), are selected for comparison with ECO. To ensure these MHS algorithms achieve their optimal performance, the parameters are adopted from their original paper, except for a uniform population size (customized) of 30 is maintained across all MHS algorithms for consistency. Detailed information of these MHS algorithms is listed in Table 4.

5.2. ECO for unconstrained problems on 23 classic optimization functions

The detailed information of 23 classic optimization functions are presented in Table 24. The experimental parameters are set as follows. The search termination criterion Maximum Function Evaluations MaxFEs = $10,000 \times D$, where D is set to 30. The number of independent runs N=25. Solutions of MHS algorithms including Min, Ave and Std on each optimization functions will be recorded.

5.2.1. Statistical analysis

The numerical results of all MHS algorithms on 23 classic optimization functions is presented in Table 7. It can be clearly observed that ECO consistently achieved optimal solutions compared to other MHS algorithms on all optimization functions.

In addition, among comparative MHS, GWO and WOA exhibited relatively competitive performance, achieving cooptimal solutions with ECO on certain optimization functions. The rank of all MHS algorithms on each function is summarized in Table 5. Although CS did not obtain many optimum solutions, the performance of CS is very stable, while the rank of PSO fluctuates a lot.

To statistically verify the performance differences between ECO and other MHS, Wilcoxon rank-sum tests are conducted. This analysis further quantifies the performance disparities between ECO and each comparator algorithm on 23 classic optimization functions, as detailed in Table 6. It is easy to notice that ECO has demonstrated obvious advantages over any MHS algorithms in every comparison. None of the MHS algorithms has achieved better numerical results than ECO in any optimization function.

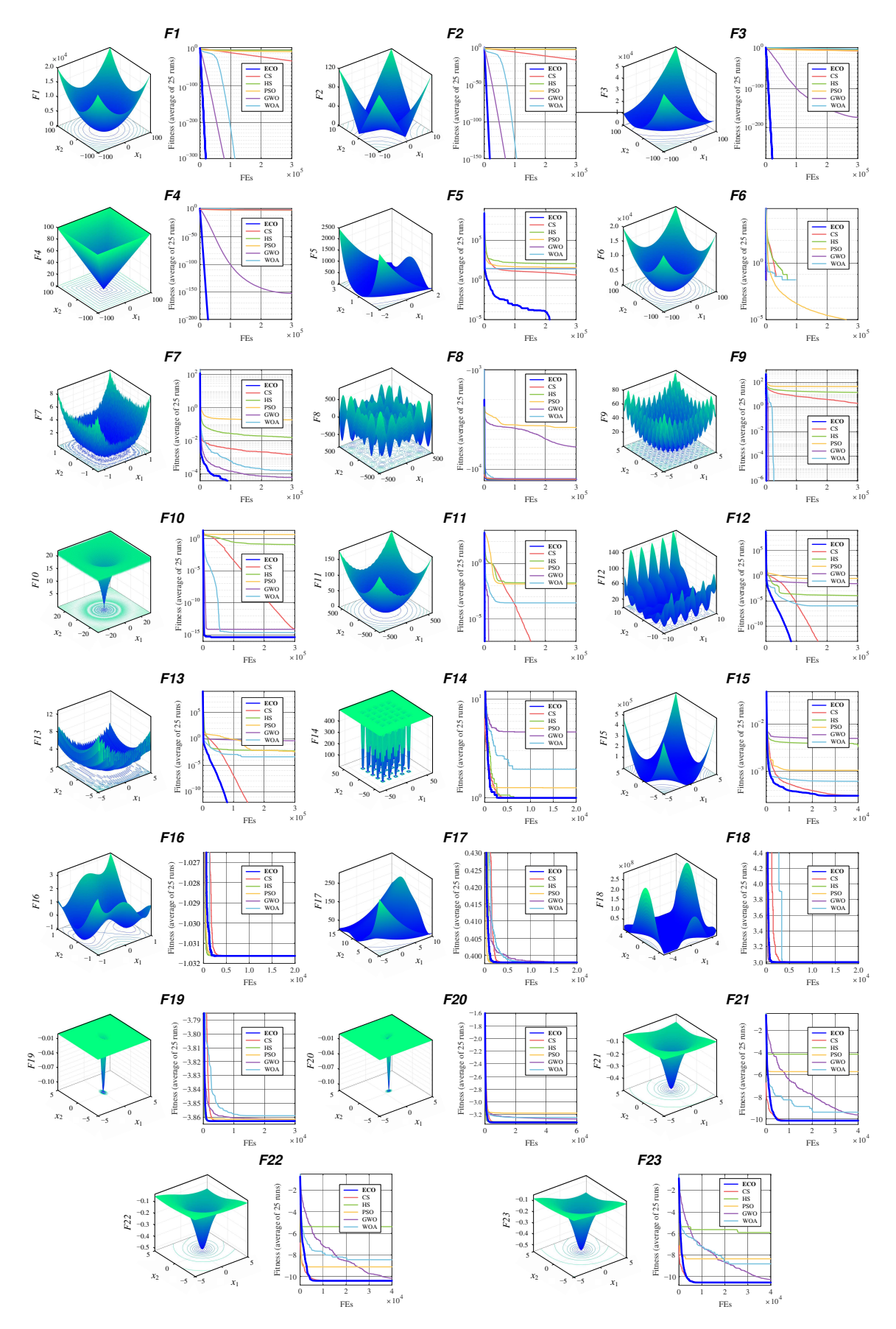


Figure 5: Mean convergence curve of ECO and competing MHS algorithms on 23 classic benchmark functions.

 Table 4

 Competing MHS algorithms and parameter settings.

MHS	Parameters settings	Ref.	Year	Cited
CS	Probability $p_a = 0.25$, Lévy parameter $\beta = 1.5$	(Yang and Deb, 2009)	2009	9512
HS	Harmony memory considering rate $HMCR = 0.95$, pitch adjustment rate $PAR = 0.3$	(Geem et al., 2001)	2001	8095
PSO	Cognitive learning factor $c_1 = 2$, social learning factor $c_2 = 2$, inertia weight $w = 0.8$	(Kennedy and Eberhart, 1995)	1995	94527
GWO	Convergence parameter a decreases from 2 to 0	(Mirjalili et al., 2014)	2014	19851
WOA	Convergence parameter a decreases from 2 to 0, logarithmic spiral shape parameter $b = 1$	(Mirjalili and Lewis, 2016)	2016	14377

Note: Citation counts are from Google Scholar as of August 15, 2025.

All parameters remain consistent with those used in the original publications.

Table 5Friedman mean rank of ECO and competing MHS algorithms on the 23 classic optimization functions benchmark.

MHS	ECO	CS	HS	PSO	GWO	WOA
Friedman	1.00	2.65	4.70	4.57	3.35	3.65
Rank	1	2	6	5	3	4

Table 6Wilcoxon rank-sum test results between ECO and competing MHS algorithms on 23 classic optimization functions.

ECO vs.	CS	HS	PSO	GWO	WOA
+/=/-	19/4/0	22/1/0	21/2/0	18/5/0	18/5/0

5.2.2. Convergence analysis

The convergence curves of ECO and comparative MHS algorithms on 23 classic optimization functions along with 3D function topology are presented in Figure 5. It can be observed that ECO exhibits a superior convergence speed on all optimization functions. At early stage, the so far optimum solution of ECO descends very quickly, indicating a vast search range, while it converges to a flat in the later stage, means that all search particles gather together to the optimum point. Apart from ECO, CS has also demonstrated good convergence speed in some functions. However, PSO performs poorly when dealing with most multimodal functions. Not only does it fail to converge rapidly, but the overall numerical results are also far from the optimum.

Notably, discontinuities are observed in the convergence curves on some optimization functions (e.g. *F*6). This phenomenon is attributed to the global optimum (zero value) achieved by MHS algorithms cannot be properly displayed on logarithmic scale employed in the convergence curve plot for a clearer visualization of curve hierarchies.

5.2.3. Exploration & exploitation analysis

Based on the classifications and characteristics of the optimization functions in the 23 classic optimization functions, the *exploration* and *exploitation* ability of MHS algorithms is suggested to be analyzed.

The exploitation capability of MHS algorithms is defined as their ability to rapidly converge toward the vicinity

of the current optimal solution during the later stages of iteration. As shown in Table 24, optimization functions F1-F7 are unimodal, containing only a single global optimum. Therefore, the ability of ECO and other MHS algorithms to reach the global optimum on these functions can be indirectly used to reflect their exploitation capabilities.

The *exploration* ability of MHS algorithms is defined as the dispersion of search particles within the search space during the early stages of iteration. Greater dispersion indicates a stronger exploration capability, enabling the algorithm to escape local optima and search for the global optimum. Optimization functions *F*8-*F*23 are multimodal, containing multiple local optima. Therefore, evaluating whether ECO and other MHS algorithms can reach the global optimum on these functions indirectly reflects their exploration capabilities.

Therefore, from Table 7 and Figure 5, it is clear that ECO possesses robust exploration and exploitation capabilities. However, no quantitative method has been available to express these abilities precisely. To address this limitation, the Hussain model (Hussain et al., 2019) was employed to calculate the percentages of exploration and exploitation, as well as their changing trends as the number of iterations increased. Note that although FEs is utilized to evalute the performance of MHS, ECO as well as many other MHS algorithms are designed by iterative search methods. Thus, a number of iterations is adopted for the analysis of the exploration and exploitation ability of ECO. The formulas are as follows:

$$Exploration = \frac{Div(k)}{Div_{\text{max}}} \times 100\%, \tag{24}$$

Exploitation =
$$\frac{Div_{\text{max}} - \text{Div}(k)}{Div_{\text{max}}} \times 100\%$$
, (25)

$$Div(k) = \frac{1}{p} \sum_{j=1}^{p} \left[\frac{1}{p} \sum_{i=1}^{p} \left| \text{median}(x_j(k)) - x_{i,j}(k) \right| \right], \quad (26)$$

$$Div_{\text{max}} = \max(Div(k)),$$
 (27)

where Div(k) represents the diversity of the MHS algorithms after the kth iteration of a single search, median $(x_j(k))$ denotes the median value of the jth dimension of all search particles after the kth iteration, $x_{i,j}(k)$ is the value of the jth

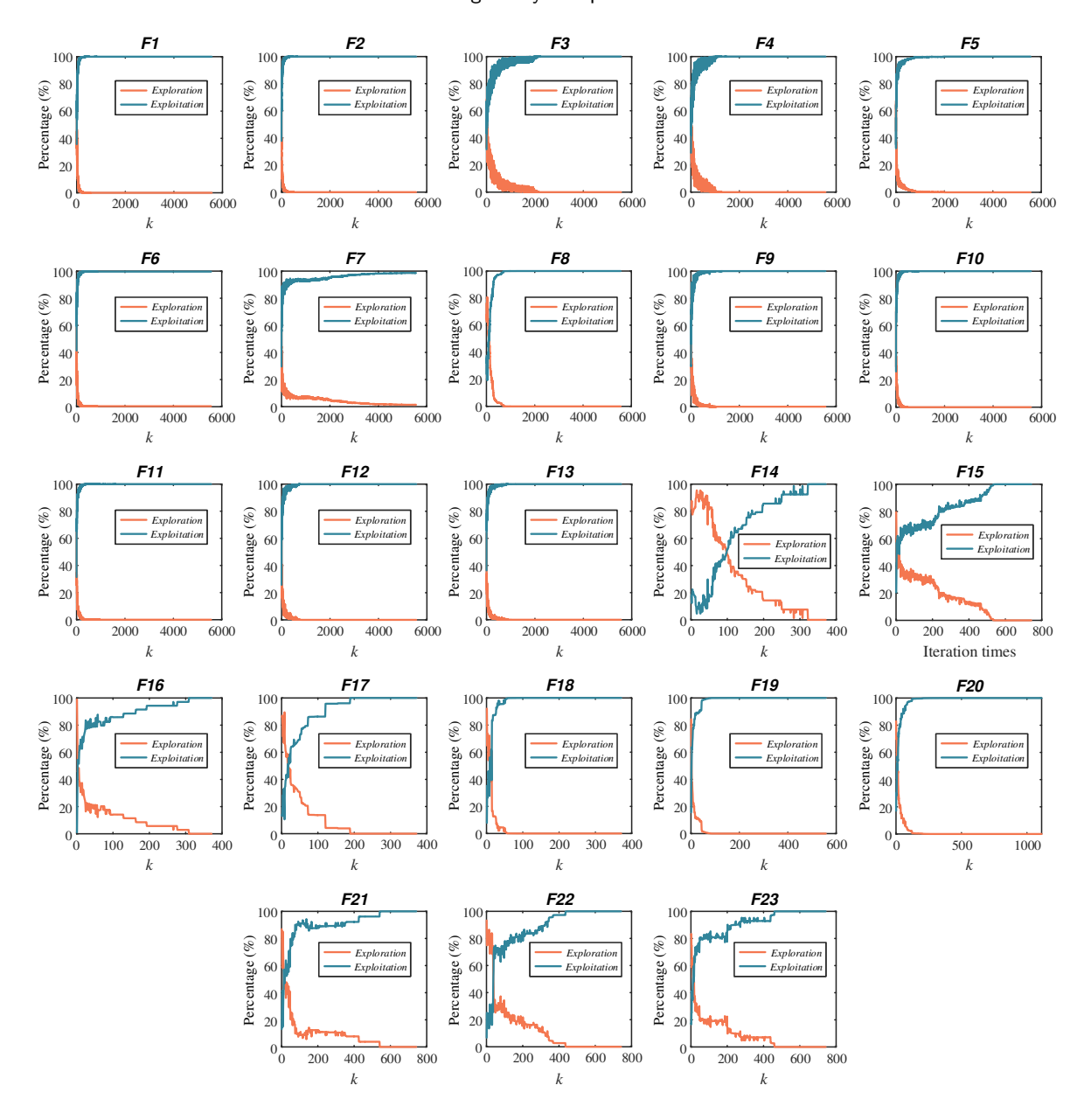


Figure 6: Exploration - exploitation balance curve of ECO on 23 classic benchmark functions.

dimension of the ith particle, and p is the total number of search particles.

Based on these calculations, the *exploration-exploitation* curve of ECO on the 23 classic optimization functions is plotted, as shown in Fig. 6. ECO maintains a high *exploration* percentage during the early stages of the search, ensuring its ability to escape local optima. As the number of iterations increases, the *exploration* percentage decreases rapidly, while the *exploitation* percentage increases, eventually reaching 100%, thereby demonstrating ECO's excellent *exploitation* ability.

5.3. ECO for constrained problems on CEC-2006

In this section, the performance of ECO in solving constrained problems is verified. The characteristics of the

optimization functions CEC-2006 test suite are shown in Table 25. For detailed constraints of these functions, please refer to the technical report (Liang et al., 2006).

Due to the fact that CEC-2006 is known for its complex constraint conditions but without overly complicated optimization functions, all MHS algorithms have the characteristic of converging relatively quickly when solving the optimization functions of this test suite. Therefore, in this section, we only focus on analyzing the numerical results of ECO and each of the comparison algorithms and verifying whether they satisfy the constraint conditions.

Following by the technical report, the experimental parameters are set as follows: the search termination criterion MaxFEs = 500,000 and the number of independent runs

 Table 7

 Numerical results of ECO and competing MHS algorithms on 23 classic optimization functions.

lo.	Index	ECO	CS	HS	PSO	GWO	WOA
71	Min	0.00000E+00	3.32792E-34	1.17101E-02	1.45960E-06	0.00000E+00	0.00000E+00
	Ave	0.00000E+00	1.24257E-31	1.57320E-02	5.56363E-06	0.00000E+00	0.00000E+00
	Std	0.00000E+00	2.00575E-31	2.49723E-03	2.95213E-06	0.00000E+00	0.00000E+00
2	Min	0.00000E+00	3.86475E-16	2.84180E-01	1.99481E-02	0.00000E+00	0.00000E+00
	Ave	0.00000E+00	1.28546E-15	3.33412E-01	1.27238E-01	0.00000E+00	0.00000E+00
	Std	0.00000E+00	6.40637E-16	3.48474E-02	1.10784E-01	0.00000E+00	0.00000E+00
3	Min	0.00000E+00	3.05721E-05	8.89746E-01	3.77799E-04	1.94130E-215	1.21362E-03
	Ave	0.00000E+00	2.76531E-04	4.73536E+00	1.05380E-03	6.74406E-175	2.98306E+01
	Std	0.00000E+00	3.30982E-04	3.90565E+00	5.38232E-04	0.00000E+00	6.58807E+01
4	Min	0.00000E+00	4.11866E-03	6.61464E-02	5.57405E-02	5.87876E-158	1.13853E-12
	Ave	0.00000E+00	2.63188E-01	7.90247E-02	1.20844E-01	3.59577E-153	7.90953E-01
	Std	0.00000E+00	2.63575E-01	4.13891E-03	5.61101E-02	1.14004E-152	2.26563E+00
75	Min	2.92753E-09	8.67840E-04	1.26157E+01	1.37017E+01	2.48292E+01	2.39297E+01
	Ave	1.96849E-07	4.15557E+00	1.13721E+02	3.55310E+01	2.63927E+01	2.42981E+01
	Std	2.19375E-07	3.65001E+00	7.14675E+01	2.27422E+01	8.87104E-01	3.17043E-01
6	Min	0.00000E+00	0.00000E+00	0.00000E+00	1.95927E-06	0.00000E+00	0.00000E+00
	Ave	0.00000E+00	0.00000E+00	0.00000E+00	5.95734E-06	0.00000E+00	0.00000E+00
	Std	0.00000E+00	0.00000E+00	0.00000E+00	4.39921E-06	0.00000E+00	0.00000E+00
7	Min	2.98786E-07	3.87959E-05	8.03928E-03	3.59086E-03	1.74696E-05	1.01427E-05
	Ave	4.17000E-06	1.55654E-03	1.61762E-02	1.88778E-01	6.31169E-05	1.62265E-04
	Std	2.74771E-06	1.41529E-03	3.20017E-03	6.79995E-01	3.73483E-05	1.50868E-04
8	Min	-1.25695E+04	-1.25695E+04	-1.25695E+04	-8.48020E+03	-7.38371E+03	-1.25695E+04
-	Ave	-1.25695E+04	-1.25695E+04	-1.25695E+04	-3.79540E+03	-5.95350E+03	-1.24978E+04
	Std	1.85009E-12	6.01099E-06	3.31192E-04	1.84225E+03	8.27409E+02	1.74804E+02
9	Min	0.00000E+00	5.68434E-14	9.74546E+00	1.89048E+01	0.00000E+00	0.00000E+00
	Ave	0.00000E+00	1.90462E+00	1.47769E+01	4.41439E+01	0.00000E+00	0.00000E+00
	Std	0.00000E+00	3.19252E+00	3.29223E+00	1.76200E+01	0.00000E+00	0.00000E+00
10	Min	4.44089E-16	3.99680E-15	8.63799E-02	2.81411E+00	3.99680E-15	4.44089E-16
10	Ave	4.44089E-16	7.78636E-15	1.23323E-01	4.43090E+00	7.43109E-15	2.33887E-15
	Std	3.00880E-31	5.01852E-15	1.37144E-02	1.00657E+00	6.48634E-16	2.23398E-15
11	Min	0.00000E+00	0.00000E+00	4.60431E-04	2.46219E-07	0.00000E+00	0.00000E+00
1 1	Ave	0.00000E+00	0.00000E+00	1.82971E-02	1.45864E-02	0.00000E+00	2.90711E-04
	Std	0.00000E+00 0.00000E+00	0.00000E+00	2.30154E-02	1.54834E-02	0.00000E+00	1.59229E-03
12	Min	1.69155E-32	1.66735E-32	7.67628E-05	7.07487E-08	6.65551E-03	3.57704E-07
12	Ave		7.93897E-29		2.90504E-01		1.07792E-06
		1.81418E-32		1.12367E-04		2.69604E-02	
12	Std	5.79191E-34	3.50427E-28	1.90215E-05	3.92543E-01	1.41768E-02	4.28570E-07
13	Min	2.70564E-32	3.93823E-32	1.40403E-03	4.38395E-07	1.00012E-01	6.53238E-06
	Ave	5.49541E-32	1.46772E-30	5.60061E-03	3.66602E-03	4.41727E-01	4.04267E-04
1.4	Std	1.36816E-32	3.65022E-30	5.22256E-03	5.26923E-03	2.04395E-01	2.00590E-03
14	Min	9.98004E-01	9.98004E-01	9.98004E-01	9.98004E-01	9.98004E-01	9.98004E-01
	Ave	9.98004E-01	9.98004E-01	9.98004E-01	1.26304E+00	4.64744E+00	1.94670E+00
	Std	3.38761E-16	4.43888E-13	3.13541E-14	5.17216E-01	4.59033E+00	2.49449E+00
15	Min	3.07486E-04	3.07486E-04	4.35158E-04	3.07486E-04	3.07487E-04	3.07765E-04
	Ave	3.07486E-04	3.07865E-04	3.37991E-03	1.06526E-03	5.08396E-03	6.22439E-04
	Std	3.65182E-19	9.28385E-07	6.78888E-03	3.65650E-03	8.57776E-03	3.78524E-04
16	Min	-1.03163E+00	-1.03163E+00	-1.03163E+00	-1.03163E+00	-1.03163E+00	-1.03163E+00
	Ave	-1.03163E+00	-1.03163E+00	-1.03163E+00	-1.03163E+00	-1.03163E+00	-1.03163E+00
	Std	0.00000E+00	7.01237E-14	1.29794E-07	0.00000E+00	5.28743E-09	1.99186E-09
17	Min	3.97887E-01	3.97887E-01	3.97887E-01	3.97887E-01	3.97887E-01	3.97887E-01
	Ave	3.97887E-01	3.97887E-01	3.97888E-01	3.97887E-01	3.97887E-01	3.97890E-01
	Std	1.12920E-16	1.53258E-11	2.41376E-07	1.12920E-16	1.80713E-07	3.63548E-06
18	Min	3.00000E+00	3.00000E+00	3.00000E+00	3.00000E+00	3.00000E+00	3.00000E+00
	Ave	3.00000E+00	3.00000E+00	8.42784E+00	3.00000E+00	3.00003E+00	3.00003E+00
	Std	4.51681E-16	1.05918E-13	1.09716E+01	6.63730E-15	3.66926E-05	3.60477E-05
19	Min	-3.86278E+00	-3.86278E+00	-3.86278E+00	-3.86278E+00	-3.86278E+00	-3.86278E+00
	Ave	-3.86278E+00	-3.86278E+00	-3.86278E+00	-3.86147E+00	-3.86172E+00	-3.8588E+00
	Std	2.71009E-15	2.71009E-15	3.74222E-07	2.98749E-03	2.36754E-03	7.99528E-03
20	Min	-3.32200E+00	-3.32200E+00	-3.32199E+00	-3.32200E+00	-3.32200E+00	-3.32199E+00
	Ave	-3.32200E+00	-3.32200E+00	-3.31010E+00	-3.17501E+00	-3.26816E+00	-3.24412E+00
	Std	1.35504E-15	3.10877E-14	3.62773E-02	1.56896E-01	6.31640E-02	7.98470E-02
21	Min	-1.01532E+01	-1.01532E+01	-1.01532E+01	-1.01532E+01	-1.01532E+01	-1.01532E+01
	Ave	-1.01532E+01	-1.01532E+01	-4.16470E+00	-5.73610E+00	-9.64488E+00	-9.38974E+00
	Std	1.80672E-15	1.07347E-11	3.04551E+00	3.50937E+00	1.55092E+00	2.00926E+00
22	Min	-1.04029E+01	-1.04029E+01	-1.04029E+01	-1.04029E+01	-1.04029E+01	-1.04029E+01
	Ave	-1.04029E+01	-1.04029E+01	-5.38010E+00	-9.11089E+00	-1.01622E+01	-8.44745E+00
	Std	0.00000E+00	9.81490E-11	3.37023E+00	2.68307E+00	1.31837E+00	3.11150E+00
	Min	-1.05364E+01	-1.05364E+00	-1.05364E+01	-1.05364E+01	-1.05364E+01	-1.05364E+01
23		-1.ひころひサレナリエ	-1.UJJU4ETUU	-1.05504ET01	-1.05504E+01	-1.05504ET01	-1.05504ET01
23	Ave	-1.05364E+01	-1.05364E+01	-5.89925E+00	-8.33944E+00	-1.02659E+01	-8.80730E+00

N=25. Solutions of MHS algorithms including Min, Ave, and Std on every optimization functions will be recorded.

From the results on Table 8, it can be seen that ECO and CS have demonstrated extremely outstanding performance in solving constrained problems, achieving the optimal Ave

on nearly half of the optimization functions. PSO also shows decent solving capabilities, but it is worth noting that although PSO does not achieve better Ave on many optimization functions, its obtained Min value can be comparable to ECO and CS, indicating that its performance ceiling is

Table 8Numerical results of ECO and competing MHS algorithms on 24 CEC-2006 optimization functions.

No.	Index	ECO	CS	HS	PSO	GWO	WOA
F1	Min	-1.50000E+01	-1.50000E+01	-1.49988E+01	-7.00000E+00	-1.49987E+01	-1.29219E+01
	Ave	-1.50000E+01	-1.39437E+01	-1.49975E+01	1.31933E+09	-1.10337E+01	-5.55741E+00
	Std	2.99111E-11	1.66762E+00	8.91424E-04	1.37100E+09	1.81035E+00	3.32401E+00
F2	Min	-1.33986E-01	-1.34340E-01	-1.33166E-01	-1.34343E-01	-1.34279E-01	-1.34343E-01
	Ave	-1.33463E-01	-1.34118E-01	-1.32478E-01	-1.33281E-01	2.24801E+02	2.24816E+02
	Std	3.56887E-04	1.91323E-04	3.14841E-04	7.57747E-04	1.12467E+03	1.12475E+03
F3	Min	-1.00050E+00	-1.00050E+00	-9.99930E-01	0.00000E+00	-1.00050E+00	-2.92901E-02
	Ave	-1.00050E+00	-1.00050E+00	-9.98269E-01	0.00000E+00	-1.20061E-01	-1.87413E-03
	Std	4.53247E-16	3.15328E-10	9.88406E-04	0.00000E+00	3.31827E-01	6.70374E-03
F4	Min	-3.06655E+04	-3.06655E+04	-3.06652E+04	-3.06655E+04	-3.06655E+04	-3.06182E+04
	Ave	-3.06655E+04	-3.06655E+04	-3.06646E+04	-3.06655E+04	-3.06653E+04	-3.03980E+04
	Std	7.42599E-12	7.42599E-12	5.25680E-01	7.42599E-12	1.05984E-01	1.44397E+02
F5	Min	5.12655E+03	1.00000E+10	5.17351E+03	5.12754E+03	6.99468E+03	5.14553E+03
	Ave	5.14771E+03	1.00000E+10	1.36019E+04	5.65480E+03	2.80211E+04	6.16259E+05
	Std	1.56830E+01	0.00000E+00	1.24032E+04	4.04337E+02	2.92030E+04	1.50544E+06
F6	Min	-6.96181E+03	-6.96181E+03	-6.96004E+03	-6.96181E+03	-6.96163E+03	-6.96178E+03
	Ave	-6.96181E+03	-6.96181E+03	-6.95881E+03	1.82611E+14	7.54428E+09	3.39493E+10
	Std	3.71300E-12	4.03487E-07	6.09729E-01	8.81538E+14	2.61115E+10	4.61991E+10
F7	Min	2.43086E+01	2.43062E+01	2.46331E+01	2.43840E+01	2.45475E+01	2.60297E+01
	Ave	2.43280E+01	2.43062E+01	2.60419E+01	2.54339E+01	1.00472E+02	3.91416E+01
	Std	1.57018E-02	4.39120E-06	8.86221E-01	1.35983E+00	2.28121E+02	1.39166E+01
F8	Min	-9.58250E-02	-9.58250E-02	-9.58250E-02	-9.58250E-02	-9.58250E-02	-9.58250E-02
	Ave	-9.58250E-02	-9.58250E-02	-9.04905E-02	-9.58250E-02	-9.58250E-02	-9.58250E-02
T 0	Std	0.00000E+00	0.00000E+00	1.84632E-02	0.00000E+00	1.86883E-10	3.83784E-12
F9	Min	6.80630E+02	6.80630E+02	6.80666E+02	6.80632E+02	6.80649E+02	6.83341E+02
	Ave	6.80631E+02	6.80630E+02	6.80768E+02	1.47474E+10	6.85116E+02	6.90691E+02
E10	Std	3.55665E-04	1.95352E-11	7.56083E-02	7.37368E+10	7.29141E+00	5.53814E+00
F10	Min	7.07909E+03	7.04925E+03	7.17694E+03	7.19626E+03	7.05644E+03	9.17120E+03
	Ave Std	7.20910E+03	7.04935E+03 3.66426E-01	1.13667E+04	2.49760E+06	7.57081E+03	2.49858E+06
F11	Min	8.28189E+01 7.5000 E- 01	7.50000E-01	3.83579E+03 7.50003E-01	8.33129E+06 7.5000 E- 01	2.95351E+02 7.50000E-01	6.60498E+06 7.50000E-01
F 11	Ave	7.5000E-01 7.50000E-01	7.5000E=01 7.50146E=01	7.51109E-01	9.80000E-01	7.5000E=01 7.50001E=01	7.50352E-01
	Std	2.26623E-16	5.42786E-04	1.40116E-03	6.92219E-02	1.14161E-06	1.75351E-03
F12	Min	-1.00000E+00	-1.00000E+00	-1.00000E+00	-1.00000E+00	-1.00000E+00	-1.00000E+00
1 12	Ave	-1.00000E+00	-1.00000E+00	-1.00000E+00	-1.00000E+00	-1.00000E+00	-1.00000E+00
	Std	0.00000E+00	0.00000E+00	8.14614E-13	0.00000E+00	1.50727E-11	4.05561E-12
F13	Min	1.76031E-01	4.81028E-01	1.00000E+08	3.15418E-01	1.00000E+08	6.44914E-02
1 10	Ave	7.11535E-01	9.60000E+07	1.00000E+08	4.03854E+06	1.00080E+08	8.40000E+07
	Std	2.10921E-01	2.00000E+07	3.57698E-01	2.01927E+07	2.76886E+05	3.74166E+07
F14	Min	-4.77466E+01	-4.77623E+01	-4.59923E+01	-4.73276E+01	-4.60146E+01	-4.52982E+01
	Ave	-4.76770E+01	-4.77623E+01	-4.26829E+01	-4.42671E+01	-4.27795E+01	-4.24557E+01
	Std	4.46072E-02	1.91641E-06	1.54905E+00	1.89938E+00	1.82702E+00	2.03895E+00
F15	Min	9.61715E+02	9.61715E+02	9.61761E+02	9.61715E+02	9.61715E+02	9.62100E+02
	Ave	9.61715E+02	9.61715E+02	9.65512E+02	7.27371E+03	1.37097E+03	2.07151E+04
	Std	0.00000E+00	0.00000E+00	3.04672E+00	3.15578E+04	2.03385E+03	5.20995E+04
F16	Min	-1.90516E+00	-1.90507E+00	-1.90483E+00	-1.90516E+00	-1.90419E+00	-1.88866E+00
	Ave	-1.90516E+00	5.20000E+09	-1.76990E+00	-1.90373E+00	-1.90271E+00	6.08665E+14
	Std	3.73894E-15	5.09902E+09	1.00498E-01	1.66618E-03	9.18783E-04	3.04332E+15
F17	Min	8.85688E+03	8.85707E+03	8.92761E+03	8.86942E+03	8.94121E+03	8.89262E+03
	Ave	8.91720E+03	8.89087E+03	9.04902E+03	8.95929E+03	4.12862E+06	1.67634E+04
	Std	2.91549E+01	1.96436E+01	1.33742E+02	6.73300E+01	2.05762E+07	1.76802E+04
F18	Min	-8.65959E-01	-6.10505E-01	-8.62316E-01	-8.65977E-01	-8.65908E-01	-8.53362E-01
	Ave	-8.64729E-01	8.40000E+09	-7.53608E-01	-7.84301E-01	-7.60727E-01	-6.75695E-01
F10	Std	9.51943E-04	3.74166E+09	9.31999E-02	1.43938E-01	1.33298E-01	1.22228E-01
F19	Min	3.45598E+01	3.27547E+01	4.22366E+01	3.35098E+01	3.32314E+01	5.42614E+01
	Ave	3.85929E+01	3.29957E+01	5.99311E+01	7.38944E+01	4.13167E+01	1.15555E+02
E20	Std	1.93540E+00	1.91972E-01	9.49342E+00	4.21077E+01	7.55958E+00	3.96872E+01
F20	Min	2.38535E+03	2.37102E+03	8.17501E+03	3.10808E+04	2.39567E+03	8.07232E+03
	Ave	2.46998E+03	2.37103E+03	1.35242E+04	4.51147E+07	4.13502E+03	7.67509E+04 4.06554E+04
F21	Std Min	6.91451E+01 1.93787E+02	1.11280E-02 1.93787E+02	2.99928E+03 1.94009E+02	1.28593E+08 2.87949E+02	2.86433E+03 4.28657E+02	4.06554E+04 2.59102E+02
1.71	Ave	1.93787E+02 1.93787E+02	1.93787E+02 1.93921E+02	1.94009E+02 2.70722E+04	2.87949E+02 2.45978E+08	4.28057E+02 7.82534E+02	2.39102E+02 1.83378E+08
	Std	1.93787E+02 4.64703E-04	6.68361E=01	7.46227E+04	4.07180E+08	7.82534E+02 2.13265E+02	6.34753E+08
F22	Min	6.67974E+19	1.00000E+10	9.89945E+28	1.45477E+38	1.17219E+28	6.31507E+28
1 44	Ave	4.21036E+22	1.00000E+10 1.00000E+10	1.40856E+30	1.72293E+39	4.51835E+33	1.48352E+34
	Std	3.96940E+22	0.00000E+10	1.46091E+30	1.77227E+39	7.52153E+33	1.58928E+34
F23	Min	-6.57118E-02	0.00000E+00	3.70634E+11	-2.99868E+02	9.00000E+02	0.00000E+00
1 23	Ave	-3.42413E-03	0.00000E+00	1.37856E+19	3.99955E+18	1.46492E+19	0.00000E+00
	Std	1.35717E-02	0.00000E+00	2.02094E+19	9.35309E+18	3.16691E+19	0.00000E+00
E2.4	Min	-5.50801E+00	-5.50801E+00	-5.50798E+00	-5.50801E+00	-5.50799E+00	-5.50457E+00
F 24							
F24	Ave	-5.50801E+00	-5.50801E+00	-5.50644E+00	-5.50801E+00	-5.50795E+00	-5.48502E+00

good but lacks stability. HS, GWO, and WOA do not have particularly outstanding performance, suggesting that their performance in solving constrained problems is limited.

The ranking based on the Friedman mean rank algorithm is shown on Table 9. ECO ranks first with outstanding performance. The results of the Wilcoxon rank-sum test are presented on Table 10. It can be seen that ECO and CS have been competing against each other in different optimization functions, and they are evenly matched in 7 optimization functions. Although PSO does not have a significantly better performance than ECO, it can also tie with ECO in 7 functions.

All solution outputs generated by MHS algorithms are rigorously verified through systematic examination. The spatial coordinates of all search particles and the obtained optimal solutions are confirmed to strictly satisfy all specified constraints while remaining within the predefined solution boundaries.

6. Comparison of ECO and 50 SOTA MHS

In previous chapter, the superior performance of ECO in addressing both unconstrained and constrained optimization problems is successfully demonstrated. To further investigate its performance potential, a candidate pool comprising 50 SOTA MHS algorithms published in academia over the past ten years, along with ECO, is established. Experiments are conducted on CEC-2014 and CEC-2017 test suites, and rankings are generated based on the obtained numerical results.

Subsequently, the top 5 MHS algorithms (excluding ECO) are selected for further competing MHS algorithms against ECO on CEC-2020 test suite. Comprehensive analyses encompassing solution accuracy and convergence speed are performed, and a qualitative analysis of ECO's characteristics is completed.

6.1. Competing algorithms and parameter settings

The parameter configurations of the 50 SOTA MHS algorithms in the algorithms candidate pool are summarized in Table 11. To ensure that all algorithms in the candidate pool perform at their optimal capacity, thereby enhancing the credibility of experimental results, all parameters of these algorithms are configured according to the optimal values reported in their original publications, with the exception of the customized population size, which is uniformly set to 30.

6.2. 51 SOTA MHS algorithms competition

In this section, the experimental details of the algorithm pool comprising 51 MHS algorithms (including ECO) are provided, as well as the experimental parameter settings. Detailed information of CEC-2014 and CEC-2017 can be found in Table 26 and Table 27. Finally, the numerical results of these MHS algorithms on the CEC-2014 and CEC-2017 test suites are analyzed, and their comprehensive performance rankings across these two benchmarks are derived.

Table 9Friedman mean rank of ECO and competing MHS algorithms on CEC-2006 benchmark.

MHS	ECO	CS	GWO	HS	PSO	WOA
Friedman	1.38	2.04	4.17	4.00	3.79	5.04
Rank	1	2	5	4	3	6

Table 10Wilcoxon rank-sum test results between ECO and competing MHS algorithms on 24 CEC-2006 optimization functions.

ECO vs.	CS	HS	PSO	GWO	WOA
+/=/-	9/7/8	24/0/0	17/7/0	24/0/0	24/0/0

Following by the technical report, the experimental parameters are set to as follows: the search termination criterion MaxFEs = $10,000 \times D$ and the number of independent runs N=51. Solutions of MHS algorithms including Min, Ave, and Std on every optimization functions will be recorded.

In this section, D=10 is adopted, as this dimensionality aligns with practical optimization scenarios, ensuring computational efficiency while maintaining result representativeness and statistical significance (in subsequent CEC-2020 experiments, scalability analyses for ECO and the top five algorithms are conducted at D=30/50/100 to validate their robustness in higher-dimensional problems). MHS algorithms are ranked 1–51 on each optimization function based on the following priority: smaller Ave, followed by Min and Std. Then, the Friedman test is adopted and Friedman mean rank across all optimization functions is calculated, and global performance rankings are generated accordingly. MHS algorithms with lower mean ranks are deemed superior in solving the CEC-2014 and CEC-2017 test suites.

After N = 51 independent repeated trials, the numerical results of all algorithms are shown in Table 29 and Table 30 (noted that only Ave values are listed due to massive data volume). It can be clearly seen that ECO has achieved the best Ave on the most optimization functions in both CEC-2014 and CEC-2017.

To identify the most competitive MHS, the numerical results are first subjected to the Friedman test, yielding p-value $< \alpha$. Consequently, all the MHS algorithms are globally ranked according to their Friedman mean ranks, with the results summarized in Table 12.

ECO is observed to achieve the first position among all MHS algorithms on CEC-2014 and CEC-2017 test suites. Besides the top five competitive MHS algorithms are ARO (Wang et al., 2022), CFOA (Jia et al., 2024), CSA (Braik, 2021), WSO (Braik et al., 2022), and INFO (Ahmadianfar et al., 2022) (in descending order of mean rank). These six algorithms are further analyzed comprehensively in the subsequent section.

Table 11
Competing MHS algorithms and parameter settings of MHS SOTA pool.

MHS	Parameters settings	Ref.	Year
ECO	1	This article	2025
AO	Exploitation adjustment parameters $\alpha = 0.1$ and $\delta = 0.1$	(Abualigah et al., 2021c)	2021
AOA	Sensitive parameter $\alpha = 5$, control parameter $\mu = 0.5$	(Abualigah et al., 2021b)	2021
ARO	Hiding parameter H decreases from 1 to $1/T$ (T is the maximal number of iterations)	(Wang et al., 2022)	2022
AVOA	Measurement parameters $L_1 = 0.8$ and $L_2 = 0.2$, fixed parameter $w = 2.5$,	(Abdollahzadeh et al., 2021)	2021
	strategy selection parameters $P_1 = 0.6$, $P_2 = 0.4$, and $P_3 = 0.6$		
BFO	Distribution radius $R = 0$, random function $U(1) = 1$, initial step-jump parameter $J(1) = 1$	(Zareian et al., 2024)	2024
BKA	Attack behavior control parameter $p = 0.9$	(Wang et al., 2024)	2024
BOA	Sensory modality $c = 0.01$, power exponent a increases from 0.1 to 0.3, switch probability $p = 0.8$	(Arora and Singh, 2019)	2019
BWO	Whale fall probability W_f decreases from 0.1 to 0.05	(Zhong et al., 2022)	2022
CFOA	Move offset r_3 changes from either -1 or 1 toward 0, parameter $r_4 = 1, 2, \text{ or } 3$	(Jia et al., 2024)	2024
COA	Integer $I = 1$ or 2	(Dehghani et al., 2023)	2023
CSA	Constants $p_1 = 0.25$, $p_2 = 1.5$, $\rho = 1$, $c_1 = 1.75$, $c_2 = 1.75$, $\alpha = 3.5$, $\beta = 3$, and $\gamma = 1$, prey perception probability $P_p = 0.1$	(Braik, 2021)	2021
CTCM DBO	Tribes size $m = 20$, experience factor $c_1 = 2$, obey factor $c_2 = 1$, escape factor $c_3 = 0.1$	(Chen et al., 2025)	2025 2023
DMO	Deflection coefficient $k = 0.1$, natural coefficient $\alpha = -1$ or 1, probability value $\lambda = 0.1$, parameters $b = 0.3$ and $S = 0.5$	(Xue and Shen, 2023)	
DOA	The number of babysitters $bs = 3$, alpha female's vocalization $peep = 2$	(Agushaka et al., 2022) (Lang and Gao, 2025)	2022 2025
	Demarcation iteration number $T_d = 0.9T_{\text{max}}$ (T_{max} is the maximal number of iterations), strategy execution ratio $u = 0.9$		
ESOA ETO	Step factors $step_a = 0.1$ and $step_b = 0.5$	(Chen et al., 2022) (Luan et al., 2024)	2022 2024
EIO	Adjustment coefficients $a = 4.6$ and $b = 1.55$ Reflectance $\alpha = 0.2$, the first-half refraction ratio $Para_1$ changes from either -2 or 2 toward 0,	(Luaii et al., 2024)	2024
FATA	the second-half refraction ratio $Para_1$ changes from 0 toward either -150 or 150	(Qi et al., 2024)	2024
FHO	The maximum number of fire hawks r is a random integer from 1 to the population size divided by 5 and rounded up	(Azizi et al., 2023b)	2023
FLA	The maximum number of the hawks r is a random integer from 1 to the population size divided by 3 and founded up. The number of water particles evaporate $N_e = 5$	(Ghasemi et al., 2024)	2023
FOX	Jump movement parameters $c_1 = 0.18$ and $c_2 = 0.82$	(Mohammed and Rashid, 2023)	2024
GGO	Parameter a decreases from 2 to 0	(El-Kenawy et al., 2024)	2023
GJO	Constants $c_1 = 1.5$ and $\beta = 1.5$, E_1 decreases from 1.5 to 0	(Chopra and Ansari, 2022)	2024
GOOSE	Parameter α decreases from 2 to 0	(Hamad and Rashid, 2024)	2024
GPC	Gravity $g = 9.8$, ramp angle $\theta = 10$, minimum friction $\mu_{k,\text{min}} = 1$, maximum friction $\mu_{k,\text{max}} = 10$, substitution probability $= 0.5$	(Harifi et al., 2021)	2024
HBA	Honey badger foraging ability parameter $\beta = 6$, constant $C = 2$	(Hashim et al., 2022)	2021
HGS	Hunger threshold $LH = 100$, parameter $l = 0.03$	(Yang et al., 2021)	2021
НО	Integers $I_1 = 1$ or 2, $I_2 = 1$ or 2, $\rho_1 = 0$ or 1, and $\rho_2 = 0$ or 1, constant $\theta = 1.5$	(Amiri et al., 2024)	2024
HOA	Hiker sweep factor $\alpha = 1, 2, \text{ or } 3$	(Oladejo et al., 2024)	2024
IAO	Quality factor Φ increases from -0.99 to 0	(Wu et al., 2024)	2024
INFO	Constants $c = 2$ and $d = 4$	(Ahmadianfar et al., 2022)	2022
MFO	Convergence constant r decreases from -1 to -2 , logarithmic spiral shape constant $b=1$	(Mirjalili, 2015)	2015
NRBO	Deciding factor $DF = 0.6$	(Sowmya et al., 2024)	2024
PDO	Food source alarm $\rho = 0.1$, food source quality $\epsilon = 2.2204E - 16$, individual prairie dog difference $\Delta = 0.005$	(Ezugwu et al., 2022)	2022
	Constant $\beta = 1.5$, cluster size factor $\rho = 0.04$, the minimum possible population size $S_{\min} = 5$,		
PEOA	probability $p = 0.33$, memory size $H = 0.2$	(Enriquez et al., 2022)	2022
DIO	Map and compass factor $R = 0.2$, the maximum generations for map-compass operation $Nc_{1\text{max}} = 150$,	(D. 10; 2014)	2014
PIO	the maximum generations for landmark operation $Nc_{2\text{max}} = 200$	(Duan and Qiao, 2014)	2014
PKO	Beating factor $BF = 8$, predatory efficiency of the pied kingfisher $PE_{\text{max}} = 0.5$ and $PE_{\text{min}} = 0$	(Bouaouda et al., 2024)	2024
PO	Adjustable parameters $PF_1 = 0.5$, $PF_2 = 0.5$, $PF_3 = 0.3$, and $U = 0.2$	(Abdollahzadeh et al., 2024)	2024
RIME	Step function parameter $w = 5$	(Su et al., 2023)	2023
RSA	Sensitive parameters $\alpha = 0.1$ and $\beta = 0.1$	(Abualigah et al., 2022)	2022
RUN	Control parameters $a = 20$ and $b = 12$	(Ahmadianfar et al., 2021)	2021
SAO	Olfaction capacity of $f = 0.75$, step length constant $SL = 0.9$	(Salawudeen et al., 2021)	2021
SCA	Constant $a = 2$	(Mirjalili, 2016)	2016
SCSO	Cat sensitivity r_G decreases from 2 to 0	(Seyyedabbasi and Kiani, 2023)	2023
SMA	Parameter v_c changes from either -1 or 1 toward 0, parameter $z = 0.03$	(Li et al., 2020)	2020
SO	Constants $c_1 = 0.5$, $c_2 = 0.05$, and $c_3 = 2$	(Hashim and Hussien, 2022)	2022
SRS	Lorentz force constant $\mu = 1$	(Goodarzimehr et al., 2022)	2022
SSA	Safety threshold $ST = 0.8$	(Xue and Shen, 2020)	2020
TSA	Switch parameter $P_{\text{switch}} = 0.3$, escape probability $P_{\text{esc}} = 0.8$	(Layeb, 2022)	2022
	Maximum undulation frequency $f_{\text{max}} = 0.75$, minimum undulation frequency $f_{\text{max}} = 0.07$,		
WSO	acceleration coefficient $\tau = 4.125$, positive constants $a_0 = 6.25$, $a_1 = 100$, and $a_2 = 0.0005$	(Braik et al., 2022)	2022

Note: All parameters remain consistent with those used in the original publications.

6.3. Performance of 6 winning MHS algorithms on CEC-2020

In this section, ECO is systematically compared with ARO, CFOA, CSA, WSO, and INFO on CEC-2020 test suite. Detailed information of CEC-2020 can be found in Table 28. A comparative analysis will be conducted to evaluate their solution accuracy and convergence rates. Additionally, a qualitative assessment of ECO will be performed to characterize its algorithmic behavior and optimization mechanisms.

Following by the technical report, the experimental parameters are set as follows: the search termination criterion

MaxFEs = $10,000 \times D$, where D = 30/50/100, and the number of independent runs N = 30. Solutions of MHS algorithms including Min, Ave, and Std on every optimization functions will be recorded.

6.3.1. Statistical analysis

The average solution values of the six algorithms are shown in Table 15, with their Friedman mean ranks and global rankings provided in Table 13.

ECO demonstrates statistically significant superiority across all tested dimensions and optimization functions, achieving a Friedman rank of 1 in all dimensional scenarios.

Table 12
Friedman mean rank of ECO and competing MHS algorithms on CEC-2014 and CEC-2017 benchmark.

MHS	Frie	dman	Mean	Rank	MHS	Fried	lman	Mean	Rank	MHS	Fried	lman	Mean	Rank
11115	CEC14	CEC17			1,1110	CEC14	CEC17			11110	CEC14	CEC17		
ECO	3.23	2.41	2.82	1	BFO	18.50	18.93	18.72	18	MFO	30.57	31.10	30.84	35
ARO	7.53	7.21	7.37	2	FLA	19.27	19.97	19.62	19	SCA	33.20	29.59	31.39	36
CFOA	10.40	6.38	8.39	3	AVOA	20.53	22.03	21.28	20	НО	29.57	33.48	31.52	37
CSA	12.63	7.79	10.21	4	CTCM	22.63	21.76	22.20	21	FHO	32.50	31.72	32.11	38
WSO	14.93	9.38	12.16	5	SSA	20.37	24.52	22.44	22	FOX	28.90	37.79	33.35	39
INFO	11.30	13.34	12.32	6	FATA	24.87	21.28	23.07	23	GOOSE	37.53	37.59	37.56	40
PKO	14.90	9.83	12.36	7	DBO	25.13	21.66	23.39	24	AOA	34.30	41.21	37.75	41
RIME	13.83	12.76	13.30	8	BKA	23.07	23.90	23.48	25	DOA	40.27	39.10	39.69	42
IAO	15.70	12.03	13.87	9	ESOA	25.07	23.45	24.26	26	SRS	36.77	44.31	40.54	43
SMA	12.63	15.14	13.89	10	GPC	24.80	24.66	24.73	27	HOA	40.80	41.83	41.31	44
SO	13.80	14.41	14.11	11	AO	27.63	26.59	27.11	28	COA	40.13	45.41	42.77	45
PEOA	16.60	15.41	16.01	12	SCSO	26.70	28.28	27.49	29	PDO	42.33	43.28	42.80	46
RUN	15.83	16.83	16.33	13	PO	29.90	27.41	28.66	30	TSA	43.40	43.17	43.29	47
SAO	17.10	16.21	16.65	14	GJO	29.13	28.83	28.98	31	RSA	42.37	45.21	43.79	48
HBA	16.07	17.34	16.71	15	NRBO	27.47	31.10	29.29	32	GGO	43.47	44.86	44.16	49
DMOA	20.63	14.48	17.56	16	ETO	28.27	31.41	29.84	33	BWO	45.67	47.55	46.61	50
HGS	16.37	20.34	18.36	17	PIO	30.17	29.66	29.91	34	BOA	51.00	51.00	51.00	51

Table 13Friedman mean rank of ECO and competing MHS algorithms on CEC-2020 benchmark.

MHS	ECO	ARO	CFOA	CSA	WSO	INFO
D = 10	1.7	3.6	3.7	3.9	3.3	4.8
D = 30	1.5	4.5	3.7	3.4	4.6	3.3
D = 50	1.2	4.0	3.3	3.3	5.1	4.1
D = 100	1.1	4.1	3.2	3.8	5.0	3.8
Mean	1.4	4.1	3.5	3.6	4.5	4.0
Rank	1	5	2	3	6	4

Notably, its performance improvement becomes more pronounced as dimensionality increases. In high-dimensional complex problems, ECO attains an optimal solution coverage rate exceeding 80%. Furthermore, it exhibits robust consistency across diverse function types, including unimodal, multimodal, hybrid, and composition functions.

Specifically, ECO dominates hybrid and composition functions regardless of dimensionality, while competitors show limited competitiveness—only performing adequately in low-dimensional simple unimodal or multimodal functions. A key observation is that ECO's advantage escalates with higher dimensions, whereas competing algorithms suffer from significant performance degradation and instability under such conditions.

The result of Wilcoxon rank-sum test are shown in Table 14. ECO demonstrates an obvious advantages in any dimension. ARO, CFOA, WSO and INFO can still defeat ECO in a few optimization functions at low dimensions, but they lack scalability and the gap between them and ECO widens further in high-dimensional problems. CSA shows certain scalability and can perform comparably to ECO in a few optimization functions in high-dimensional problems.

Table 14Wilcoxon rank-sum test results between ECO and competing MHS algorithms on 10 CEC-2020 optimization functions.

ECO vs.	ARO	CFOA	CSA	WSO	INFO
D = 10	5/4/1	8/1/1	7/3/0	4/4/2	8/1/1
D = 30	10/0/0	8/2/0	7/3/0	9/1/0	6/1/3
D = 50	10/0/0	7/3/0	7/2/1	9/1/0	7/3/0
D = 100	10/0/0	9/1/0	9/0/1	9/1/0	9/1/0

The solution value distributions can be found in Fig. 10. The numerical results of the vast majority of MHS algorithms show considerable fluctuations, while ECO demonstrates excellent stability. Moreover, the range of numerical results of ECO is significantly lower than that of the others, and only a few data points are considered as abnormal data, further demonstrating the superiority of its stability. In most optimization functions, the search range of MHS algorithms does not fluctuate significantly with the change of dimensions, except for F8 and F9 where the fluctuations are large for all MHS. This indicates that these two optimization functions have higher requirements for performance and scalability.

Ranking variations across functions are in Fig. 11 and dimensional scalability via Friedman ranks are in Fig. 7. From these two figures, we can clearly and intuitively see the advantages of ECO over other MHS. Moreover, as the dimension increases, the performance of ECO becomes increasingly prominent.

6.3.2. Convergence analysis

Subsequently, the convergence speed of these six algorithms is analyzed, and the trajectory of the best-found solutions during each function evaluation is plotted, as shown in Fig. 8.

Table 15
Numerical results of ECO and competing MHS algorithms on 10 CEC-2020 optimization functions.

MHS	Dim	F1	F2	F3	F4	F5	F6	F7	F8	F9	F10
ECO	10	1.69888E+02	1.42045E+03	7.19530E+02	1.90975E+03	1.94903E+03	1.60129E+03	2.13286E+03	2.29502E+03	2.61573E+03	2.89884E+03
	30	3.91671E+02	3.66733E+03	7.97826E+02	2.63556E+03	7.55108E+03	2.09889E+03	6.67077E+03	2.30000E+03	2.88873E+03	2.88612E+03
	50	4.94529E+02	6.65836E+03	9.39196E+02	1.08577E+04	3.36816E+04	2.77739E+03	2.08574E+04	5.16050E+03	3.06083E+03	3.04034E+03
	100	1.18207E+03	1.36097E+04	1.47342E+03	2.85145E+03	2.68771E+05	4.66695E+03	1.01203E+05	1.69576E+04	3.98784E+03	3.25929E+03
ARO	10	3.42848E+02	1.49398E+03	7.29484E+02	1.90113E+03	3.38028E+03	1.73383E+03	2.12820E+03	2.29942E+03	2.68156E+03	2.92546E+03
	30	3.94139E+03	3.93538E+03	9.29419E+02	6.21110E+03	1.52616E+05	2.71890E+03	7.50830E+04	2.40883E+03	2.94995E+03	2.90654E+03
	50	3.03010E+03	7.01877E+03	1.29413E+03	1.56479E+04	2.40186E+05	3.32166E+03	2.25225E+05	8.47836E+03	3.25668E+03	3.07747E+03
	100	7.02664E+03	1.52491E+04	2.60114E+03	4.64283E+03	1.28709E+06	5.47491E+03	8.05184E+05	1.79007E+04	4.50041E+03	3.31934E+03
CFOA	10	1.12471E+03	1.40630E+03	7.16901E+02	1.92728E+03	2.14414E+03	1.64285E+03	2.35023E+03	2.30345E+03	2.71921E+03	2.91564E+03
	30	2.75871E+03	4.05992E+03	8.43367E+02	1.34002E+04	8.75759E+03	2.28803E+03	8.71131E+03	2.30091E+03	2.91081E+03	2.93369E+03
	50	2.11318E+03	6.82116E+03	1.08323E+03	4.96019E+04	4.78035E+04	2.93099E+03	2.55479E+04	5.93024E+03	3.15252E+03	3.08426E+03
	100	4.94413E+03	1.44001E+04	1.97587E+03	5.67482E+05	6.36463E+05	5.61387E+03	2.12387E+05	1.73370E+04	4.16077E+03	3.31593E+03
CSA	10	4.62711E+02	1.67352E+03	7.21313E+02	1.93845E+03	2.03602E+03	1.62964E+03	2.24498E+03	2.30104E+03	2.73399E+03	2.91734E+03
	30	2.17745E+03	4.87468E+03	8.37848E+02	2.64744E+03	1.91104E+04	2.19487E+03	1.55280E+04	3.61051E+03	2.88251E+03	2.91991E+03
	50	2.46879E+03	8.74254E+03	1.03142E+03	1.10791E+04	6.83825E+04	2.91324E+03	5.41499E+04	9.28727E+03	3.04084E+03	3.08196E+03
	100	4.63556E+03	1.93136E+04	1.75849E+03	9.21852E+05	7.00463E+05	5.30729E+03	2.61920E+05	2.14430E+04	3.94856E+03	3.35186E+03
WSO	10	1.75987E+03	1.35203E+03	7.20344E+02	1.90305E+03	1.95305E+03	1.68288E+03	2.15446E+03	2.30934E+03	2.66714E+03	2.92416E+03
	30	4.08451E+03	3.81710E+03	1.03409E+03	5.85880E+03	1.22908E+05	2.44882E+03	1.06668E+05	2.65454E+03	3.36959E+03	2.90142E+03
	50	6.46388E+05	6.61789E+03	1.50047E+03	1.93992E+04	2.44446E+05	3.34518E+03	2.30928E+05	9.00932E+03	4.08150E+03	3.09319E+03
	100	1.27077E+09	1.36704E+04	2.96418E+03	6.75223E+03	8.60074E+05	6.07244E+03	4.74302E+05	1.93469E+04	5.12064E+03	3.56305E+03
INFO	10	1.00000E+02	1.74049E+03	7.33594E+02	1.91262E+03	2.11628E+03	1.73302E+03	2.38399E+03	2.30221E+03	2.75011E+03	2.92850E+03
	30	1.00005E+02	4.93076E+03	9.78514E+02	2.08993E+03	6.93494E+03	2.68436E+03	4.54806E+03	4.87569E+03	2.97208E+03	2.89892E+03
	50	5.21487E+03	8.55075E+03	1.38576E+03	1.44744E+04	4.36648E+04	3.55656E+03	2.12228E+04	9.80709E+03	3.29871E+03	3.05075E+03
	100	6.18795E+03	1.66468E+04	2.79274E+03	8.35616E+03	3.39367E+05	6.03451E+03	1.01659E+05	1.87630E+04	4.75243E+03	3.29834E+03

Table 16
Running time of ECO and competing MHS algorithms on 10 CEC-2020 optimization functions. (s)

MHS	Dim	F1	F2	F3	F4	F5	F6	F7	F8	F9	F10
ECO	10	4.31040E-01	7.74742E-01	7.16554E-01	1.62407E+00	7.04584E-01	6.42884E-01	6.16835E-01	7.86299E-01	5.93578E-01	8.03347E-01
ECO	30	2.07100E+00	3.52747E+00	3.07518E+00	1.11802E+01	3.01587E+00	2.72003E+00	2.47034E+00	4.52550E+00	3.79571E+00	4.71135E+00
	50	5.67906E+00	8.24728E+00	7.18549E+00	2.96526E+01	6.87163E+00	6.19320E+00	5.53178E+00	1.24913E+01	1.04824E+01	1.41239E+01
	100	2.27279E+01	3.26872E+01	2.88803E+01	1.17047E+02	2.54116E+01	2.28979E+01	2.19469E+01	5.56340E+01	7.92824E+01	8.47433E+01
ARO	100	4.35250E-01	7.89020E-01	9.09498E-01		6.22750E-01	6.39111E-01		8.60994E-01	9.01189E-01	8.04275E-01
AKO					1.85143E+00			6.43027E-01			
	30	1.72977E+00	3.11141E+00	3.73268E+00	1.20073E+01	2.60956E+00	2.59001E+00	2.55522E+00	4.57462E+00	5.25541E+00	4.31749E+00
	50	3.61266E+00	8.45121E+00	8.40096E+00	3.12434E+01	5.91156E+00	5.79367E+00	5.81235E+00	1.20998E+01	1.44883E+01	1.24271E+01
	100	1.93731E+01	3.52224E+01	3.24682E+01	9.62594E+01	2.34039E+01	2.25076E+01	2.22787E+01	5.77965E+01	7.32816E+01	8.33125E+01
CFOA	10	5.85671E-01	1.17459E+00	1.10932E+00	2.05669E+00	1.00332E+00	9.87418E-01	9.81864E-01	1.25355E+00	1.26321E+00	1.15775E+00
	30	2.89915E+00	4.67128E+00	4.24166E+00	1.24285E+01	3.79200E+00	3.82002E+00	3.65507E+00	6.10269E+00	6.74691E+00	5.91844E+00
	50	5.73514E+00	1.01166E+01	9.10402E+00	3.06642E+01	8.18482E+00	8.18426E+00	7.68986E+00	1.56674E+01	1.83432E+01	1.66216E+01
	100	2.47765E+01	3.55354E+01	3.30792E+01	1.15659E+02	2.98228E+01	2.95077E+01	2.80334E+01	7.22829E+01	9.33584E+01	8.25371E+01
CSA	10	2.31508E-01	5.07219E-01	4.49608E-01	1.32104E+00	4.23513E-01	4.08596E-01	4.17977E-01	6.57453E-01	7.09714E-01	6.14459E-01
	30	1.30594E+00	2.58812E+00	2.14141E+00	9.81862E+00	1.97243E+00	1.92934E+00	1.89887E+00	4.26376E+00	5.07073E+00	4.09166E+00
	50	3.17508E+00	6.58361E+00	5.30041E+00	2.71422E+01	4.89930E+00	4.82495E+00	4.59791E+00	1.24219E+01	1.52209E+01	1.30421E+01
	100	1.73462E+01	2.83169E+01	2.45521E+01	1.05974E+02	2.23749E+01	2.20530E+01	2.12498E+01	6.41834E+01	8.19153E+01	8.15078E+01
WSO	10	2.43052E-01	5.19790E-01	4.88000E-01	1.38570E+00	4.20614E-01	4.24238E-01	4.37287E-01	6.69746E-01	7.20860E-01	6.70885E-01
	30	1.24798E+00	2.70474E+00	2.44490E+00	1.05234E+01	2.25886E+00	2.15021E+00	2.15473E+00	4.46101E+00	5.33803E+00	4.65093E+00
	50	4.24796E+00	6.89170E+00	6.34003E+00	2.84547E+01	5.86161E+00	5.51713E+00	5.48484E+00	1.29704E+01	1.63298E+01	1.50714E+01
	100	2.16513E+01	3.02859E+01	2.79530E+01	1.10282E+02	2.62237E+01	2.49906E+01	2.45243E+01	6.69416E+01	8.95692E+01	8.43015E+01
INFO	10	1.52645E+00	1.71057E+00	1.62719E+00	2.36673E+00	1.50125E+00	1.47060E+00	1.48580E+00	1.87718E+00	1.62176E+00	1.49007E+00
	30	5.26475E+00	7.04464E+00	6.08856E+00	1.36835E+01	5.94762E+00	5.87776E+00	5.80222E+00	8.74829E+00	8.49977E+00	7.30375E+00
	50	1.29370E+01	1.51803E+01	1.31402E+01	3.45510E+01	1.29127E+01	1.25794E+01	1.23995E+01	2.02022E+01	2.24309E+01	1.97355E+01
	100	4.24096E+01	5.27719E+01	4.57193E+01	1.30895E+02	4.41324E+01	4.40347E+01	4.50802E+01	8.33793E+01	9.57086E+01	8.92145E+01

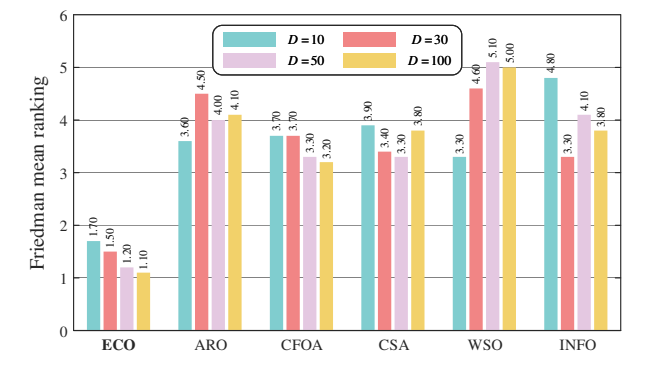


Figure 7: Scalability of ECO and competing MHS algorithms on CEC-2020 benchmark (D = 10/30/50/100).

The experimental results reveal three distinct optimization phases in ECO's performance. During the early exploration stage, ECO demonstrates significantly faster convergence than competing algorithms, indicating superior exploratory capabilities. This is followed by a transitional midphase where ECO's convergence rate exhibits a deliberate deceleration, allowing competing methods to temporarily gain performance advantages. However, in the final exploitation stage, ECO regains its rapid convergence characteristics, ultimately achieving optimal solutions across most test functions and dimensional configurations. This triphasic behavior, characterized by strong initial exploration, adaptive mid-stage refinement, and powerful final exploitation, enables ECO to consistently outperform alternative approaches

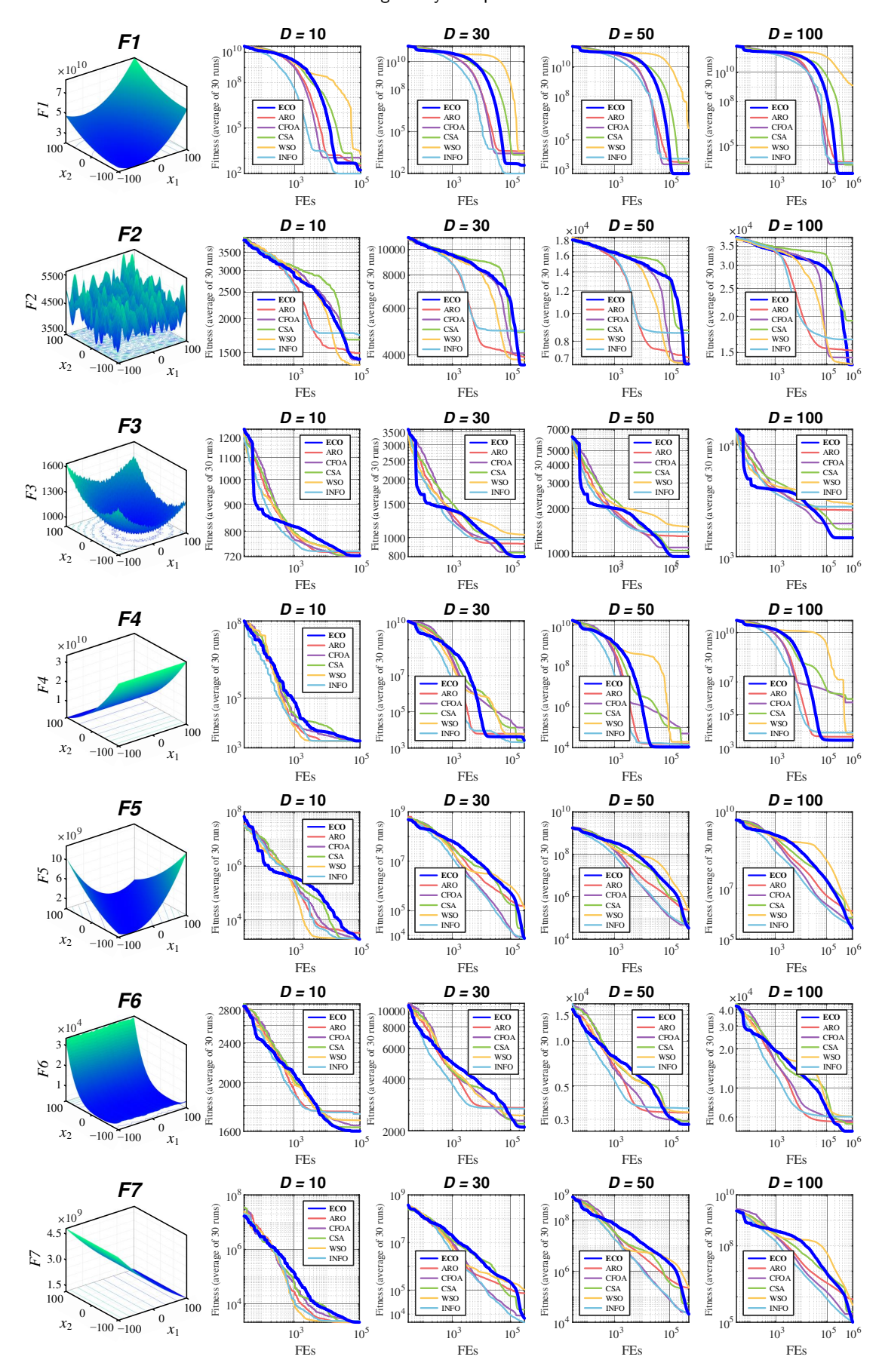


Figure 8: Mean convergence curve of ECO and competing MHS algorithms on 10 optimization functions of CEC-2020.

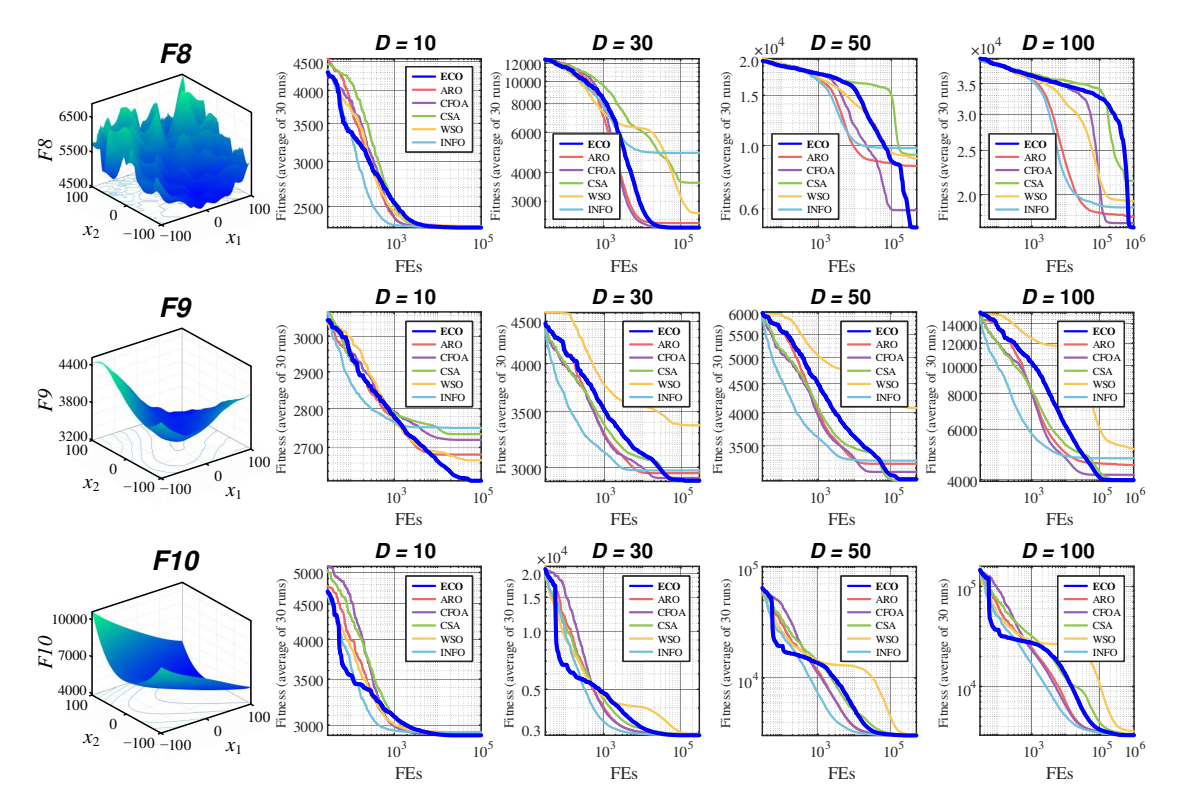


Figure 8: Mean convergence curve of ECO and competing MHS algorithms on 10 optimization functions of CEC-2020 (continued).

while maintaining robust performance across diverse problem landscapes.

6.3.3. Qualitative analysis

A comprehensive qualitative analysis of ECO's solution process is performed, as illustrated in Fig. 9. The visualization framework systematically presents four key analytical components for each test function: three-dimensional topological plots (with two-dimensional projections for clarity) depict the function landscape, followed by spatial distributions of searched regions using representative particle subsets. Solution trajectories are characterized through three complementary metrics: 1) the best-found solution curve; 2) population-wide average solution curve; and 3) dynamic *exploration-exploitation* balance profile. Finally, value trajectories of the optimal particle in the primary dimensions provide evolutionary signatures of convergence behavior.

The evaluation framework examined six representative functions spanning four CEC-2020 categories, revealing three fundamental behavioral patterns. First, comprehensive global search capability is evidenced by particle distributions spanning the entire search space, with concentrated exploration near global optima regions—a manifestation of ECO's equilibrium between exploration and exploitation. Second, distinct phase transition characteristics emerge: initial iterations exhibit marked divergence between average and elite particle values (reflecting exploratory dominance), while terminal phases demonstrate unanimous value convergence across all 30 particles (confirming precise exploitation). Third, the quantitative *exploration-exploitation*

balance metric provides empirical validation of this dynamic transition process, exhibiting characteristic sigmoidal progression from exploration-dominant to exploitation-focused search states.

6.3.4. Running time comparison analysis

Finally, the computational efficiency of the six winning MHS algorithms is examined to compare their processing speeds. As all algorithms are executed N=30 times across all dimensions of each optimization function, the average computational runtime is presented in Table 16.

Analysis reveals that CSA and WSO exhibit the highest computational efficiency, with ECO performing comparably close behind. Conversely, INFO demonstrates the slowest processing speed, exhibiting an average runtime approximately triple that of the other algorithms. Furthermore, it is observed that the relative computational efficiency of all MHS algorithms remains largely consistent across varying dimensions. However, a simple linear relationship between problem dimensionality and solving time is not identified for these algorithms. This characteristic is intrinsically linked to their unique operational mechanisms.

Overall, ECO demonstrates remarkably high solution accuracy without sacrificing much computational runtime, showcasing commendable overall performance.

7. ECO for engineering problems

In this chapter, the performance of ECO in solving realworld engineering problems are verified. The engineering

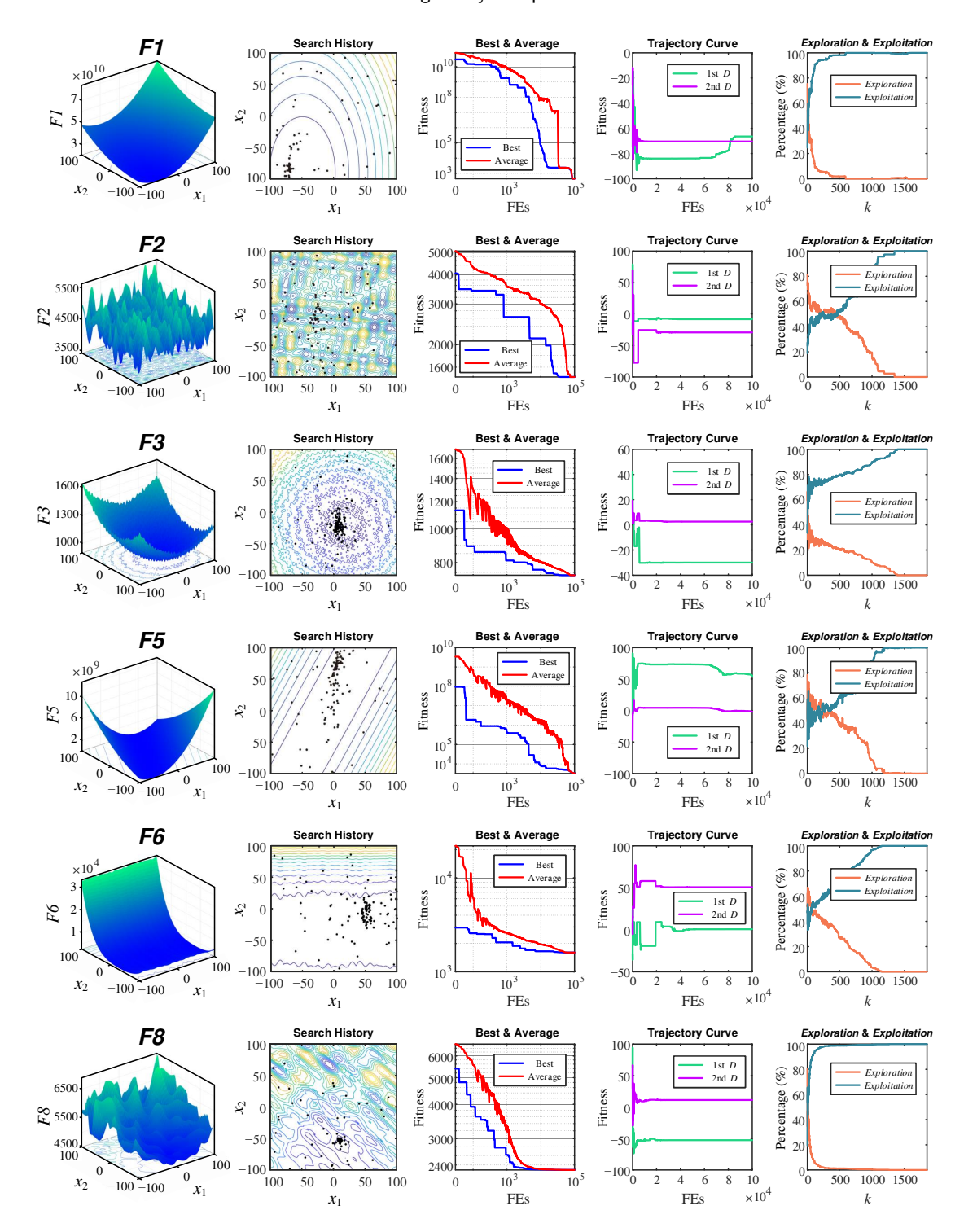


Figure 9: Qualitative analysis of ECO on 6 typical optimization functions of CEC-2020.

problems in the CEC-2020-RW test suite are known for their relatively complex optimization functions and constraints, and their solution difficulty is higher than that of the CEC-2006 test suite. We selected five classic mechanical design problems as benchmarks: (1) RC15: weight minimization of a speed reducer; (2) RC17: tension/compression spring design (case-1); (3) RC19: welded beam design, (4) RC20:

three-bar truss design; and (5) RC31: gear train design (Kumar et al., 2020c).

To enhance the persuasiveness of the experimental results, we select five SOTA MHS algorithms that have been widely applied in engineering fields, along with four best-performing algorithms on "CEC2020 competition on real-world single objective constrained optimization" which exactly adopt CEC-2020-RW as test suite, in order to explore

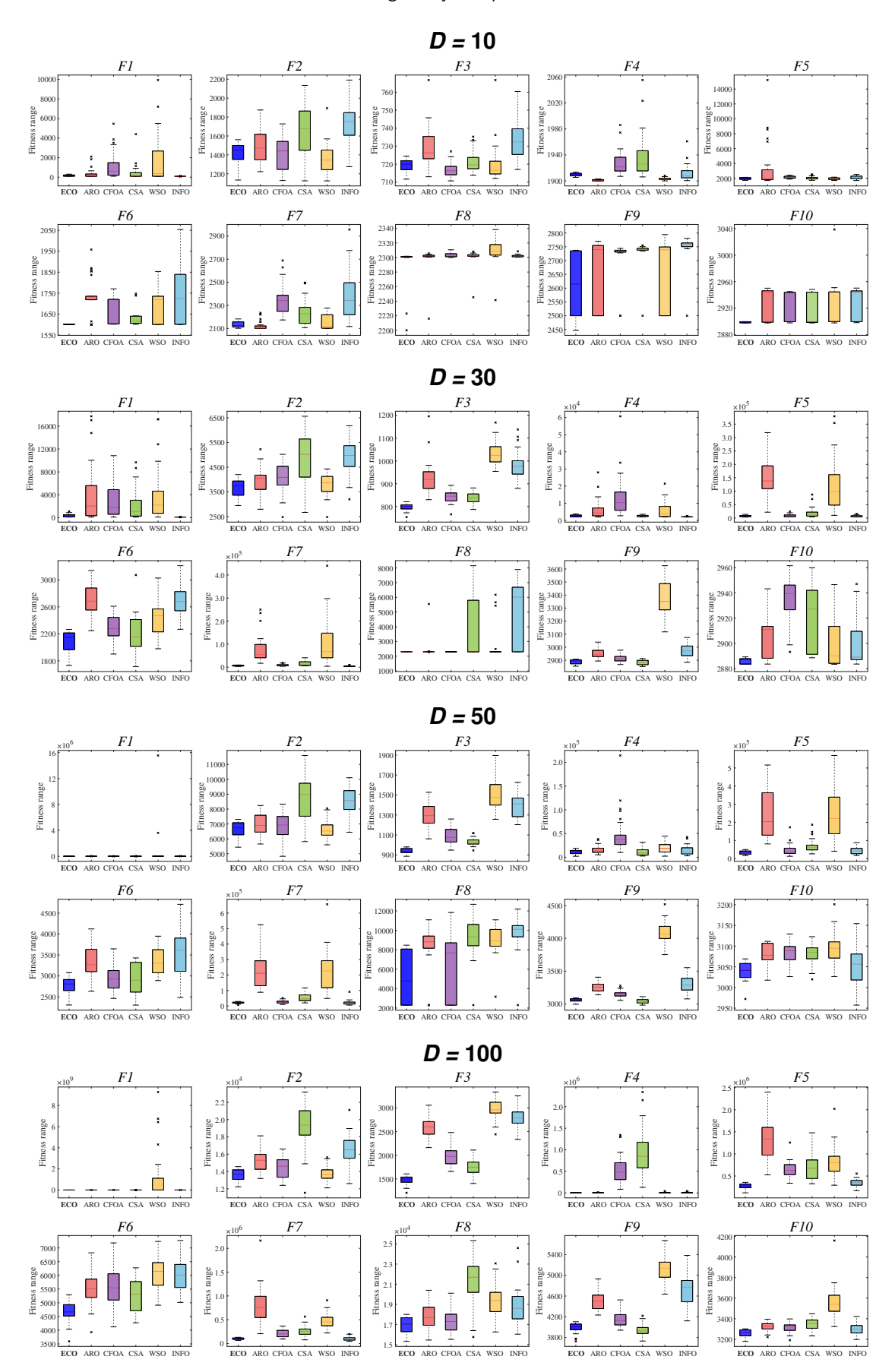


Figure 10: Range of numerical results of ECO and competing MHS algorithms on 10 optimization functions of CEC-2020.

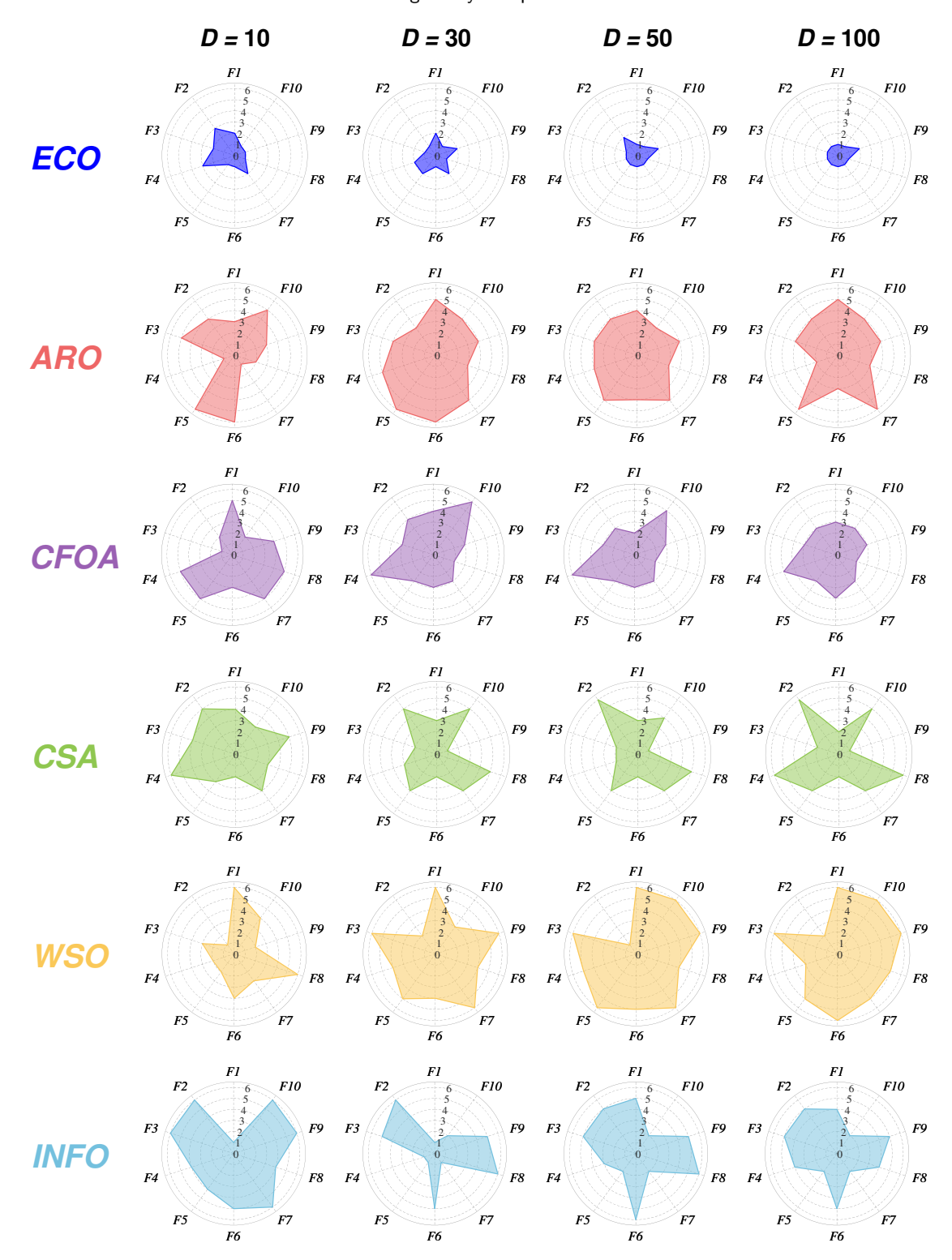


Figure 11: Rank of ECO and competing MHS algorithms on 10 optimization functions of CEC-2020.

whether ECO can demonstrate its potential and prospects in engineering applications.

According to the technical report, the experimental parameters are set as follows: the number of independent runs

N = 25 and the search termination criterion are defined as

MaxFEs =
$$\begin{cases} 1 \times 10^5, & D \le 10 \\ 2 \times 10^5, & 10 < D \le 30 \\ 4 \times 10^5, & 30 < D \le 50 \\ 8 \times 10^5, & 50 < D \le 150 \\ 10^6, & 150 < D \end{cases}$$
(28)

Table 17
Competing MHS algorithms and parameter settings.

MHS	Parameters settings	Ref.	Year
NSM-SFS	Start point $N_p = 50$, maximum diffusion number $q = 1$	(Kahraman et al., 2023)	2023
FDB-SFS	Start point $N_p = 50$, maximum diffusion number $q = 1$	(Aras et al., 2021)	2021
FDB-AGDE	Population size $P = 50$, parameter $p = 0.1$	(Guvenc et al., 2021)	2021
L-SHADE	Initial population size $N^{\text{init}} = 18 \times D$, parameters $r^{\text{arc}} = 2.6$ and $p = 0.11$, historical memory size $H = 6$	(Tanabe and Fukunaga, 2014)	2014
LRFDB-COA	Number of coyotes = $N_p \times N_c$, number of packs $N_p = 20$, number of coyotes per pack $N_c = 5$	(Duman et al., 2021)	2021
SASS	Population size $N=60$, historical memory size $H=6$, top-rank proportion for ϵ initialization $\theta_t=0.9$, and minimum decay exponent for ϵ -level updating $\gamma_{min}=3$	(Kumar et al., 2020b)	2020
ϵ sCMAgES	Parent population size $\mu = \lfloor \lambda/3 \rfloor$, offspring population size $\lambda = 4 + \lfloor 3 \log D \rfloor$, initial step size $\sigma^0 = 1$, step-size evolution path $P_{\sigma} = 0$, and covariance matrix evolution path $P_{c} = 0$	(Kumar et al., 2020a)	2020
EnMODE	Initial population size $NP^{\text{min}} = 200$, minimum population size $NP^{\text{min}} = 4$, window size $W = 50$, archive rate $A = 1.4$, and memory size $H = 5$	(Sallam et al., 2020)	2020
COLSHADE	Population parameters $r^{N^{\text{init}}}=18$ and $r^{\text{arc}}=2.6$, proportion of best solutions $p=0.11$, size of cyclical memories $H=6$, stable distribution parameters $\alpha=0.5$, $\beta=1$, $\gamma=0.01$, and $\delta=0$, minimum probability for mutations $q_{\min}=10^{-3}$, update probability rate $\mu=0.25$, and final tolerance $\epsilon_f=10^{-4}$	(Gurrola-Ramos et al., 2020)	2020

Note: All parameters remain consistent with those used in the original publications.

For each optimization function, the Min, Ave, and Std of MHS algorithms, as well as the coordinates of the search particles corresponding to the optimization objectives of the engineering problems, will be recorded.

7.1. Competing algorithms and parameter settings

The five highly competitive MHS algorithms selected for comparison are NSM-SFS (Kahraman et al., 2023), FDB-SFS (Aras et al., 2021), FDB-AGDE (Guvenc et al., 2021), L-SHADE (Tanabe and Fukunaga, 2014), and LRFDB-COA (Duman et al., 2021). As indicated in Table 17, all five algorithms incorporate enhancement mechanisms such as NSM and FDB to improve optimization capabilities, contributing to their widespread adoption in engineering applications. Additionally, the four top-performing algorithms from the CEC-2020 real-world single objective constrained optimization competition are employed for comparison, namely SASS (Kumar et al., 2020b) (competition winner), ϵ sCMAgES (Kumar et al., 2020a), EnMODE (Sallam et al., 2020), and COLSHADE (Gurrola-Ramos et al., 2020).

All parameters are configured according to the optimal settings reported in the respective source publications. Notably, both NSM-SFS and FDB-AGDE employ three distinct search mechanisms (denoted as case-1, case-2, and case-3). Empirical testing on the five engineering problems selected for this study determines that NSM-SFS (case-1) and FDB-AGDE (case-3) deliver superior performance.

It should be emphasized that parameter tuning for the four competition-winning algorithms is computationally intensive, as their configurations are specifically optimized for the CEC-2020-RW problem set. The parameter values summarized in Table 17 are the optimal mechanisms for these algorithms.

7.2. Weight minimization of a speed reducer

This is the RC15 problem in CEC-2020-RW. The weight minimization of a speed reducer problem is a complex non-linear optimization project in mechanical braking systems, aimed at minimizing the total weight of a speed reducer while adhering to constraints related to gear teeth bending

stress, shaft stress, surface stress, and transverse shaft deflection. The structure of the speed reducer is illustrated in Fig. 12. This problem involves seven decision variables: surface width $(b=x_1)$, gear module $(m=x_2)$, pinion teeth count $(p=x_3)$, lengths of the 1st and 2nd shafts between bearings $(l_1=x_4,\ l_2=x_5)$, and diameters of the 1st and 2nd shafts $(d_1=x_6,\ d_2=x_7)$, as follows:

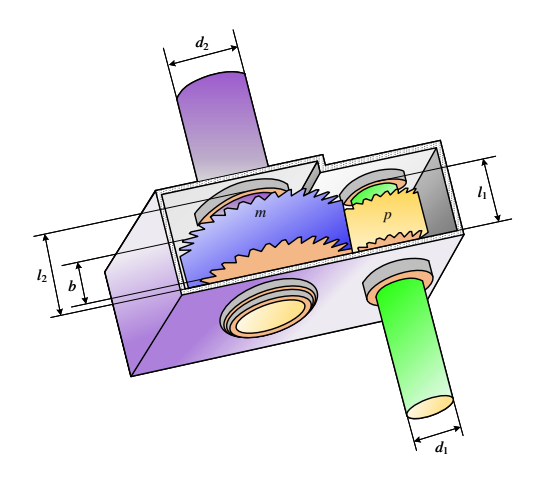


Figure 12: Weight minimization of a speed reducer.

$$X = \begin{bmatrix} x_1, x_2, x_3, x_4, x_5, x_6, x_7 \end{bmatrix} = \begin{bmatrix} b, m, p, l_1, l_2, d_1, d_2 \end{bmatrix}.$$
 (29)

The objective is to minimize:

$$f(\mathbf{X}) = 0.7854x_1x_2^2 (3.3333x_3^2 + 14.9334x_3 - 43.0934)$$
$$-1.508x_1 (x_6^2 + x_7^2) + 7.4777 (x_6^3 + x_7^3)$$
$$+ 0.7854 (x_4x_6^2 + x_5x_7^2),$$
 (30)

subject to:

$$g_1(\mathbf{X}) = \frac{27}{x_1 x_2^2 x_3} - 1 \le 0, (31)$$

$$g_2(X) = \frac{397.5}{x_1 x_2^2 x_3^2} - 1 \le 0, (32)$$

$$g_3(\boldsymbol{X}) = \frac{1.93x_4^3}{x_2x_3x_6^4} - 1 \le 0, (33)$$

$$g_4(X) = \frac{1.93x_5^3}{x_2x_3x_7^4} - 1 \le 0, (34)$$

$$g_5(X) = \frac{\sqrt{\left(\frac{745x_5}{x_2x_3}\right)^2 + 1.69 \times 10^7}}{110x_6^3} - 1 \le 0,$$
 (35)

$$g_6(X) = \frac{\sqrt{\left(\frac{745x_5}{x_2x_3}\right)^2 + 1.57 \times 10^5}}{85x_7^3} - 1 \le 0,$$
 (36)

$$g_7(X) = \frac{x_2 x_3}{40} - 1 \le 0, (37)$$

$$g_8(X) = \frac{5x_2}{x_1} - 1 \le 0, (38)$$

$$g_9(X) = \frac{x_1}{12x_2} - 1 \le 0, (39)$$

$$g_{10}(X) = \frac{1.5x_6 + 1.9}{x_4} - 1 \le 0, (40)$$

$$g_{11}(X) = \frac{1.1x_7 + 1.9}{x_5} - 1 \le 0. \tag{41}$$

Variable ranges are defined as follows:

$$\begin{aligned} 2.6 &\leq x_1 \leq 3.6, & 0.7 \leq x_2 \leq 0.8, \\ 17 &\leq x_3 \leq 28, & 7.3 \leq x_4 \leq 8.3, \\ 7.3 &\leq x_5 \leq 8.3, & 2.9 \leq x_6 \leq 3.9, & 5.0 \leq x_7 \leq 5.5. \end{aligned} \tag{42}$$

As shown in Table 18, ECO and eight comparative algorithms achieve the optimal solution. However, FDB-AGDE exhibits significantly inferior performance, with three key performance metrics diverging by five orders of magnitude (10⁵) from those of the other algorithms. Comprehensive numerical validation confirms that all constraints are satisfied.

7.3. Tension/compression spring design

This is the RC17 problem appearing in CEC-2020-RW. The tension/compression spring design problem aims to minimize the weight of a spring subject to several engineering constraints. The spring depicted in Fig. 13 must meet the requirements on shear stress, surge frequency, and deflection to ensure optimal performance. The design variables include the wire diameter $(d = x_1)$, the mean coil diameter $(D = x_2)$, and the number of active coils $(N = x_3)$, which must be precisely estimated to achieve the optimal design configuration. Thus,

$$X = [x_1, x_2, x_3] = [d, D, N].$$
 (43)

The objective is to minimize:

$$f(X) = (x_3 + 2)x_2x_1^2, (44)$$

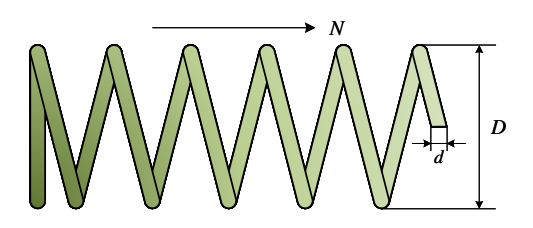


Figure 13: Tension/compression spring design.

subject to:

$$g_1(X) = 1 - \frac{x_3^3}{71785x_1^4} \le 0,$$
 (45)

$$g_2(X) = \frac{4x_2^2 - x_1x_2}{12566(x_2x_1^3 - x_1^4)} + \frac{1}{5108x_1^2} \le 0,$$
 (46)

$$g_3(X) = 1 - \frac{140.45x_1}{x_2 x_2^2} \le 0, (47)$$

$$g_4(X) = \frac{x_1 + x_2}{1.5} - 1 \le 0. \tag{48}$$

Variable ranges are defined as follows:

$$0.05 \le x_1 \le 2.00$$
, $0.25 \le x_2 \le 1.30$, $2.00 \le x_3 \le 15.0$. (49)

As presented in Table 19, COLSHADE achieves the smallest mean value among all algorithms, indicating superior solution stability. L-SHADE and ϵ sCMAgES also attain the optimal solution, but their solution ranges exhibit significant fluctuation. ECO, EnMODE, and SASS demonstrate competitive performance. Comprehensive numerical validation confirms all constraints are satisfied.

7.4. Welded beam design

This is the RC19 problem from CEC-2020-RW. The welded beam design problem, as illustrated in Fig. 14, aims to minimize the total manufacturing cost of a welded beam by optimizing four design variables: height $(h = x_1)$, length $(l = x_2)$, thickness $(t = x_3)$, and width $(b = x_4)$, subject to seven constraints. The decision variable vector is

$$X = [x_1, x_2, x_3, x_4] = [h, l, t, b].$$
 (50)

The objective of this mathematical problem is to minimize:

$$f(X) = 1.1047x_1x_2 + 0.04811x_3x_4(14.0 + x_2),$$
 (51)

subject to:

$$g_1(X) = \tau(X) - \tau_{\text{max}} \le 0,$$
 (52)

$$g_2(X) = \sigma(X) - \sigma_{\text{max}} \le 0, \tag{53}$$

$$g_3(X) = \delta(X) - \delta_{\text{max}} \le 0, \tag{54}$$

$$g_{A}(X) = x_{1} - x_{A} \le 0, \tag{55}$$

$$g_5(X) = P - P_c(X) \le 0,$$
 (56)

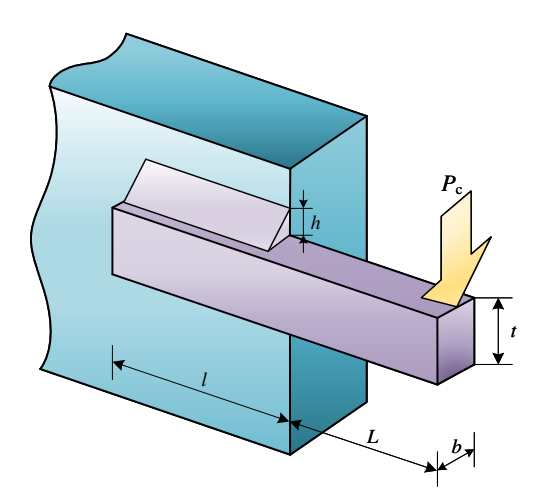


Figure 14: Welded beam design.

$$\begin{split} g_6(X) &= 0.125 - x_1 \leq 0, \\ g_7(X) &= 1.1047 x_1 x_2 + 0.04811 x_3 x_4 (14.0 + x_2) - 5.0 \leq 0, \\ &(58) \end{split}$$

where

$$\tau(X) = \sqrt{(t')^2 + 2t't''\frac{x_2}{2R} + (t'')^2},$$

$$t' = \frac{P}{\sqrt{2x_1x_2}}, \quad t'' = \frac{MR}{J}, \quad M = P\left(L + \frac{x_2}{2}\right),$$

$$R = \sqrt{\frac{x_2^2}{4} + \left(\frac{x_1 + x_3}{2}\right)^2},$$

$$J = 2\left(\sqrt{2x_1x_2}\left[\frac{x_2^2}{4} + \left(\frac{x_1 + x_3}{2}\right)^2\right]\right),$$

$$\sigma(X) = \frac{6PL}{x_4x_3^2}, \quad \delta(X) = \frac{6PL^3}{Ex_3x_4},$$

$$P_{c}(X) = \frac{4.0134E\sqrt{\frac{x_{3}^{2}x_{4}^{2}}{36}}}{L^{2}} \left(1 - \frac{x_{3}}{2L}\sqrt{\frac{E}{4G}}\right),$$

$$\begin{split} P &= 6000, \quad L = 14, \quad E = 30 \times 10^6, \quad G = 12 \times 10^6, \\ \tau_{\text{max}} &= 13600, \quad \sigma_{\text{max}} = 30000, \quad \delta_{\text{max}} = 0.25. \end{split}$$

Variable ranges are defined as follows:

$$0.1 \le x_3, x_2 \le 10, \quad 0.1 \le x_4 \le 2, \quad 0.125 \le x_1 \le 2.$$
 (59)

The optimization results for the welded beam design problem across all MHS algorithms are presented in Table 20. All algorithms yield identical results, with the solutions satisfying the design constraints and demonstrating robust performance. Comprehensive numerical validation confirms these findings.

7.5. Three-bar truss design

This is the RC20 problem in CEC-2020-RW. The three-bar truss design problem aims to determine the optimal values of three variables, which include the areas of three bars $(A_1 = A_3, A_2)$, and minimize the weight of the truss while meeting specific constraints. The general structure of the truss is depicted in Fig. 15.

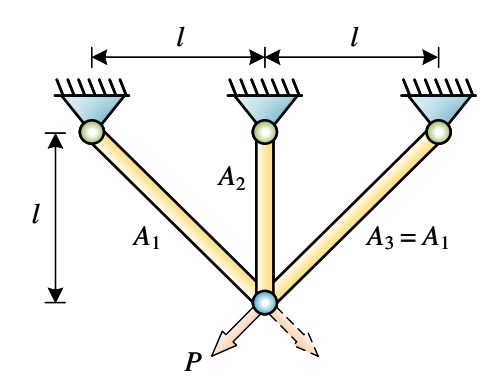


Figure 15: Three bar truss design.

The design variables are defined as follows:

$$X = [x_1, x_2] = [A_1, A_2].$$
 (60)

The objective is to minimize:

$$f(X) = \left(2\sqrt{2}x_1 + x_2\right)l, (61)$$

subject to:

$$g_1(X) = \frac{\sqrt{2}x_1 + x_2}{\sqrt{2}x_1^2 + 2x_1x_2}P - \sigma \le 0, \tag{62}$$

$$g_2(X) = \frac{x_2}{\sqrt{2}x_1^2 + 2x_1x_2}P - \sigma \le 0, \tag{63}$$

$$g_3(X) = \frac{1}{\sqrt{2}x_2 + x_1} P - \sigma \le 0, \tag{64}$$

where

$$l = 100 \text{ cm}, \quad P = 2 \text{ kN/cm}^2, \quad \sigma = 2 \text{ kN/cm}^2.$$

The variable ranges are defined as follows:

$$0 \le x_1, x_2 \le 1. \tag{65}$$

As shown in Table 21, ECO and eight compared algorithms achieve the optimal solution for this problem. However, LRFDB-COA exhibits significant performance deviation, with all key metrics being over three orders of magnitude worse than those of the other MHS algorithms. Comprehensive numerical validation confirms that all constraints are satisfied.

7.6. Gear train design

This is the RC31 problem appearing in CEC-2020-RW. The gear train design problem aims to minimize the cost associated with the gear ratio of the gear train depicted in Fig. 16. The problem involves four integer variables: T_a , T_b , T_d , and T_f , which represent the number of teeth on four different gearwheels. The gear ratio is defined as $T_bT_d/(T_aT_f)$.

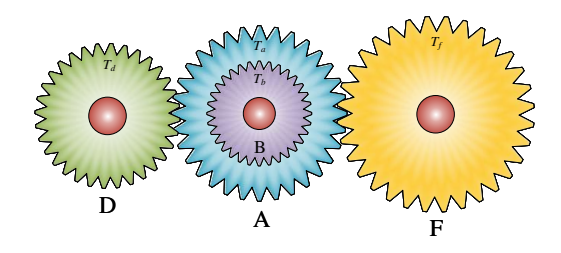


Figure 16: Gear train design.

The design variables are defined as follows:

$$X = [x_1, x_2, x_3, x_4] = [T_a, T_b, T_d, T_f].$$
 (66)

The objective is to minimize:

$$f(X) = \left(\frac{1}{6.931} - \frac{T_b T_d}{T_a T_f}\right)^2,\tag{67}$$

subject to:

$$g_i(x_i) = 12 - x_i \le 0, \quad i = 1, 2, 3, 4,$$
 (68)

$$g_i(x_i) = 60 - x_i \le 0, \quad i = 5, 6, 7, 8.$$
 (69)

Variable ranges are defined as follows:

$$0.01 \le x_1, x_2, x_3, x_4 \le 60. \tag{70}$$

As presented in Table 22, ECO and the four top-performing MHS algorithms from the CEC-2020 real-world single objective constrained optimization competition demonstrates exceptional performance on this problem. Specifically, they achieve the optimal values for all three metrics (Min, Ave, and Std). Comparatively, other benchmark algorithms exhibit substantially lower solution stability. Comprehensive numerical validation confirms that all constraints are satisfied.

7.7. Rank of all MHS algorithms on CEC-2020-RW

As shown in Table 23, among the five engineering problems evaluated, COLSHADE achieves superior performance, followed by EnMODE and SASS in second and third places, respectively. ECO surpasses ϵ sCMAgES, securing fourth position on this benchmark. Conversely, FDB-AGDE and LRFDB-COA demonstrate notably poorer performance, ranking lowest among all MHS algorithms.

The most important finding from the detailed analysis of the four highest-performing algorithms reveals that their

parameters are specifically optimized for the CEC-2020-RW problem set. This benchmark-specific tuning results in computationally intensive solution processes with exceptional target-problem efficacy, explaining their superior performance on this suite. However, when applied to alternative test sets, these algorithms exhibit significantly reduced computational efficiency due to their narrow optimization scope. Consequently, they lack the computational generality inherent in ECO's more versatile architecture.

8. Conclusion

This article proposes a novel MHS algorithm called ECO to tackle complex, non-convex constrained optimization problems characterized by numerous local optima. Inspired by the processes of energy flow and material cycling within ecosystems, ECO uses a mathematical model to simulate the ecological cycle, incorporating tailored update strategies for the producers, consumers, and decomposers. Specifically, consumer update strategies involve targeted predation mechanisms for herbivores, carnivores, and omnivores, while decomposer strategies comprise optimal, local random, and global random decomposition mechanisms.

To comprehensively evaluate the optimization performance of the ECO algorithm, three types of comparative experiments are conducted. For the first evaluation, five widely cited algorithms, including CS, HS, PSO, GWO, and WOA, are selected as comparative baselines. ECO is tested on 23 classical unconstrained optimization functions and 24 constrained benchmark problems from the IEEE CEC-2006 test suite, alongside these five algorithms. The numerical results obtained by all MHS algorithms are analyzed and the Wilcoxon rank-sum test and the Friedman test are conducted. The results demonstrate that ECO consistently outperforms these algorithms, exhibiting clear advantages in convergence speed, solution accuracy, and the ability to escape local optima when solving both unconstrained and constrained optimization tasks.

For the second evaluation, an algorithm pool of 50 SOTA MHS algorithms is established, and ECO is compared with all of them on the IEEE CEC-2014 and CEC-2017 test suites. Based on the experimental results, six top-performing algorithms—ECO, ARO, CFOA, CSA, WSO, and INFO—are selected for further evaluation on the IEEE CEC-2020 test suite. The numerical results obtained by all MHS algorithms are analyzed, and both the Wilcoxon rank-sum test and the Friedman test are conducted. The results show that ECO achieves the best overall optimization performance among them. This pioneering algorithm-pool experiment confirms ECO's superiority over a wide range of advanced algorithms introduced in recent years.

For the third evaluation, comprehensive comparative simulations are conducted to validate ECO's applicability for solving real-world complex optimization problems. The benchmark algorithms include five improved SOTA MHS algorithms, comprising NSM-SFS, FDB-SFS, FDB-AGDE, L-SHADE, and LRFDB-COA, and four top-performing

Table 18

Numerical results obtained by ECO and competing MHS algorithms on RC15 (weight minimization of a speed reducer).

	ECO	SASS	EnMODE	NSM-SFS	FDB-SFS	FDB-AGDE	ϵ sCMAgES	L-SHADE	COLSHADE	LRFDB-COA
x ₁	3.50000000	3.50000000	3.50000000	3.50000000	3.50000000	3.50000000	3.50000000	3.50000000	3.50000000	3.50000000
x_2	0.70000000	0.70000000	0.70000000	0.70000000	0.70000000	0.70000000	0.70000000	0.70000000	0.70000000	0.70000000
x_3	17.0000000	17.0000000	17.0000000	17.0000000	17.0000000	17.0000000	17.0000000	17.0000000	17.0000000	17.0000000
x_{4}	7.30000000	7.30000000	7.30000000	7.30000000	7.30000000	7.30000000	7.30000000	7.30000000	7.30000000	7.30000000
x 5	7.71531991	7.71531991	7.71531991	7.71531991	7.71531991	7.71531991	7.71531991	7.71531991	7.71531991	7.71531991
x_6	3.35054095	3.35054095	3.35054095	3.35054095	3.35054095	3.35054095	3.35054095	3.35054095	3.35054095	3.35054095
x_7	5.28665446	5.28665446	5.28665446	5.28665446	5.28665446	5.28665446	5.28665446	5.28665446	5.28665446	5.28665446
Min	2994.42447	2994.42447	2994.42447	2994.42447	2994.42447	2994.42447	2994.42447	2994.42447	2994.42447	2994.42447
Ave	2994.42447	2994.42447	2994.42447	2994.42447	2994.42447	2994.42447	2994.42447	2994.42447	2994.42447	2994.42447
Std	9.2825E-13	9.2825E-13	9.2825E-13	9.2825E-13	9.2825E-13	1.0229E-08	9.2825E-13	9.2825E-13	9.2825E-13	9.2825E-13

Table 19
Numerical results obtained by ECO and competing MHS algorithms on RC17 (tension/compression spring design, case-1).

MHS	ECO	SASS	EnMODE	NSM-SFS	FDB-SFS	FDB-AGDE	ϵ sCMAgES	L-SHADE	COLSHADE	LRFDB-COA
x_1	0.05169231	0.05168906	0.05168906	0.05168904	0.05168901	0.05168906	0.05168907	0.05168907	0.05168907	0.05172036
x_2	0.35679602	0.35671784	0.35671783	0.35671715	0.35671643	0.35671777	0.35671784	0.35671784	0.35671784	0.35747109
x_3	11.2843781	11.2889601	11.2889602	11.2890006	11.2890426	11.2889638	11.2889601	11.2889601	11.2889601	11.2449453
Min	0.01266523	0.01266523	0.01266523	0.01266523	0.01266523	0.01266523	0.01266523	0.01266523	0.01266523	0.01266524
Ave	0.01266525	0.01266523	0.01266523	0.01266525	0.01266533	0.01266527	0.01266526	0.01266950	0.01266523	0.01266538
Std	3.8839E-09	1.3880E-11	4.9233E-12	1.8822E-08	9.4667E-06	2.2047E-06	8.9366E-07	6.5781E-05	2.7225E-12	1.0027E-06

 Table 20

 Numerical results obtained by ECO and competing MHS algorithms on RC19 (welded beam design).

	ECO	SASS	EnMODE	NSM-SFS	FDB-SFS	FDB-AGDE	ϵ sCMAgES	L-SHADE	COLSHADE	LRFDB-COA
x ₁	0.20572964	0.20572964	0.20572964	0.20572964	0.20572964	0.20572964	0.20572964	0.20572964	0.20572964	0.20572964
x_2	3.25312004	3.25312004	3.25312004	3.25312004	3.25312004	3.25312004	3.25312004	3.25312004	3.25312004	3.25312004
x_3	9.03662391	9.03662391	9.03662391	9.03662391	9.03662391	9.03662391	9.03662391	9.03662391	9.03662391	9.03662391
x_{4}	0.20572964	0.20572964	0.20572964	0.20572964	0.20572964	0.20572964	0.20572964	0.20572964	0.20572964	0.20572964
Min	1.69524716	1.69524716	1.69524716	1.69524716	1.69524716	1.69524716	1.69524716	1.69524716	1.69524716	1.69524716
Ave	1.69524716	1.69524716	1.69524716	1.69524716	1.69524716	1.69524716	1.69524716	1.69524716	1.69524716	1.69524716
Std	2.2662E-16	2.2662E-16	2.2662E-16	2.2662E-16						

 Table 21

 Numerical results obtained by ECO and competing MHS algorithms on RC20 (three-bar truss design).

	ECO	SASS	EnMODE	NSM-SFS	FDB-SFS	FDB-AGDE	esCMAgES	L-SHADE	COLSHADE	LRFDB-COA
x_1	0.78867513	0.78867513	0.78867513	0.78867513	0.78867514	0.78867514	0.78867513	0.78867513	0.78867513	0.78867507
x_2	0.40824830	0.40824830	0.40824830	0.40824830	0.40824829	0.40824829	0.40824829	0.40824829	0.40824829	0.40824848
Min	263.895843	263.895843	263.895843	263.895843	263.895843	263.895843	263.895843	263.895843	263.895843	263.895843
Ave	263.895843	263.895843	263.895843	263.895843	263.895843	263.895843	263.895843	263.895843	263.895843	263.895843
Std	5.8016E-14	3.1422E-11								

Table 22
Numerical results obtained by ECO and competing MHS algorithms on RC31 (gear train design).

	ECO	SASS	EnMODE	NSM-SFS	FDB-SFS	FDB-AGDE	ϵ sCMAgES	L-SHADE	COLSHADE	LRFDB-COA
x_1	49.3000403	49.3000403	49.3000403	49.2889111	49.3824442	49.4918951	49.3000403	49.3698757	49.3000403	48.6638793
x_2	19.3605917	19.3605917	19.3605917	16.0674738	15.7965736	16.0983856	19.3605917	16.0521244	19.3605917	18.5973568
x_3	15.8481360	15.8481360	15.8481360	18.9821250	19.3517569	19.3860636	15.8481360	19.2014224	15.8481360	16.2893830
x_4	42.8673784	42.8673784	42.8673784	43.3920358	43.4353539	42.6301489	42.8673784	42.5424910	42.8673784	43.2077863
Min	2.7009E-12	2.7009E-12	2.7009E-12	2.7010E-12	2.7017E-12	2.7010E-12	2.7009E-12	2.7015E-12	2.7009E-12	2.7009E-12
Ave	2.7009E-12	2.7009E-12	2.7009E-12	1.5408E-11	3.7588E-10	1.8669E-11	2.7009E-12	2.0184E-11	2.7009E-12	1.4927E-11
Std	0.0000E+00	0.0000E+00	0.0000E+00	1.0324E-11	4.7952E-10	2.1711E-10	0.0000E+00	2.4235E-10	0.0000E+00	1.0189E-11

Table 23
Friedman mean rank of ECO and competing MHS algorithms on CEC-2020-RW benchmark.

MHS	ECO	SASS	EnMODE	NSM-SFS	FDB-SFS	FDB-AGDE	ϵ sCMAgES	L-SHADE	COLSHADE	LRFDB-COA
RC15	1	1	1	1	1	10	1	1	1	1
RC17	4	3	2	5	8	7	6	10	1	9
RC19	1	1	1	1	1	1	1	1	1	1
RC20	1	1	1	1	1	1	1	1	1	10
RC31	1	1	1	7	10	8	1	9	1	6
Friedman Rank	1.6 4	1.4 3	1.2 2	3.0	4.2 7	5.4 9	2 5	4.4 8	1.0 1	5.4 9

algorithms from the IEEE CEC-2020 real-world single objective constrained optimization benchmark, namely SASS, &CMAgES, EnMODE, and COLSHADE. These algorithms are evaluated on five engineering problems from the IEEE CEC-2020-RW test suite. All numerical results undergo rigorous analysis, complemented by the Friedman statistical test for performance ranking. The results show that ECO achieves performance comparable to that of these SOTA algorithms, thereby demonstrating its strong potential for tackling complex real-world scenarios.

In conclusion, ECO demonstrates rapid convergence, high-precision solutions, and a strong ability to escape local optima, outperforming the vast majority of existing SOTA MHS algorithms in terms of optimization performance. Its simplicity, freedom from hyperparameter pre-setting, and superior capability in solving complex optimization problems make it a highly effective tool. Future research will focus on extending ECO to multi-objective optimization tasks to further broaden its applicability.

CRediT authorship contribution statement

Boyu Ma: Conceptualization, Methodology, Software, Validation, Formal analysis, Investigation, Resources, Data curation, Writing - original draft, Writing - review & editing, Visualization, Supervision, Project administration. Jiaxiao Shi: Methodology, Software, Validation, Formal analysis, Investigation, Resources, Data curation, Writing - original draft, Writing - review & editing, Visualization. Yiming Ji: Formal analysis, Writing - review & editing, Visualization. Zhengpu Wang: Writing - review & editing, Visualization.

References

- Abdel-Basset, M., El-Shahat, D., Jameel, M., Abouhawwash, M., 2023a. Exponential distribution optimizer (edo): a novel math-inspired algorithm for global optimization and engineering problems. Artificial Intelligence Review 56, 9329–9400.
- Abdel-Basset, M., El-Shahat, D., Jameel, M., Abouhawwash, M., 2023b. Young's double-slit experiment optimizer: A novel metaheuristic optimization algorithm for global and constraint optimization problems. Computer Methods in Applied Mechanics and Engineering 403, 115652.
- Abdel-Basset, M., Mohamed, R., Azeem, S.A.A., Jameel, M., Abouhawwash, M., 2023c. Kepler optimization algorithm: A new metaheuristic algorithm inspired by kepler's laws of planetary motion. Knowledge-based systems 268, 110454.
- Abdel-Basset, M., Mohamed, R., Jameel, M., Abouhawwash, M., 2023d. Nutcracker optimizer: A novel nature-inspired metaheuristic algorithm for global optimization and engineering design problems. Knowledge-Based Systems 262, 110248.
- Abdollahzadeh, B., Gharehchopogh, F.S., Mirjalili, S., 2021. African vultures optimization algorithm: A new nature-inspired metaheuristic algorithm for global optimization problems. Computers & Industrial Engineering 158, 107408.
- Abdollahzadeh, B., Khodadadi, N., Barshandeh, S., Trojovskỳ, P., Gharehchopogh, F.S., El-kenawy, E.S.M., Abualigah, L., Mirjalili, S., 2024.Puma optimizer (po): a novel metaheuristic optimization algorithm and its application in machine learning. Cluster Computing 27, 5235–5283.
- Abualigah, L., Abd Elaziz, M., Sumari, P., Geem, Z.W., Gandomi, A.H., 2022. Reptile search algorithm (rsa): A nature-inspired meta-heuristic optimizer. Expert Systems with Applications 191, 116158.

- Abualigah, L., Diabat, A., Mirjalili, S., Abd Elaziz, M., Gandomi, A.H., 2021a. The arithmetic optimization algorithm. Computer Methods in Applied Mechanics and Engineering 376, 113609.
- Abualigah, L., Diabat, A., Mirjalili, S., Abd Elaziz, M., Gandomi, A.H., 2021b. The arithmetic optimization algorithm. Computer methods in applied mechanics and engineering 376, 113609.
- Abualigah, L., Yousri, D., Abd Elaziz, M., Ewees, A.A., Al-Qaness, M.A., Gandomi, A.H., 2021c. Aquila optimizer: a novel meta-heuristic optimization algorithm. Computers & Industrial Engineering 157, 107250.
- Agushaka, J.O., Ezugwu, A.E., Abualigah, L., 2022. Dwarf mongoose optimization algorithm. Computer methods in applied mechanics and engineering 391, 114570.
- Agushaka, J.O., Ezugwu, A.E., Abualigah, L., 2023. Gazelle optimization algorithm: a novel nature-inspired metaheuristic optimizer. Neural Computing and Applications 35, 4099–4131.
- Ahmadianfar, I., Heidari, A.A., Gandomi, A.H., Chu, X., Chen, H., 2021.Run beyond the metaphor: An efficient optimization algorithm based on runge kutta method. Expert Systems with Applications 181, 115079.
- Ahmadianfar, I., Heidari, A.A., Noshadian, S., Chen, H., Gandomi, A.H., 2022. Info: An efficient optimization algorithm based on weighted mean of vectors. Expert Systems with Applications 195, 116516.
- Amiri, M.H., Mehrabi Hashjin, N., Montazeri, M., Mirjalili, S., Khodadadi, N., 2024. Hippopotamus optimization algorithm: a novel nature-inspired optimization algorithm. Scientific Reports 14, 5032.
- Aras, S., Gedikli, E., Kahraman, H.T., 2021. A novel stochastic fractal search algorithm with fitness-distance balance for global numerical optimization. Swarm and Evolutionary Computation 61, 100821.
- Arora, S., Singh, S., 2019. Butterfly optimization algorithm: a novel approach for global optimization. Soft Computing 23, 715–734.
- Atashpaz-Gargari, E., Lucas, C., 2007. Imperialist competitive algorithm: An algorithm for optimization inspired by imperialistic competition, in: 2007 IEEE Congress on Evolutionary Computation, IEEE. pp. 4661–4667.
- Awad, N.H., Ali, M.Z., Suganthan, P.N., 2017. Ensemble sinusoidal differential covariance matrix adaptation with euclidean neighborhood for solving cec2017 benchmark problems, in: 2017 IEEE congress on evolutionary computation (CEC), IEEE. pp. 372–379.
- Awad, N.H., Ali, M.Z., Suganthan, P.N., Reynolds, R.G., 2016. An ensemble sinusoidal parameter adaptation incorporated with 1-shade for solving cec2014 benchmark problems, in: 2016 IEEE Congress on Evolutionary Computation (CEC), IEEE. pp. 2958–2965.
- Azizi, M., Aickelin, U., A. Khorshidi, H., Baghalzadeh Shishehgarkhaneh, M., 2023a. Energy valley optimizer: a novel metaheuristic algorithm for global and engineering optimization. Scientific Reports 13, 226.
- Azizi, M., Talatahari, S., Gandomi, A.H., 2023b. Fire hawk optimizer: A novel metaheuristic algorithm. Artificial Intelligence Review 56, 287– 363
- Beyer, H.G., Schwefel, H.P., 2002. Evolution strategies a comprehensive introduction. Natural computing 1, 3–52.
- Bouaouda, A., Hashim, F.A., Sayouti, Y., Hussien, A.G., 2024. Pied kingfisher optimizer: a new bio-inspired algorithm for solving numerical optimization and industrial engineering problems. Neural Computing and Applications 36, 15455–15513.
- Boyd, S., Vandenberghe, L., 2004. Convex optimization. Cambridge university press.
- Braik, M., Hammouri, A., Atwan, J., Al-Betar, M.A., Awadallah, M.A., 2022. White shark optimizer: A novel bio-inspired meta-heuristic algorithm for global optimization problems. Knowledge-Based Systems 243, 108457.
- Braik, M.S., 2021. Chameleon swarm algorithm: A bio-inspired optimizer for solving engineering design problems. Expert Systems with Applications 174, 114685.
- Carrasco, J., García, S., Rueda, M., Das, S., Herrera, F., 2020. Recent trends in the use of statistical tests for comparing swarm and evolutionary computing algorithms: Practical guidelines and a critical review. Swarm and Evolutionary Computation 54, 100665.
- Chen, X., Xu, B., Mei, C., Ding, Y., Li, K., 2018. Teaching–learning–based artificial bee colony for solar photovoltaic parameter estimation. Applied

- Energy 212, 1578-1588.
- Chen, Z., Francis, A., Li, S., Liao, B., Xiao, D., Ha, T.T., Li, J., Ding, L., Cao, X., 2022. Egret swarm optimization algorithm: an evolutionary computation approach for model free optimization. Biomimetics 7, 144.
- Chen, Z., Li, S., Khan, A.T., Mirjalili, S., 2025. Competition of tribes and cooperation of members algorithm: An evolutionary computation approach for model free optimization. Expert Systems with Applications 265, 125908.
- Chopra, N., Ansari, M.M., 2022. Golden jackal optimization: A novel nature-inspired optimizer for engineering applications. Expert Systems with Applications 198, 116924.
- Chuang, C.L., Jiang, J.A., 2007. Integrated radiation optimization: inspired by the gravitational radiation in the curvature of space-time, in: 2007 IEEE Congress on Evolutionary Computation, IEEE. pp. 3157–3164.
- Das, B., Mukherjee, V., Das, D., 2020. Student psychology based optimization algorithm: A new population based optimization algorithm for solving optimization problems. Advances in Engineering software 146, 102804.
- Dehghani, M., Montazeri, Z., Trojovská, E., Trojovský, P., 2023. Coati optimization algorithm: A new bio-inspired metaheuristic algorithm for solving optimization problems. Knowledge-Based Systems 259, 110011
- Dehghani, M., Trojovská, E., Zuščák, T., 2022. A new human-inspired metaheuristic algorithm for solving optimization problems based on mimicking sewing training. Scientific reports 12, 17387.
- Derrac, J., García, S., Molina, D., Herrera, F., 2011. A practical tutorial on the use of nonparametric statistical tests as a methodology for comparing evolutionary and swarm intelligence algorithms. Swarm and Evolutionary Computation 1, 3–18.
- Dorigo, M., Maniezzo, V., Colorni, A., 1996. Ant system: optimization by a colony of cooperating agents. IEEE transactions on systems, man, and cybernetics, part b (cybernetics) 26, 29–41.
- Duan, H., Qiao, P., 2014. Pigeon-inspired optimization: a new swarm intelligence optimizer for air robot path planning. International journal of intelligent computing and cybernetics 7, 24–37.
- Duman, S., Kahraman, H.T., Guvenc, U., Aras, S., 2021. Development of a lévy flight and fdb-based coyote optimization algorithm for global optimization and real-world acopf problems. Soft Computing 25, 6577– 6617.
- Duman, S., Kahraman, H.T., Kati, M., 2023. Economical operation of modern power grids incorporating uncertainties of renewable energy sources and load demand using the adaptive fitness-distance balancebased stochastic fractal search algorithm. Engineering Applications of Artificial Intelligence 117, 105501.
- Eftimov, T., Korošec, P., Seljak, B.K., 2017. A novel approach to statistical comparison of meta-heuristic stochastic optimization algorithms using deep statistics. Information Sciences 417, 186–215.
- Eiben, A.E., Schippers, C.A., 1998. On evolutionary exploration and exploitation. Fundamenta Informaticae 35, 35–50.
- El-Kenawy, E.S.M., Khodadadi, N., Mirjalili, S., Abdelhamid, A.A., Eid, M.M., Ibrahim, A., 2024. Greylag goose optimization: nature-inspired optimization algorithm. Expert Systems with Applications 238, 122147.
- Enriquez, E.A.T., Mendoza, R.G., Velasco, A.C.T., 2022. Philippine eagle optimization algorithm. IEEE Access 10, 29089–29120.
- Ezugwu, A.E., Agushaka, J.O., Abualigah, L., Mirjalili, S., Gandomi, A.H., 2022. Prairie dog optimization algorithm. Neural Computing and Applications 34, 20017–20065.
- Fan, Q., Huang, H., Li, Y., Han, Z., Hu, Y., Huang, D., 2021. Beetle antenna strategy based grey wolf optimization. Expert Systems with Applications 165, 113882.
- Friedman, M., 1940. A comparison of alternative tests of significance for the problem of m rankings. The annals of mathematical statistics 11, 86–92.
- Geem, Z.W., Kim, J.H., Loganathan, G.V., 2001. A new heuristic optimization algorithm: harmony search. simulation 76, 60–68.
- Ghasemi, M., Golalipour, K., Zare, M., Mirjalili, S., Trojovský, P., Abualigah, L., Hemmati, R., 2024. Flood algorithm (fla): an efficient inspired

- meta-heuristic for engineering optimization. The Journal of Supercomputing 80, 22913–23017.
- Ghasemian, H., Ghasemian, F., Vahdat-Nejad, H., 2020. Human urbanization algorithm: A novel metaheuristic approach. Mathematics and Computers in Simulation 178, 1–15.
- Givi, H., Hubalovska, M., 2023. Skill optimization algorithm: A new human-based metaheuristic technique. Computers, Materials & Continua 74.
- Goldberg, D.E., 1989. Genetic algorithms in search, optimization, and machine learning Addison-Wesley, Reading, Massachusetts.
- Gong, W., Cai, Z., Liang, D., 2014. Engineering optimization by means of an improved constrained differential evolution. Computer Methods in Applied Mechanics and Engineering 268, 884–904.
- Goodarzimehr, V., Shojaee, S., Hamzehei-Javaran, S., Talatahari, S., 2022. Special relativity search: A novel metaheuristic method based on special relativity physics. Knowledge-Based Systems 257, 109484.
- Gurrola-Ramos, J., Hernàndez-Aguirre, A., Dalmau-Cedeño, O., 2020. Colshade for real-world single-objective constrained optimization problems, in: 2020 IEEE congress on evolutionary computation (CEC), IEEE. pp. 1–8.
- Guvenc, U., Duman, S., Kahraman, H.T., Aras, S., Katı, M., 2021. Fitness–distance balance based adaptive guided differential evolution algorithm for security-constrained optimal power flow problem incorporating renewable energy sources. Applied Soft Computing 108, 107421.
- Hamad, R.K., Rashid, T.A., 2024. Goose algorithm: a powerful optimization tool for real-world engineering challenges and beyond. Evolving Systems 15, 1249–1274.
- Hansen, N., Ostermeier, A., 2001. Completely derandomized selfadaptation in evolution strategies. Evolutionary computation 9, 159– 195.
- Harifi, S., Mohammadzadeh, J., Khalilian, M., Ebrahimnejad, S., 2021. Giza pyramids construction: an ancient-inspired metaheuristic algorithm for optimization. Evolutionary Intelligence 14, 1743–1761.
- Hashim, F.A., Houssein, E.H., Hussain, K., Mabrouk, M.S., Al-Atabany, W., 2022. Honey badger algorithm: New metaheuristic algorithm for solving optimization problems. Mathematics and Computers in Simulation 192, 84–110.
- Hashim, F.A., Houssein, E.H., Mabrouk, M.S., Al-Atabany, W., Mirjalili, S., 2019. Henry gas solubility optimization: A novel physics-based algorithm. Future Generation Computer Systems 101, 646–667.
- Hashim, F.A., Hussain, K., Houssein, E.H., Mabrouk, M.S., Al-Atabany, W., 2021. Archimedes optimization algorithm: a new metaheuristic algorithm for solving optimization problems. Applied intelligence 51, 1531–1551.
- Hashim, F.A., Hussien, A.G., 2022. Snake optimizer: A novel metaheuristic optimization algorithm. Knowledge-Based Systems 242, 108320.
- Hatamlou, A., 2013. Black hole: A new heuristic optimization approach for data clustering. Information sciences 222, 175–184.
- Heidari, A.A., Mirjalili, S., Faris, H., Aljarah, I., Mafarja, M., Chen, H., 2019. Harris hawks optimization: Algorithm and applications. Future generation computer systems 97, 849–872.
- Holland, J.H., 1992. Genetic algorithms. Scientific american 267, 66–73.
 Houssein, E.H., Oliva, D., Samee, N.A., Mahmoud, N.F., Emam, M.M.,
 2023. Liver cancer algorithm: A novel bio-inspired optimizer. Computers in Biology and Medicine 165, 107389.
- Hussain, K., Salleh, M.N.M., Cheng, S., Shi, Y., 2019. On the exploration and exploitation in popular swarm-based metaheuristic algorithms. Neural Computing and Applications 31, 7665–7683.
- Issa, M., Hassanien, A.E., Oliva, D., Helmi, A., Ziedan, I., Alzohairy, A., 2018. Asca-pso: Adaptive sine cosine optimization algorithm integrated with particle swarm for pairwise local sequence alignment. Expert Systems with Applications 99, 56–70.
- Javidy, B., Hatamlou, A., Mirjalili, S., 2015. Ions motion algorithm for solving optimization problems. Applied soft computing 32, 72–79.
- Jia, H., Peng, X., Lang, C., 2021. Remora optimization algorithm. Expert Systems with Applications 185, 115665.

- Jia, H., Rao, H., Wen, C., Mirjalili, S., 2023. Crayfish optimization algorithm. Artificial Intelligence Review 56, 1919–1979.
- Jia, H., Wen, Q., Wang, Y., Mirjalili, S., 2024. Catch fish optimization algorithm: a new human behavior algorithm for solving clustering problems. Cluster Computing 27, 13295–13332.
- Jiang, X., Li, S., 2017. Bas: Beetle antennae search algorithm for optimization problems. URL: https://arxiv.org/abs/1710.10724, arXiv:1710.10724.
- Jung, S.H., 2003. Queen-bee evolution for genetic algorithms. Electronics letters 39. 1.
- Kahraman, H.T., Aras, S., Gedikli, E., 2020. Fitness-distance balance (fdb): a new selection method for meta-heuristic search algorithms. Knowledge-Based Systems 190, 105169.
- Kahraman, H.T., Bakir, H., Duman, S., Katı, M., Aras, S., Guvenc, U., 2022. Dynamic fdb selection method and its application: modeling and optimizing of directional overcurrent relays coordination. Applied Intelligence, 1–36.
- Kahraman, H.T., Katı, M., Aras, S., Taşci, D.A., 2023. Development of the natural survivor method (nsm) for designing an updating mechanism in metaheuristic search algorithms. Engineering Applications of Artificial Intelligence 122, 106121.
- Karaboga, D., 2010. Artificial bee colony algorithm. Scholarpedia 5, 6915.
 Kashan, A.H., 2009. League championship algorithm: a new algorithm for numerical function optimization, in: 2009 International Conference of Soft Computing and Pattern Recognition, IEEE. pp. 43–48.
- Kaveh, A., Dadras, A., 2017. A novel meta-heuristic optimization algorithm: Thermal exchange optimization. Advances in engineering software 110, 69–84.
- Kaveh, A., Mahdavi, V.R., 2014. Colliding bodies optimization: a novel meta-heuristic method. Computers & Structures 139, 18–27.
- Kaveh, A., Talatahari, S., 2010. A novel heuristic optimization method: charged system search. Acta mechanica 213, 267–289.
- Kaveh, A., Zolghadr, A., 2016. A novel meta-heuristic algorithm: tug of war optimization. International Journal of Optimization in Civil Engineering 6, 469–492.
- Kennedy, J., Eberhart, R., 1995. Particle swarm optimization, in: Proceedings of ICNN'95-international conference on neural networks, Ieee. pp. 1942–1948.
- Khishe, M., Mosavi, M.R., 2020. Chimp optimization algorithm. Expert systems with applications 149, 113338.
- Kirkpatrick, S., Gelatt, C.D., Vecchi, M.P., 1983. Optimization by simulated annealing. Science 220, 671–680.
- Koza, J.R., 1994. Genetic programming as a means for programming computers by natural selection. Statistics and computing 4, 87–112.
- Kumar, A., Das, S., Zelinka, I., 2020a. A modified covariance matrix adaptation evolution strategy for real-world constrained optimization problems, in: Proceedings of the 2020 genetic and evolutionary computation conference companion, pp. 11–12.
- Kumar, A., Das, S., Zelinka, I., 2020b. A self-adaptive spherical search algorithm for real-world constrained optimization problems, in: Proceedings of the 2020 genetic and evolutionary computation conference companion, pp. 13–14.
- Kumar, A., Wu, G., Ali, M.Z., Mallipeddi, R., Suganthan, P.N., Das, S., 2020c. A test-suite of non-convex constrained optimization problems from the real-world and some baseline results. Swarm and evolutionary computation 56, 100693.
- Lang, Y., Gao, Y., 2025. Dream optimization algorithm (doa): A novel metaheuristic optimization algorithm inspired by human dreams and its applications to real-world engineering problems. Computer Methods in Applied Mechanics and Engineering 436, 117718.
- Layeb, A., 2022. Tangent search algorithm for solving optimization problems. Neural Computing and Applications 34, 8853–8884.
- Li, S., Chen, H., Wang, M., Heidari, A.A., Mirjalili, S., 2020. Slime mould algorithm: A new method for stochastic optimization. Future generation computer systems 111, 300–323.
- Li, Y., Han, T., Zhou, H., Tang, S., Zhao, H., 2022. A novel adaptive l-shade algorithm and its application in uav swarm resource configuration problem. Information Sciences 606, 350–367.

- Liang, J.J., Qu, B.Y., Suganthan, P.N., et al., 2013. Problem definitions and evaluation criteria for the cec 2014 special session and competition on single objective real-parameter numerical optimization. Computational Intelligence Laboratory, Zhengzhou University, Zhengzhou China and Nanyang Technological University, Singapore, Technical Report 635, 490
- Liang, J.J., Runarsson, T.P., Mezura-Montes, E., Clerc, M., Suganthan, P.N., Coello, C.C., Deb, K., 2006. Problem definitions and evaluation criteria for the cec 2006 special session on constrained real-parameter optimization. Journal of Applied Mechanics 41, 8–31.
- Lipowski, A., Lipowska, D., 2012. Roulette-wheel selection via stochastic acceptance. Physica A: Statistical Mechanics and its Applications 391, 2193–2196.
- Luan, T.M., Khatir, S., Tran, M.T., De Baets, B., Cuong-Le, T., 2024. Exponential-trigonometric optimization algorithm for solving complicated engineering problems. Computer Methods in Applied Mechanics and Engineering 432, 117411.
- Mirjalili, S., 2015. Moth-flame optimization algorithm: A novel natureinspired heuristic paradigm. Knowledge-based systems 89, 228–249.
- Mirjalili, S., 2016. Sca: a sine cosine algorithm for solving optimization problems. Knowledge-based systems 96, 120–133.
- Mirjalili, S., Lewis, A., 2016. The whale optimization algorithm. Advances in engineering software 95, 51–67.
- Mirjalili, S., Mirjalili, S.M., Hatamlou, A., 2016. Multi-verse optimizer: a nature-inspired algorithm for global optimization. Neural Computing and Applications 27, 495–513.
- Mirjalili, S., Mirjalili, S.M., Lewis, A., 2014. Grey wolf optimizer. Advances in engineering software 69, 46–61.
- Moein, S., Logeswaran, R., 2014. Kgmo: A swarm optimization algorithm based on the kinetic energy of gas molecules. Information Sciences 275, 127–144.
- Mohamed, A.W., Hadi, A.A., Fattouh, A.M., Jambi, K.M., 2017. Lshade with semi-parameter adaptation hybrid with cma-es for solving cec 2017 benchmark problems, in: 2017 IEEE Congress on evolutionary computation (CEC), IEEE. pp. 145–152.
- Mohamed, A.W., Mohamed, A.K., 2019. Adaptive guided differential evolution algorithm with novel mutation for numerical optimization. International Journal of Machine Learning and Cybernetics 10, 253– 277
- Mohammed, H., Rashid, T., 2023. Fox: a fox-inspired optimization algorithm. Applied Intelligence 53, 1030–1050.
- Moosavi, S.H.S., Bardsiri, V.K., 2019. Poor and rich optimization algorithm: A new human-based and multi populations algorithm. Engineering Applications of Artificial Intelligence 86, 165–181.
- Moosavian, N., Roodsari, B.K., 2014. Soccer league competition algorithm: A novel meta-heuristic algorithm for optimal design of water distribution networks. Swarm and Evolutionary Computation 17, 14–24.
- Mousavirad, S.J., Ebrahimpour-Komleh, H., 2017. Human mental search: a new population-based metaheuristic optimization algorithm. Applied Intelligence 47, 850–887.
- Nocedal, J., Wright, S.J., 1999. Numerical optimization. Springer.
- Odum, E.P., Barrett, G.W., 1971. Fundamentals of ecology Philadelphia: Saunders.
- Oladejo, S.O., Ekwe, S.O., Mirjalili, S., 2024. The hiking optimization algorithm: a novel human-based metaheuristic approach. Knowledge-Based Systems 296, 111880.
- Ozkaya, B., Duman, S., Kahraman, H.T., Guvenc, U., 2024. Optimal solution of the combined heat and power economic dispatch problem by adaptive fitness-distance balance based artificial rabbits optimization algorithm. Expert Systems with Applications 238, 122272.
- Ozkaya, B., Kahraman, H.T., Duman, S., Guvenc, U., 2023. Fitness-distance-constraint (fdc) based guide selection method for constrained optimization problems. Applied Soft Computing 144, 110479.
- Połap, D., Woźniak, M., 2021. Red fox optimization algorithm. Expert Systems with Applications 166, 114107.
- Qais, M.H., Hasanien, H.M., Turky, R.A., Alghuwainem, S., Tostado-Véliz, M., Jurado, F., 2022. Circle search algorithm: A geometry-based metaheuristic optimization algorithm. Mathematics 10, 1626.

- Qi, A., Zhao, D., Heidari, A.A., Liu, L., Chen, Y., Chen, H., 2024. Fata: an efficient optimization method based on geophysics. Neurocomputing 607, 128289
- Rao, R.V., Savsani, V.J., Vakharia, D.P., 2011. Teaching–learning-based optimization: A novel method for constrained mechanical design optimization problems. Computer-aided design 43, 303–315.
- Rashedi, E., Nezamabadi-Pour, H., Saryazdi, S., 2009. Gsa: a gravitational search algorithm. Information sciences 179, 2232–2248.
- Salawudeen, A.T., Mu'azu, M.B., Yusuf, A., Adedokun, A.E., 2021. A novel smell agent optimization (sao): An extensive cec study and engineering application. Knowledge-Based Systems 232, 107486.
- Salimi, H., 2015. Stochastic fractal search: a powerful metaheuristic algorithm. Knowledge-based systems 75, 1–18.
- Sallam, K.M., Elsayed, S.M., Chakrabortty, R.K., Ryan, M.J., 2020. Multi-operator differential evolution algorithm for solving real-world constrained optimization problems, in: 2020 IEEE Congress on Evolutionary Computation (CEC), pp. 1–8. doi:10.1109/CEC48606.2020.9185722.
- Seyyedabbasi, A., Kiani, F., 2023. Sand cat swarm optimization: A nature-inspired algorithm to solve global optimization problems. Engineering with computers 39, 2627–2651.
- Shah-Hosseini, H., 2011. Principal components analysis by the galaxy-based search algorithm: a novel metaheuristic for continuous optimisation. International journal of computational science and engineering 6, 132–140.
- Simon, D., 2008. Biogeography-based optimization. IEEE transactions on evolutionary computation 12, 702–713.
- Sowmya, R., Premkumar, M., Jangir, P., 2024. Newton-raphson-based optimizer: A new population-based metaheuristic algorithm for continuous optimization problems. Engineering Applications of Artificial Intelligence 128, 107532.
- Srivastava, A., Das, D.K., 2022. A bottlenose dolphin optimizer: An application to solve dynamic emission economic dispatch problem in the microgrid. Knowledge-Based Systems 243, 108455.
- Storn, R., Price, K., 1997. Differential evolution a simple and efficient heuristic for global optimization over continuous spaces. Journal of global optimization 11, 341–359.
- Su, H., Zhao, D., Heidari, A.A., Liu, L., Zhang, X., Mafarja, M., Chen, H., 2023. Rime: A physics-based optimization. Neurocomputing 532, 183–214.
- Talbi, H., Draa, A., 2017. A new real-coded quantum-inspired evolutionary algorithm for continuous optimization. Applied Soft Computing 61, 765–791.
- Tanabe, R., Fukunaga, A., 2013. Success-history based parameter adaptation for differential evolution, in: 2013 IEEE congress on evolutionary computation, IEEE. pp. 71–78.
- Tanabe, R., Fukunaga, A.S., 2014. Improving the search performance of shade using linear population size reduction, in: 2014 IEEE congress on evolutionary computation (CEC), IEEE. pp. 1658–1665.
- Tanyildizi, E., Demir, G., 2017. Golden sine algorithm: a novel mathinspired algorithm. Advances in Electrical & Computer Engineering 17
- Tao, H., Aldlemy, M.S., Ahmadianfar, I., Goliatt, L., Marhoon, H.A., Homod, R.Z., Togun, H., Yaseen, Z.M., 2025. Optimizing engineering design problems using adaptive differential learning teaching-learningbased optimization: Novel approach. Expert Systems with Applications 126425.
- Tu, J., Chen, H., Wang, M., Gandomi, A.H., 2021. The colony predation algorithm. Journal of Bionic Engineering 18, 674–710.
- Wang, G.G., 2018. Moth search algorithm: a bio-inspired metaheuristic algorithm for global optimization problems. Memetic Computing 10, 151–164.
- Wang, J., Wang, W.c., Hu, X.x., Qiu, L., Zang, H.f., 2024. Black-winged kite algorithm: a nature-inspired meta-heuristic for solving benchmark functions and engineering problems. Artificial Intelligence Review 57, 98.
- Wang, L., Cao, Q., Zhang, Z., Mirjalili, S., Zhao, W., 2022. Artificial rabbits optimization: A new bio-inspired meta-heuristic algorithm for solving engineering optimization problems. Engineering Applications

- of Artificial Intelligence 114, 105082.
- Wei, Z., Huang, C., Wang, X., Han, T., Li, Y., 2019. Nuclear reaction optimization: A novel and powerful physics-based algorithm for global optimization. IEEE Access 7, 66084–66109.
- Wilcoxon, F., 1945a. Wilcoxon ranking test for unpaired measurements. Biometrics Bull 1, 80.
- Wilcoxon, F., 1945b. Wilcoxon signed-rank test calculator.
- Wolpert, D.H., Macready, W.G., 1997. No free lunch theorems for optimization. IEEE transactions on evolutionary computation 1, 67–82.
- Wu, G., Mallipeddi, R., Suganthan, P.N., 2017. Problem definitions and evaluation criteria for the cec 2017 competition on constrained real-parameter optimization. National University of Defense Technology, Changsha, Hunan, PR China and Kyungpook National University, Daegu, South Korea and Nanyang Technological University, Singapore, Technical Report.
- Wu, X., Li, S., Jiang, X., Zhou, Y., 2024. Information acquisition optimizer: a new efficient algorithm for solving numerical and constrained engineering optimization problems. The Journal of Supercomputing 80, 25736–25791.
- Xiao, Y., Cui, H., Hussien, A.G., Hashim, F.A., 2024. Msao: A multistrategy boosted snow ablation optimizer for global optimization and real-world engineering applications. Advanced Engineering Informatics 61, 102464.
- Xue, J., Shen, B., 2020. A novel swarm intelligence optimization approach: sparrow search algorithm. Systems science & control engineering 8, 22–34.
- Xue, J., Shen, B., 2023. Dung beetle optimizer: A new meta-heuristic algorithm for global optimization. The Journal of Supercomputing 79, 7305–7336
- Yang, X.S., Deb, S., 2009. Cuckoo search via lévy flights, in: 2009 World congress on nature & biologically inspired computing (NaBIC), Ieee. pp. 210–214.
- Yang, Y., Chen, H., Heidari, A.A., Gandomi, A.H., 2021. Hunger games search: Visions, conception, implementation, deep analysis, perspectives, and towards performance shifts. Expert Systems with Applications 177, 114864.
- Yao, X., Liu, Y., Lin, G., 1999. Evolutionary programming made faster. IEEE Transactions on Evolutionary computation 3, 82–102.
- Yue, C.T., K. V. Price, P. N. Suganthan, J.J.L.M.Z.A.B.Y.Q.N.H.A., Biswas, P., 2019. Problem definitions and evaluation criteria for the cec 2020 special session and competition on single objective bound constrained numerical optimization. Computational Intelligence Laboratory, Zhengzhou University, Zhengzhou China, Technical Report 10.
- Zareian, L., Rahebi, J., Shayegan, M.J., 2024. Bitterling fish optimization (bfo) algorithm. Multimedia Tools and Applications 83, 75893–75926.
- Zhang, C., Ding, S., 2021. A stochastic configuration network based on chaotic sparrow search algorithm. Knowledge-Based Systems 220, 106924.
- Zhang, Q., Wang, R., Yang, J., Ding, K., Li, Y., Hu, J., 2017. Collective decision optimization algorithm: A new heuristic optimization method. Neurocomputing 221, 123–137.
- Zhao, S., Zhang, T., Ma, S., Chen, M., 2022a. Dandelion optimizer: A nature-inspired metaheuristic algorithm for engineering applications. Engineering Applications of Artificial Intelligence 114, 105075.
- Zhao, S., Zhang, T., Ma, S., Wang, M., 2023a. Sea-horse optimizer: a novel nature-inspired meta-heuristic for global optimization problems. Applied Intelligence 53, 11833–11860.
- Zhao, W., Wang, L., Mirjalili, S., 2022b. Artificial hummingbird algorithm: A new bio-inspired optimizer with its engineering applications. Computer Methods in Applied Mechanics and Engineering 388, 114194.
- Zhao, W., Wang, L., Zhang, Z., 2019. Atom search optimization and its application to solve a hydrogeologic parameter estimation problem. Knowledge-Based Systems 163, 283–304.
- Zhao, W., Wang, L., Zhang, Z., Fan, H., Zhang, J., Mirjalili, S., Khodadadi, N., Cao, Q., 2024. Electric eel foraging optimization: A new bioinspired optimizer for engineering applications. Expert Systems with Applications 238, 122200.

- Zhao, W., Wang, L., Zhang, Z., Mirjalili, S., Khodadadi, N., Ge, Q., 2023b.
 Quadratic interpolation optimization (qio): A new optimization algorithm based on generalized quadratic interpolation and its applications to real-world engineering problems. Computer Methods in Applied Mechanics and Engineering 417, 116446.
- Zhao, W., Zhang, Z., Wang, L., 2020. Manta ray foraging optimization: An effective bio-inspired optimizer for engineering applications. Engineering Applications of Artificial Intelligence 87, 103300.
- Zhong, C., Li, G., Meng, Z., 2022. Beluga whale optimization: A novel nature-inspired metaheuristic algorithm. Knowledge-based systems 251, 109215.

Table 24Description of 23 classic optimization functions.

No.	$f(\vec{\mathbf{x}})$	D	Search space	$f(\vec{x}^*)$
<i>F</i> 1	$\sum_{i=1}^D x_i^2$	D	$[-100, 100]^D$	0
F2	$\sum_{i=1}^{D} x_i + \prod_{i=1}^{D} x_i $	D	$[-10, 10]^D$	0
F3	$\sum_{i=1}^D (\sum_{j=1}^i x_j)^2$	D	$[-100, 100]^D$	0
F4	$\max_i\{ x_i , 1 \leq i \leq D\}$	D	$[-100, 100]^D$	0
F5	$\sum_{i=1}^{D-1} [100(x_{i+1} - x_i^2)^2 + (x_i - 1)^2]$	D	$[-30, 30]^D$	0
F6	$\sum_{i=1}^{D} (\lfloor x_i + 0.5 \rfloor)^2$	D	$[-100, 100]^D$	0
F 7	$\sum_{i=1}^{D} i x_i^4 + rand$	D	$[-1.28, 1.28]^D$	0
F8	$-\sum_{i=1}^{D} x_i \sin \sqrt{ x_i }$	D	$[-500, 500]^D$	-418.98 × D
F9	$\sum_{i=1}^{D} [x_i^2 - 10\cos(2\pi x_i) + 10]$	D	$[-5.12, 5.12]^D$	0
F10	$-20e^{\left(-0.2\sqrt{\frac{1}{D}\sum_{i=1}^{D}x_{i}^{2}}\right)} - e^{\left[\frac{1}{D}\sum_{i=1}^{D}\cos(2\pi x_{i})\right]} + 20 + e$	D	$[-32, 32]^D$	0
F11	$\frac{1}{4000} \sum_{i=1}^{D} x_i^2 - \prod_{i=1}^{D} \cos\left(\frac{x_i}{\sqrt{i}}\right) + 1$	D	$[-600, 600]^D$	0
F12	$\frac{\pi}{D} \{ 10 \sin^2(\pi y_1) + \sum_{i=1}^{D-1} (y_i - 1)^2 [1 + 10 \sin^2(\pi y_{i+1})] + (y_D - 1)^2 \} + \sum_{i=1}^{D} u(x_i, 10, 100, 4)$	D	$[-50, 50]^D$	0
F13	$0.1\{\sin^2(3\pi x_1) + \sum_{i=1}^{D-1}(x_i-1)^2[1+\sin^2(3\pi x_{i+1})] + (x_D-1)^2[1+\sin^2(2\pi x_D)]\} + \sum_{i=1}^D u(x_i,5,100,4)$	D	$[-50, 50]^D$	0
F14	$\left[\frac{1}{500} + \sum_{j=1}^{25} \frac{1}{j + \sum_{i=1}^{2} (x_i - a_{ij})^6}\right]^{-1}$	2	[-65.536, 65.536] ^D	0.9980
F15	$\sum_{i=1}^{11} \left[a_i - \frac{x_1(b_i^2 + b_i x_2)}{b_i^2 + b_i x_3 + x_4} \right]^2$	4	$[-5,5]^D$	0.0003075
F16	$4x_1^2 - 2.1x_1^4 + \frac{1}{3}x_1^6 + x_1x_2 - 4x_2^2 + 4x_2^4$	2	$[-5,5]^D$	-1.0316
F17	$\left(x_2 - \frac{5.1}{4\pi^2}x_1^2 + \frac{5}{\pi}x_1 - 6\right)^2 + 10\left(1 - \frac{1}{8\pi}\right)\cos x_1 + 10$	2	$[-5, 10] \times [0, 15]$	0.3979
F18	$\left[1 + (x_1 + x_2 + 1)^2 (19 - 14x_1 + 3x_1^2 - 14x_2 + 6x_1x_2 + 3x_2^2)\right] \times \left[30 + (2x_1 - 3x_2)^2 \times (18 - 32x_1 + 12x_1^2 + 48x_2 - 36x_1x_2 + 27x_2^2)\right]$	2	$[-2,2]^D$	3
F19	$-\sum_{i=1}^{4} c_i e^{-\sum_{j=1}^{3} a_{ij} (x_j - p_{ij})^2}$	3	$[0,1]^D$	-3.8628
F20	$-\sum_{i=1}^{4} c_i e^{-\sum_{j=1}^{6} a_{ij}(x_j - p_{ij})^2}$	6	$[0,1]^D$	-3.3220
F21	$-\sum_{i=1}^{5} \left[(x - a_i)(x - a_i)^{\mathrm{T}} + c_i \right]^{-1}$	4	$[0, 10]^D$	-10.1532
F22	$-\sum_{i=1}^{7} \left[(x - a_i)(x - a_i)^{\mathrm{T}} + c_i \right]^{-1}$	4	$[0, 10]^D$	-10.4029
F23	$-\sum_{i=1}^{10} \left[(x - a_i)(x - a_i)^{\mathrm{T}} + c_i \right]^{-1}$	4	$[0, 10]^D$	-10.5364

Note: Functions F1-F7 are unimodal functions and F8-F23 are multimodal functions. Functions F14-F23 have fixed D. More detailed information about the 23 classic optimization functions can be found in (Yao et al., 1999).

Table 25Description of 24 CEC-2006 optimization functions.

No.	$f(\vec{x})$	D	G_{num}	$f(\vec{x}^*)$
F 1	$5\sum_{i=1}^{4} x_i - 5\sum_{i=1}^{4} x_i^2 - \sum_{i=5}^{13} x_i$	13	9	-15.000000
F2	$- \left \frac{\sum_{i=1}^{D} \cos^4(x_i) - 2 \prod_{i=1}^{D} \cos^2(x_i)}{\sqrt{\sum_{i=1}^{D} ix_i^2}} \right $	20	2	-0.8036191
F3	$-\left(\sqrt{D} ight)^D\prod_{i=1}^D x_i$	10	1	-1.0005001
F4	$5.3578547x_3^2 + 0.8356891x_1x_5 + 37.293239x_1 - 40792.141$	5	6	-30665.539
F5	$3x_1 + 0.000001x_1^3 + 2x_2 + (0.000002/3)x_2^3$	4	5	5126.4967
F6	$(x_1 - 10)^3 + (x_2 - 20)^3$	2	2	-6961.8139
F7	$x_1^2 + x_2^2 + x_1x_2 - 14x_1 - 16x_2 + (x_3 - 10)^2 + 4(x_4 - 5)^2 + (x_5 - 3)^2 + 2(x_6 - 1)^2 + 5x_7^2$	10	8	24.306209
	$+7(x_8 - 11)^2 + 2(x_9 - 10)^2 + (x_{10} - 7)^2 + 45$			
F8	$-\frac{\sin^3(2\pi x_1)\sin(2\pi x_2)}{x_1^3(x_1+x_2)}$	2	2	-0.0958250
F9	$(x_1 - 10)^2 + 5(x_2 - 12)^2 + x_3^4 + 3(x_4 - 11)^2 + 10x_5^6 + 7x_6^2 + x_7^4 - 4x_6x_7 - 10x_6 - 8x_7$	7	4	680.63006
F10	$x_1 + x_2 + x_3$	8	6	7049.2480
F11	$x_1^2 + (x_2 - 1)^2$	2	1	0.7499000
F12	$-\left[100 - \left(x_1 - 5\right)^2 - \left(x_2 - 5\right)^2 - \left(x_3 - 5\right)^2\right] / 100$	3	1	-1.0000000
F13	$e^{x_1x_2x_3x_4x_5}$	5	3	0.0539415
F14	$\sum_{i=1}^{10} x_i \left(c_i + \ln \frac{x_i}{\sum_{j=1}^{10} x_j} \right)$	10	3	-47.764888
F15	$1000 - x_1^2 - 2x_2^2 - x_3^2 - x_1x_2 - x_1x_3$	3	2	961.71502
F16	$0.000117y_{14} + 0.1365 + 0.00002358y_{13} + 0.000001502y_{16} + 0.0321y_{12} + 0.004324y_5 + \\$	5	38	-1.9051553
	$0.0001 \frac{c_{15}}{c_{16}} + 37.48 \frac{y_2}{c_{12}} - 0.0000005843 y_{17}$			
F17	$f_1(x_1) + f_2(x_2)$	6	4	8853.5397
	$f_1(x_1) = \begin{cases} 30x_1 & 0 \le x_1 < 300\\ 31x_1 & 300 \le x_1 < 400 \end{cases}$ $\begin{cases} 28x_2 & 0 \le x_2 < 100 \end{cases}$			
	$f_2(x_2) = \begin{cases} 28x_2 & 0 \le x_2 < 100 \\ 29x_2 & 100 \le x_2 < 200 \\ 30x_2 & 200 \le x_2 < 1000 \end{cases}$ $-0.5(x_1x_4 - x_2x_3 + x_3x_9 - x_5x_9 + x_5x_8 - x_6x_7)$			
F10	$\begin{cases} 30x_2 & 200 \le x_2 < 1000 \end{cases}$	0	10	0.0660 25 4
F18		9	13	-0.8660254
F19	$\sum_{j=1}^{5} \sum_{i=1}^{5} c_{ij} x_{(10+i)} x_{(10+j)} + 2 \sum_{j=1}^{5} d_j x_{(10+j)}^3 - \sum_{i=1}^{10} b_i x_i$	15	5	32.655593
F20	$\sum_{i=1}^{24} a_i x_i$	24	20	0.2049794
F21	x_1	7	6	193.72451
F22	x_1	22	20	236.43098
F23	$-9x_5 - 15x_8 + 6x_1 + 16x_2 + 10(x_6 + x_7)$	9	6	-400.05510
F24	$-x_1-x_2$	2	2	-5.5080133

Note: The G_{num} refers to the number of constraints.

The specific constraints and search space of \vec{x} can be found in the technical report of CEC-2006 (Liang et al., 2006).

Table 26
Description of 30 CEC-2014 optimization functions.

No.	Descriptions	D	Search space	$f(\vec{x}^*)$
<i>F</i> 1	Function of Rotated High Conditioned Elliptic	D	$[-100, 100]^D$	100
F2	Function of Rotated Bent Cigar	D	$[-100, 100]^D$	200
F3	Function of Rotated Discus	D	$[-100, 100]^D$	300
F4	Function of Shifted and Rotated Rosenbrock	D	$[-100, 100]^D$	400
F5	Function of Shifted and Rotated Ackley	D	$[-100, 100]^D$	500
F6	Function of Shifted and Rotated Weierstrass	D	$[-100, 100]^D$	600
F7	Function of Shifted and Rotated Griewank	D	$[-100, 100]^D$	700
F8	Function of Shifted Rastrigin	D	$[-100, 100]^D$	800
F9	Function of Shifted and Rotated Rastrigin	D	$[-100, 100]^D$	900
F10	Function of Shifted Schwefel	D	$[-100, 100]^D$	1000
<i>F</i> 11	Function of Shifted and Rotated Schwefel	D	$[-100, 100]^D$	1100
<i>F</i> 12	Function of Shifted and Rotated Katsuura	D	$[-100, 100]^D$	1200
F13	Function of Shifted and Rotated HappyCat	D	$[-100, 100]^D$	1300
F14	Function of Shifted and Rotated HGBat	D	$[-100, 100]^D$	1400
F15	Function of Shifted and Rotated Expanded Griewank's plus Rosenbrock	D	$[-100, 100]^D$	1500
F16	Function of Shifted and Rotated Expanded Scaffer	D	$[-100, 100]^D$	1600
F17	Function 1 Hybrid	D	$[-100, 100]^D$	1700
F18	Function 2 Hybrid	D	$[-100, 100]^D$	1800
F19	Function 3 Hybrid	D	$[-100, 100]^D$	1900
F20	Function 4 Hybrid	D	$[-100, 100]^D$	2000
F21	Function 5 Hybrid	D	$[-100, 100]^D$	2100
F22	Function 6 Hybrid	D	$[-100, 100]^D$	2200
F23	Function 1 Composition	D	$[-100, 100]^D$	2300
F24	Function 2 Composition	D	$[-100, 100]^D$	2400
F25	Function 3 Composition	D	$[-100, 100]^D$	2500
F26	Function 4 Composition	D	$[-100, 100]^D$	2600
F27	Function 5 Composition	D	$[-100, 100]^D$	2700
F28	Function 6 Composition	D	$[-100, 100]^D$	2800
F29	Function 7 Composition	D	$[-100, 100]^D$	2900
F30	Function 8 Composition	D	$[-100, 100]^D$	3000

Note: Functions F1-F3 are unimodal functions, F4-F16 are multimodal functions, F17-F22 are hybrid functions, and F23-F30 are composition functions. The formulation of $f(\vec{x})$ can be found in the technical report of CEC-2014 (Liang et al., 2013).

Table 27Description of 29 CEC-2017 optimization functions.

No.	Descriptions	D	Search space	$f(\vec{x}^*)$
<i>F</i> 1	Function of Shifted and Rotated Bent Cigar	D	$[-100, 100]^D$	100
F3	Function of Shifted and Rotated Zakharov	D	$[-100, 100]^D$	300
F4	Function of Shifted and Rotated Rosenbrock	D	$[-100, 100]^D$	400
F5	Function of Shifted and Rotated Rastrigin	D	$[-100, 100]^D$	500
F6	Function of Shifted and Rotated Expanded Scaffer	D	$[-100, 100]^D$	600
F7	Function of Shifted and Rotated Lunacek Bi-Rastrigin	D	$[-100, 100]^D$	700
F8	Function of Shifted and Rotated Non-Continuous Rastrigin	D	$[-100, 100]^D$	800
F9	Function of Shifted and Rotated Levy	D	$[-100, 100]^D$	900
F10	Function of Shifted and Rotated Schwefel	D	$[-100, 100]^D$	1000
F11	Function 1 Hybrid	D	$[-100, 100]^D$	1100
<i>F</i> 12	Function 2 Hybrid	D	$[-100, 100]^D$	1200
F13	Function 3 Hybrid	D	$[-100, 100]^D$	1300
F14	Function 4 Hybrid	D	$[-100, 100]^D$	1400
F15	Function 5 Hybrid	D	$[-100, 100]^D$	1500
F16	Function 6 Hybrid	D	$[-100, 100]^D$	1600
F17	Function 7 Hybrid	D	$[-100, 100]^D$	1700
F18	Function 8 Hybrid	D	$[-100, 100]^D$	1800
F19	Function 9 Hybrid	D	$[-100, 100]^D$	1900
F20	Function 10 Hybrid	D	$[-100, 100]^D$	2000
F21	Function 1 Composition	D	$[-100, 100]^D$	2100
F22	Function 2 Composition	D	$[-100, 100]^D$	2200
F23	Function 3 Composition	D	$[-100, 100]^D$	2300
F24	Function 4 Composition	D	$[-100, 100]^D$	2400
F25	Function 5 Composition	D	$[-100, 100]^D$	2500
F26	Function 6 Composition	D	$[-100, 100]^D$	2600
F27	Function 7 Composition	D	$[-100, 100]^D$	2700
F28	Function 8 Composition	D	$[-100, 100]^D$	2800
F29	Function 9 Composition	D	$[-100, 100]^D$	2900
F30	Function 10 Composition	D	$[-100, 100]^D$	3000

Note: Functions F1-F3 are unimodal functions, F4-F10 are multimodal functions, F11-F20 are hybrid functions, and F21-F30 are composition functions. The formulation of $f(\vec{x})$ can be found in the technical report of CEC-2017 (Wu et al., 2017).

Table 28Description of 10 CEC-2020 optimization functions.

Туре	No.	Descriptions	D	Search space	$f(\vec{x}^*)$
Unimodal	<i>F</i> 1	Shifted and Rotated Bent Cigar Function (CEC 2017 F1)	D	$[-100, 100]^D$	100
Basic	F2	Shifted and Rotated Schwefel's Function (CEC 2014 F11)	D	$[-100, 100]^D$	1100
	F3	Shifted and Rotated Lunacek Bi-Rastrigin Function (CEC 2017 F7)	D	$[-100, 100]^D$	700
	F4	Expanded Rosenbrock's plus Griewangk's Function (CEC 2017 F19)	D	$[-100, 100]^D$	1900
Hybrid	F5	Hybrid Function 1 ($N = 3$, CEC 2014 $F17$)	D	$[-100, 100]^D$	1700
-	F6	Hybrid Function 2 ($N = 4$, CEC 2017 $F16$)	D	$[-100, 100]^D$	1600
	F7	Hybrid Function 3 ($N = 5$, CEC 2014 $F21$)	D	$[-100, 100]^D$	2100
Composition	F8	Composition Function 1 ($N = 3$, CEC 2017 $F22$)	D	$[-100, 100]^D$	2200
•	F9	Composition Function 2 ($N = 4$, CEC 2017 $F24$)	D	$[-100, 100]^D$	2400
	F10	Composition Function 3 ($N = 5$, CEC 2017 $F25$)	D	$[-100, 100]^D$	2500

Note: Function F1 is unimodal functions, F2-F4 are basic functions, F5-F7 are hybrid functions, and F8-F10 are composition functions. The formulation of $f(\vec{x})$ can be found in the technical report of CEC-2020 (Yue et al., 2019).

Table 29
Numerical results of ECO and competing MHS algorithms on 30 CEC-2014 optimization functions.

MHS	F1	F2	F3	F4	F5	F6	F7	F8	F9	F10	F11	F12	F13	F14	F15	F16	F17	F18	F19	F20	F21	F22	F23	F24	F25	F26	F27	F28	F29	F30
ECO	1.262E+03	2.208E+02	3.035E+02	4.035E+02	5.182E+02	6.003E+02	7.000E+02	8.047E+02	9.110E+02	1.007E+03	1.425E+03	1.200E+03	1.300E+03	1.400E+03	1.500E+03	1.602E+03	1.895E+03	1.848E+03	1.900E+03	2.029E+03	2.131E+03	2.208E+03	2.493E+03	2.515E+03	2.632E+03	2.700E+03	2.702E+03	3.000E+03	3.175E+03	3.775E+02
AO										1.475E+03																				
AOA	1.387E+07	1.776E+09	1.665E+04	6.681E+02	5.200E+02	6.095E+02	7.753E+02	8.324E+02	9.383E+02	1.623E+03	1.981E+03	1.200E+03	1.300E+03	1.407E+03	1.611E+03	1.603E+03	4.191E+04	1.076E+04	1.927E+03	5.855E+03	6.937E+03	2.386E+03	2.500E+03	2.580E+03	2.699E+03	2.704E+03	2.883E+03	3.000E+03	4.412E+03	1.008E+04
ARO	2.652E+03	2.747E+02	3.001E+02	4.202E+02	5.200E+02	6.015E+02	7.001E+02	8.021E+02	9.158E+02	1.066E+03	1.494E+03	1.200E+03	1.300E+03	1.400E+03	1.501E+03	1.602E+03	2.732E+03	1.951E+03	1.900E+03	2.007E+03	2.128E+03	2.235E+03	2.500E+03	2.541E+03	2.692E+03	2.700E+03	2.826E+03	3.039E+03	3.163E+03	3.805E+03
AVOA	1.178E+05	3.212E+03	9.870E+02	4.239E+02	5.200E+02	6.057E+02	7.003E+02	8.087E+02	9.326E+02	1.118E+03	1.915E+03	1.200E+03	1.300E+03	1.400E+03	1.503E+03	1.603E+03	6.175E+03	1.022E+04	1.903E+03	4.806E+03	7.026E+03	2.243E+03	2.500E+03	2.581E+03	2.698E+03	2.700E+03	2.880E+03	3.000E+03	3.565E+03	4.216E+03
BFO	3.202E+04	3.249E+03	1.469E+03	4.247E+02	5.193E+02	6.033E+02	7.000E+02	8.212E+02	9.212E+02	1.712E+03	1.981E+03	1.200E+03	1.300E+03	1.400E+03	1.502E+03	1.603E+03	6.278E+03	6.278E+03	1.902E+03	2.937E+03	2.851E+03	2.259E+03	2.629E+03	2.534E+03	2.672E+03	2.700E+03	2.704E+03	3.274E+03	3.371E+03	4.229E+03
BKA	5.519E+05	1.150E+08	1.582E+03	4.335E+02	5.201E+02	6.060E+02	7.080E+02	8.297E+02	9.303E+02	1.599E+03	1.863E+03	1.200E+03	1.300E+03	1.400E+03	1.505E+03	1.603E+03	3.221E+03	1.924E+03	1.904E+03	2.163E+03	2.655E+03	2.283E+03	2.500E+03	2.577E+03	2.693E+03	2.700E+03	2.854E+03	3.000E+03	3.441E+03	4.756E+03
BOA	1.282E+09	3.865E+10	3.247E+08	1.220E+04	5.211E+02	6.157E+02	8.516E+02	9.845E+02	1.101E+03	3.458E+03	4.102E+03	1.205E+03	1.308E+03	1.449E+03	2.342E+05	1.604E+03	2.035E+08	6.777E+08	2.079E+03	1.267E+07	1.037E+07	2.879E+03	2.850E+03	3.846E+03	2.719E+03	2.930E+03	3.747E+03	6.828E+03	3.784E+07	3.436E+05
BWO	4.699E+08	9.403E+09	1.203E+04	3.451E+03	5.204E+02	6.100E+02	8.273E+02	8.755E+02	9.679E+02	2.356E+03	2.896E+03	1.201E+03	1.305E+03	1.433E+03	7.957E+03	1.603E+03	7.468E+05	1.712E+06	1.932E+03	2.939E+05	6.416E+05	2.432E+03	2.500E+03	2.599E+03	2.699E+03	2.708E+03	2.913E+03	3.001E+03	3.283E+04	4.295E+04
CFOA	9.764E+03	1.098E+03	8.623E+02	4.249E+02	5.196E+02	6.009E+02	7.001E+02	8.078E+02	9.079E+02	1.346E+03	1.426E+03	1.200E+03	1.300E+03	1.400E+03	1.500E+03	1.601E+03	2.197E+03	2.016E+03	1.901E+03	2.063E+03	2.391E+03	2.226E+03	2.629E+03	2.515E+03	2.663E+03	2.700E+03	2.899E+03	3.176E+03	3.231E+03	3.640E+03
COA	1.171E+08	5.130E+09	1.198E+04	1.979E+03	5.203E+02	6.095E+02	7.879E+02	8.717E+02	9.612E+02	2.367E+03	2.707E+03	1.201E+03	1.303E+03	1.425E+03	4.104E+03	1.603E+03	3.583E+05	1.643E+04	1.924E+03	6.314E+03	1.065E+04	2.391E+03	2.500E+03	2.598E+03	2.699E+03	2.704E+03	2.898E+03	3.000E+03	3.137E+03	8.638E+03
CSA	3.402E+04	7.321E+02	7.018E+02	4.214E+02	5.200E+02	6.028E+02	7.001E+02	8.108E+02	9.101E+02	1.201E+03	1.585E+03	1.200E+03	1.300E+03	1.400E+03	1.501E+03	1.602E+03	2.078E+03	1.903E+03	1.902E+03	2.052E+03	2.288E+03	2.220E+03	2.629E+03	2.527E+03	2.667E+03	2.700E+03	2.998E+03	3.217E+03	2.438E+05	3.598E+03
CTCM	3.573E+04	1.578E+03	2.529E+03	4.179E+02	5.201E+02	6.042E+02	7.002E+02	8.258E+02	9.235E+02	1.402E+03	1.711E+03	1.200E+03	1.300E+03	1.400E+03	1.501E+03	1.603E+03	4.439E+03	5.261E+03	1.902E+03	3.448E+03	3.108E+03	2.285E+03	2.625E+03	2.564E+03	2.690E+03	2.706E+03	3.031E+03	3.530E+03	1.331E+05	4.751E+03
DBO	1.098E+06	6.285E+03	1.152E+03	4.551E+02	5.202E+02	6.052E+02	7.002E+02	8.215E+02	9.329E+02	1.377E+03	1.960E+03	1.200E+03	1.300E+03	1.400E+03	1.502E+03	1.603E+03	1.041E+04	7.985E+03	1.903E+03	2.701E+03	8.987E+03	2.258E+03	2.617E+03	2.545E+03	2.675E+03	2.700E+03	2.839E+03	3.260E+03	6.126E+04	4.105E+03
DMOA	5.713E+05	5.011E+03	3.876E+03	4.032E+02	5.203E+02	6.057E+02								1.400E+03						3.259E+03						2.700E+03	3.123E+03	3.106E+03	3.107E+03	3.296E+03
DOA			9.380E+03	5.806E+02						2.250E+03				1.408E+03				2.898E+03					2.554E+03				3.053E+03		1.450E+06	1.148E+04
ESOA										1.456E+03										3.511E+03										5.547E+03
ETO		4.822E+07						8.199E+02						1.400E+03						7.647E+03										3.303E+03
FATA			3.127E+03					8.141E+02						1.400E+03						3.288E+03										4.330E+03
FHO			4.239E+03							2.585E+03				1.400E+03						2.507E+03										8.599E+03
FLA										1.483E+03										2.095E+03										4.047E+03
FOX								8.592E+02						1.400E+03						6.711E+03										3.302E+03
GGO			2.704E+04			6.076E+02				2.046E+03				1.412E+03						3.555E+04								3.892E+03	1.640E+07	
GJO			5.815E+03					8.224E+02			1.806E+03			1.400E+03						5.031E+03									2.543E+05	
GOOSE			3.992E+03					8.528E+02 8.207E+02		2.373E+03				1.400E+03 1.400E+03						4.585E+03									7.706E+05 3.467E+03	
GPC								8.207E+02 8.109E+02						1.400E+03 1.400E+03						6.258E+03 2.093E+03										3.691E+03 5.256E+03
HGS			1.808E+03					8.000E+02			1.602E+03			1.400E+03						6.909E+03									3.131E+03	
HGS		5.326E+07	6.052E+03					8.360E+02												4.667E+03										5.436E+03
HOA								8.300E+02 8.390E+02												8.695E+03										
IAO		6.267E+07	1.090E+03	4.134E+02		6.074E+02 6.037E+02		8.203E+02						1.400E+03						2.018E+03							2.828E+03		3.135E+03	
INFO		2.000E+02				6.035E+02					1.800E+03			1.400E+03						2.029E+03						2.700E+03			1.181E+05	
MEO			1.854E+04			6.044E+02				1.576E+03										2.170E+04						2.700E+03		3 199E+03	3.916E+03	
NRBO				4.357E+02						1.777E+03										3.299E+03										4 392E+03
PDO		4.177E+09	1.648E+04	8.757E+02																1.804E+04							3.051E+03	3.259E+03	3.782E+04	9.069E+03
PEOA	1.560E+05	1.221E+03		4.290E+02										1.400E+03						2.109E+03									4.029E+03	5.183E+03
PIO	2.608E+06	4.476E+08	3.211E+03	4.524E+02	5.203E+02	6.063E+02	7.047E+02	8.364E+02	9.433E+02	1.905E+03	2.368E+03	1.201E+03	1.300E+03	1.400E+03						2.200E+03									4.787E+03	4.448E+03
РКО	1.472E+05	4.855E+03	1.906E+03	4.235E+02	5.200E+02	6.027E+02	7.000E+02	8.103E+02	9.142E+02	1.199E+03	1.714E+03	1.200E+03	1.300E+03	1.400E+03	1.500E+03	1.602E+03	1.318E+04	4.174E+03	1.901E+03	3.046E+03	2.659E+03	2.215E+03	2.629E+03	2.518E+03	2.692E+03	2.700E+03	2.977E+03	3.177E+03	6.104E+04	3.526E+03
РО	6.823E+06	8.168E+05	3.449E+03	4.286E+02	5.201E+02	6.058E+02	7.008E+02	8.386E+02	9.378E+02	1.670E+03	2.000E+03	1.200E+03	1.300E+03	1.400E+03						5.401E+03									5.653E+03	4.728E+03
RIME	9.649E+04	3.724E+03	3.413E+02	4.181E+02	5.199E+02	6.022E+02	7.001E+02	8.000E+02	9.116E+02	1.071E+03	1.461E+03	1.200E+03	1.300E+03	1.400E+03	1.501E+03	1.602E+03	6.326E+03	1.396E+04	1.901E+03	2.124E+03	2.365E+03	2.252E+03	2.629E+03	2.525E+03	2.678E+03	2.700E+03	2.983E+03	3.224E+03	6.886E+04	3.893E+03
RSA	8.708E+07	6.017E+09	8.183E+03	1.228E+03	5.203E+02	6.092E+02	7.874E+02	8.720E+02	9.556E+02	2.007E+03	2.382E+03	1.201E+03	1.302E+03	1.411E+03	2.741E+03	1.603E+03	4.432E+05	2.468E+05	1.914E+03	1.087E+04	4.250E+05	2.355E+03	2.500E+03	2.598E+03	2.700E+03	2.703E+03	2.961E+03	3.215E+03	1.142E+05	7.695E+03
RUN	6.749E+03	1.684E+03	4.148E+02	4.160E+02	5.200E+02	6.051E+02	7.002E+02	8.205E+02	9.365E+02	1.169E+03	1.550E+03	1.200E+03	1.300E+03	1.400E+03	1.502E+03	1.602E+03	3.046E+03	5.748E+03	1.902E+03	2.090E+03	3.490E+03	2.266E+03	2.500E+03	2.573E+03	2.699E+03	2.700E+03	2.854E+03	3.000E+03	3.555E+03	4.279E+03
SAO	2.429E+04	4.224E+03	2.722E+03	4.252E+02	5.195E+02	6.011E+02	7.000E+02	8.128E+02	9.138E+02	1.292E+03	1.592E+03	1.200E+03	1.300E+03	1.400E+03	1.500E+03	1.602E+03	5.345E+03	1.069E+04	1.901E+03	7.338E+03	7.833E+03	2.258E+03	2.629E+03	2.527E+03	2.693E+03	2.700E+03	3.038E+03	3.225E+03	4.557E+05	3.795E+03
SCA	6.382E+06	5.107E+08	3.321E+03	4.484E+02	5.200E+02	6.060E+02	7.086E+02	8.345E+02	9.365E+02	1.849E+03	2.272E+03	1.201E+03	1.300E+03	1.400E+03	1.506E+03	1.603E+03	1.956E+04	1.790E+04	1.904E+03	2.713E+03	8.593E+03	2.252E+03	2.639E+03	2.547E+03	2.695E+03	2.700E+03	3.013E+03	3.253E+03	6.274E+03	4.330E+03
SCSO	6.206E+06	7.080E+07	5.440E+03	4.375E+02	5.200E+02	6.056E+02	7.014E+02	8.284E+02	9.372E+02	1.591E+03	1.882E+03	1.200E+03	1.300E+03	1.400E+03	1.503E+03	1.603E+03	1.658E+04	8.985E+03	1.903E+03	4.889E+03	8.488E+03	2.283E+03	2.500E+03	2.594E+03	2.700E+03	2.700E+03	2.874E+03	3.000E+03	3.847E+03	4.508E+03
SMA	1.121E+05	7.135E+03	8.527E+02	4.209E+02	5.200E+02	6.040E+02	7.002E+02	8.004E+02	9.126E+02	1.164E+03	1.630E+03	1.200E+03	1.300E+03	1.400E+03	1.501E+03	1.602E+03	9.632E+03	1.752E+04	1.901E+03	3.163E+03	3.036E+03	2.223E+03	2.500E+03	2.529E+03	2.683E+03	2.700E+03	2.886E+03	3.000E+03	3.534E+03	3.650E+03
SO	2.137E+04	1.046E+03	9.774E+02	4.192E+02	5.203E+02	6.033E+02	7.001E+02	8.124E+02	9.180E+02	1.259E+03	1.722E+03	1.200E+03	1.300E+03	1.400E+03	1.501E+03	1.602E+03	4.178E+03	3.478E+03	1.901E+03	2.144E+03	2.383E+03	2.255E+03	2.500E+03	2.541E+03	2.691E+03	2.700E+03	2.877E+03	3.000E+03	5.910E+04	3.880E+03
SRS	2.858E+07	5.818E+09	8.667E+03	7.300E+02	5.203E+02	6.092E+02	8.416E+02	8.582E+02	9.544E+02	1.874E+03	2.379E+03	1.200E+03	1.302E+03	1.412E+03	2.883E+03	1.603E+03	2.583E+05	1.152E+04	1.911E+03	8.516E+03	3.281E+04	2.348E+03	2.500E+03	2.599E+03	2.700E+03	2.713E+03	2.900E+03	3.000E+03	3.100E+03	3.200E+03
SSA	3.745E+04	2.098E+03	3.115E+02	4.208E+02	5.200E+02	6.047E+02	7.002E+02	8.207E+02	9.413E+02	1.564E+03	1.952E+03	1.200E+03	1.300E+03	1.400E+03	1.502E+03	1.603E+03	4.973E+03	9.703E+03	1.903E+03	2.156E+03	2.472E+03	2.294E+03	2.500E+03	2.595E+03	2.700E+03	2.700E+03	2.900E+03	3.000E+03	3.160E+03	3.519E+03
TSA	1.999E+07	2.176E+09	1.273E+04	7.037E+02	5.203E+02	6.079E+02	7.549E+02	8.422E+02	9.443E+02	1.964E+03	2.293E+03	1.201E+03	1.301E+03	1.413E+03	1.719E+03	1.603E+03	3.515E+05	2.388E+05	1.927E+03	1.116E+04	1.157E+05	2.376E+03	2.589E+03	2.587E+03	2.699E+03	2.704E+03	3.148E+03	3.729E+03	1.205E+06	3.400E+04
wso		C 450F - 00	2.0425 - 02	4.147E+02	5 109E 02	6 020E : 02	7.004F±02	8.052F±02	9 108F±02	1 101F±03	1.408E+03	1.201E+03	1 300E+03	1.400E+03	1.501E+03	1.602E+03	1.962E+03	1.819E+03	1 901E+03	2.008E+03	2.163E±03	2.247F±03	2.620F±03	2.531F±03	2.683F±03	2.703E+03	3 009E+03	3 270E+03	1.645E+05	3.795E+03

Table 30
Numerical results of ECO and competing MHS algorithms on 29 CEC-2017 optimization functions.

MHS	F1	F3	F4	F5	F6	F7	F8	F9	F10	F11	F12	F13	F14	F15	F16	F17	F18	F19	F20	F21	F22	F23	F24	F25	F26	F27	F28	F29	F30
ECO	1.535E+02	3.000E+02	4.003E+02	5.091E+02	6.000E+02	7.197E+02	8.123E+02	9.000E+02	1.283E+03	1.103E+03	3.432E+03	1.444E+03	1.428E+03	1.520E+03	1.601E+03	1.717E+03	1.900E+03	1.910E+03	2.002E+03	2.200E+03	2.296E+03	2.610E+03	2.649E+03	2.902E+03	2.867E+03	3.092E+03	3.090E+03	3.157E+03	3.827E+03
AO	3.652E+05	3.565E+02	4.064E+02	5.268E+02	6.136E+02	7.518E+02	8.220E+02	1.014E+03	1.883E+03	1.171E+03	2.977E+06	1.733E+04	1.846E+03	4.740E+03	1.753E+03	1.767E+03	2.681E+04	6.866E+03	2.108E+03	2.279E+03	2.305E+03	2.635E+03	2.762E+03	2.924E+03	3.015E+03	3.099E+03	3.407E+03	3.228E+03	6.036E+0
AOA	3.779E+09			5.565E+02			8.299E+02			1.215E+03								1.671E+04			2.652E+03						3.613E+03	3.426E+03	
ARO	8.199E+02			5.159E+02			8.157E+02			1.109E+03								1.901E+03				2.607E+03					3.187E+03	3.183E+03	
AVOA	3.631E+03 4.346E+03			5.319E+02 5.240E+02			8.252E+02 8.230E+02		1.707E+03 1.997E+03				1.523E+03 1.488E+03	2.399E+03 1.767E+03	1.761E+03 1.728E+03			6.289E+03 2.595E+03			2.307E+03 2.301E+03	2.638E+03 2.620E+03		2.934E+03 2.943E+03	0.00.000		3.315E+03 3.296E+03	3.231E+03 3.220E+03	
BKA	4.346E+03			5.240E+02 5.378E+02			8.230E+02 8.225E+02						1.488E+03 1.473E+03		1.728E+03 1.734E+03			2.595E+03 1.955E+03				2.620E+03 2.646E+03		2.943E+03 2.925E+03			3.296E+03 3.237E+03	3.220E+03 3.226E+03	
BOA	3.827E+10		4.133E+02 4.884E+03	6.931E+02			9.662E+02				1.539E+09		2.852E+06		3.002E+03			7.676E+07			5.067E+03			8.136E+03			3.237E+03	4.566E+03	
BWO	1.572E+10			6.126E+02			8.576E+02											5.687E+06			3.089E+03						3.865E+03	3.514E+03	
CFOA			4.011E+02	5.087E+02			8.073E+02						1.447E+03	1.622E+03	1.629E+03			1.937E+03				2.609E+03		2.919E+03			3.227E+03	3.156E+03	3.532E+0
COA	1.110E+10	1.061E+04	1.125E+03	5.930E+02	6.490E+02	8.044E+02	8.551E+02	1.467E+03	2.609E+03	2.233E+03	3.282E+08	3.819E+05	1.534E+03	8.869E+03	2.090E+03	1.806E+03	1.973E+07	5.948E+03	2.248E+03	2.368E+03	3.062E+03	2.730E+03	2.843E+03	3.457E+03	4.136E+03	3.198E+03	3.752E+03	3.444E+03	7.159E+0
CSA	5.366E+02	3.000E+02	4.048E+02	5.097E+02	6.014E+02	7.218E+02	8.087E+02	9.030E+02	1.529E+03	1.113E+03	5.601E+03	1.685E+03	1.437E+03	1.562E+03	1.634E+03	1.737E+03	2.020E+03	1.939E+03	2.027E+03	2.292E+03	2.297E+03	2.617E+03	2.735E+03	2.922E+03	2.891E+03	3.093E+03	3.273E+03	3.158E+03	1.010E+0:
CTCM	2.188E+03	3.000E+02	4.049E+02	5.382E+02	6.136E+02	7.368E+02	8.185E+02	1.070E+03	1.639E+03	1.132E+03	1.326E+04	5.351E+03	2.202E+03	2.474E+03	1.792E+03	1.757E+03	6.483E+03	5.072E+03	2.096E+03	2.301E+03	2.301E+03	2.694E+03	2.734E+03	2.910E+03	3.189E+03	3.152E+03	3.253E+03	3.236E+03	7.635E+0
DBO	7.591E+03	3.000E+02	4.229E+02	5.342E+02	6.069E+02	7.508E+02	8.291E+02	9.328E+02	1.777E+03	1.160E+03	1.545E+06	1.260E+04	1.507E+03	1.847E+03	1.759E+03	1.758E+03	1.930E+04	2.122E+03	2.064E+03	2.209E+03	2.306E+03	2.638E+03	2.602E+03	2.926E+03	3.040E+03	3.100E+03	3.310E+03	3.239E+03	4.845E+0
DMOA	2.055E+03	3.006E+02	4.038E+02	5.178E+02	6.000E+02	7.325E+02	8.168E+02	9.000E+02	2.440E+03	1.103E+03	6.074E+04	5.043E+03	1.478E+03	2.038E+03	1.604E+03	1.737E+03	1.346E+04	2.134E+03	2.021E+03	2.284E+03	2.301E+03	2.628E+03	2.756E+03	2.913E+03	2.997E+03	3.139E+03	3.280E+03	3.220E+03	3.777E+0
DOA	2.063E+09			5.550E+02			8.363E+02													2.315E+03							3.424E+03	3.317E+03	
ESOA	1.002E+09			5.210E+02			8.159E+02			1.223E+03			1.806E+03					2.745E+03			2.380E+03						3.358E+03	3.201E+03	
ETO	2.455E+08			5.319E+02			8.238E+02		1.966E+03					3.345E+03				1.402E+04				2.643E+03		2.943E+03			3.317E+03	3.235E+03	
FATA	1.665E+05			5.334E+02			8.229E+02						1.457E+03		1.837E+03			2.252E+03				2.629E+03			2.903E+03		3.343E+03 3.643E+03	3.212E+03 3.248E+03	
FHO FLA	1.818E+08 3.060E+03			5.308E+02 5.326E+02			8.238E+02 8.224E+02											2.525E+03 1.989E+03			2.336E+03 2.300E+03				3.114E+03 3.119E+03		3.643E+03 3.282E+03	3.248E+03 3.282E+03	
FOX	3.000E+03			5.326E+02 5.762E+02			8.442E+02								2.210E+03			1.989E+03 4.687E+03			2.553E+03			2.945E+03 2.932E+03	3.119E+03 3.988E+03		3.282E+03 3.324E+03	3.282E+03 3.555E+03	
GGO				5.608E+02			8.353E+02											2.905E+05			2.763E+03			3.128E+03	0.0.002		3.690E+03	3.375E+03	
GJO	3.557E+08	2.820E+03	4.304E+02	5.283E+02			8.255E+02											1.211E+04			2.350E+03			2.943E+03	3.137E+03	3.105E+03	3.342E+03	3.205E+03	6.879E+05
GOOSE	4.811E+04	3.001E+02	4.003E+02	5.800E+02			8.649E+02						2.086E+03		2.169E+03			2.439E+03			2.400E+03			2.921E+03	4.206E+03	3.258E+03	3.348E+03	3.566E+03	3.593E+05
GPC	2.072E+08	1.576E+03	4.485E+02	5.295E+02	6.152E+02	7.613E+02	8.222E+02	1.089E+03	1.549E+03	1.131E+03	9.204E+04	8.706E+03	3.480E+03	2.570E+03	1.763E+03	1.740E+03	2.250E+04	8.134E+03	2.053E+03	2.283E+03	2.357E+03	2.640E+03	2.762E+03	2.935E+03	3.056E+03	3.097E+03	3.244E+03	3.183E+03	3.751E+05
HBA	2.607E+03	3.000E+02	4.023E+02	5.183E+02	6.003E+02	7.343E+02	8.157E+02	9.014E+02	1.800E+03	1.132E+03	1.812E+04	2.845E+03	1.501E+03	1.565E+03	1.701E+03	1.749E+03	6.735E+03	2.044E+03	2.071E+03	2.294E+03	2.300E+03	2.636E+03	2.725E+03	2.928E+03	3.072E+03	3.120E+03	3.377E+03	3.244E+03	2.762E+06
HGS	6.559E+03	3.000E+02	4.039E+02	5.208E+02	6.004E+02	7.323E+02	8.187E+02	9.000E+02	1.516E+03	1.120E+03	2.522E+04	9.923E+03	1.690E+03	3.145E+03	1.730E+03	1.745E+03	2.226E+04	7.430E+03	2.008E+03	2.309E+03	2.416E+03	2.626E+03	2.741E+03	2.942E+03	3.297E+03	3.104E+03	3.357E+03	3.208E+03	2.576E+05
НО	1.587E+08	1.162E+03		5.466E+02		7.649E+02	8.282E+02	1.268E+03	2.067E+03	1.193E+03	2.782E+06	1.156E+04	1.646E+03	3.498E+03	1.863E+03	1.774E+03	2.535E+04	1.091E+04	2.137E+03	2.300E+03	2.320E+03	2.658E+03	2.677E+03	2.944E+03	3.230E+03	3.127E+03	3.375E+03	3.299E+03	2.066E+06
HOA	5.314E+09	9.894E+03		5.551E+02			8.306E+02			1.987E+03				6.988E+03	1.938E+03			1.543E+05			2.505E+03				3.788E+03	3.244E+03	3.631E+03	3.291E+03	2.746E+06
IAO	1.909E+08						8.183E+02			1.111E+03			1.412E+03		1.649E+03			1.903E+03			2.314E+03			2.931E+03	3.006E+03		3.216E+03	3.167E+03	
INFO	1.000E+02			5.194E+02			8.209E+02				1.646E+03				1.725E+03			1.913E+03			2.302E+03			2.924E+03	010112100		3.299E+03	3.234E+03	
MFO	1.168E+07			5.358E+02			8.373E+02		1.972E+03		1.093E+06		4.908E+03	1.007E+04	1.762E+03			1.634E+04			2.312E+03				3.141E+03		3.343E+03	3.233E+03	
NRBO	2.994E+08 5.793E+09			5.423E+02 5.873E+02			8.373E+02								1.795E+03			2.076E+03			2.352E+03			2.951E+03 3.180E+03			3.346E+03 3.482E+03	3.249E+03 3.374E+03	
PEOA	2.170E+03						8.555E+02 8.183E+02			3.054E+03								1.766E+05 2.307E+03			2.775E+03				0100120100		3.482E+03	3.374E+03 3.203E+03	
PIO	2.170E+03			5.412E+02		7.968E+02		1.106E+03			9.743E+06		1.461E+03	1.916E+03	1.679E+03			2.262E+03				2.636E+03		2.958E+03	3.148E+03		3.215E+03	3.217E+03	
PKO	3 104E+03			5.150E+02			8.124E+02				3.985E+04		1.480E+03		1.642E+03			3.592E+03			2.290E+03				2.949E+03		3.159E+03	3.165E+03	
PO				5.383E+02			8.294E+02														2.305E+03			2.935E+03			3.282E+03	3.225E+03	
RIME	3.365E+03	3.000E+02	4.083E+02	5.111E+02	6.000E+02	7.198E+02	8.112E+02	9.000E+02	1.327E+03	1.107E+03	1.441E+04	1.195E+04	1.453E+03	1.751E+03	1.749E+03	1.756E+03	5.052E+03	1.991E+03	2.026E+03	2.305E+03	2.300E+03	2.616E+03	2.724E+03	2.927E+03	3.014E+03	3.096E+03	3.284E+03	3.174E+03	3.370E+05
RSA	9.505E+09	8.783E+03	9.954E+02	5.750E+02	6.445E+02	8.064E+02	8.512E+02	1.519E+03	2.452E+03	4.235E+03	2.933E+08	2.508E+07	3.868E+03	1.001E+04	2.071E+03	1.827E+03	3.738E+07	6.530E+05	2.277E+03	2.278E+03	2.985E+03	2.698E+03	2.848E+03	3.329E+03	3.966E+03	3.198E+03	3.695E+03	3.345E+03	9.212E+06
RUN	3.883E+03	3.000E+02	4.004E+02	5.292E+02	6.137E+02	7.510E+02	8.259E+02	1.005E+03	1.577E+03	1.122E+03	9.527E+03	6.058E+03	1.505E+03	1.525E+03	1.759E+03	1.758E+03	1.714E+04	5.360E+03	2.074E+03	2.213E+03	2.304E+03	2.622E+03	2.737E+03	2.915E+03	2.999E+03	3.094E+03	3.329E+03	3.200E+03	5.130E+03
SAO	2.545E+03	3.000E+02	4.001E+02	5.148E+02	6.001E+02	7.207E+02	8.123E+02	9.004E+02	1.580E+03	1.107E+03	9.513E+03	1.172E+04	7.239E+03	4.389E+03	1.678E+03	1.743E+03	2.220E+04	1.322E+04	2.068E+03	2.304E+03	2.301E+03	2.617E+03	2.744E+03	2.930E+03	3.015E+03	3.095E+03	3.354E+03	3.197E+03	3.926E+0
SCA	5.926E+08	1.164E+03	4.377E+02	5.423E+02	6.167E+02	7.654E+02	8.356E+02	9.740E+02	2.154E+03	1.177E+03	7.012E+06	2.584E+04	1.566E+03	1.871E+03	1.710E+03	1.771E+03	7.234E+04	3.282E+03	2.079E+03	2.236E+03	2.353E+03	2.649E+03	2.763E+03	2.949E+03	3.058E+03	3.102E+03	3.255E+03	3.214E+03	6.055E+0
SCSO	5.086E+07			5.397E+02			8.285E+02			1.155E+03											2.319E+03			2.935E+03	3.030E+03	3.105E+03	3.311E+03	3.234E+03	5.988E+0:
SMA	7.810E+03			5.133E+02			8.155E+02			1.111E+03					1.729E+03			2.637E+03			2.339E+03			2.927E+03	3.152E+03		3.292E+03	3.179E+03	
SO				5.165E+02			8.167E+02														2.302E+03						3.279E+03	3.198E+03	
SRS				5.643E+02		8.019E+02						2.757E+06		1.069E+04	2.123E+03			1.104E+05				2.684E+03		3.190E+03			3.663E+03	3.330E+03	
SSA	4.028E+03	3.000E+02		5.330E+02		7.684E+02					1.450E+04							1.986E+03			2.340E+03				0.00.00		3.393E+03	3.254E+03	3.741E+0:
TSA WSO	2.412E+09	1.328E+04	0.00001.00	5.601E+02			8.329E+02														2.674E+03				3.647E+03 2.936E+03		3.586E+03	3.376E+03	4.557E+06
wSO	9.302E+02	5.051E+02	4.018E+02	3.15/E+02	0.004E+02	7.202E+02	6.090E+02	9.093E+02	1.584E+03	1.125E+03	5.510E+03	1.418E+03	1.430E+03	1.519E+03	1.009E+03	1./28E+03	1.82/E+03	1.905E+03	2.026E+03	2.279E+03	2.308E+03	2.050E+03	2.0/8E+03	2.919E+03	2.930E+03	5.115E+03	5.189E+03	5.1/1E+03	1.144E±0